STARS

University of Central Florida

STARS

Electronic Theses and Dissertations, 2004-2019

2005

Numerical Modeling Of Dissimilatory Iron Reduction In Sediments At A Field Site

Chun-Wen Chen
University of Central Florida

Part of the Environmental Engineering Commons

Find similar works at: https://stars.library.ucf.edu/etd

University of Central Florida Libraries http://library.ucf.edu

STARS Citation

University of Central Florida

STARS

Showcase of Text, Archives, Research & Scholarship

NUMERICAL MODELING OF DISSIMILATORY IRON REDUCTION IN SEDIMENTS AT A FIELD SITE

by

CHUN-WEN (ARVIN) CHEN
B.S. National Yunlin University of Science & Technology, 2000

A thesis submitted in partial fulfillment of the requirements
for the degree of Master of Science
in the Department of Civil and Environmental Engineering
in the College of Engineering and Computer Science
at the University of Central Florida
Orlando, Florida

Summer Term
2005

ABSTRACT

The primary purpose of this study is to identify the "universal" rate formulations with scaled-dependent parameters for the biological reduction of hematite. Three possible rate formulations were proposed to describe the bioreduction rate of hematite, and two kinds of simulation were conducted to validate the formulations and parameters with both batch and column experimental data: a reaction-based biogeochemical (batch) modeling with BIOGEOCHEM 1.0 and a reactive biogeochemical transport (column) modeling via HYDROGEOCHEM 4.0. Based on the results of simulations, only the dual Monod kinetic with inhibition rate formulation with respect to the concentrations of lactate, $\equiv$FeOOH, and Fe^{2+} under certain initial concentration of dissimilatory metal-reducing bacterium could fit the experimental data well. Our results also revealed that the equilibrium reaction rate for the surface hydration of hematite may have to be substituted with the kinetic rate formulation.

ACKNOWLEDGMENTS

First of all, I would like to convey my deep appreciation and respect to my advisor, Dr. Gour-Tsyh (George) Yeh, for his patient guidance and financial support during my graduate studies. I admire him not only for his comprehensive knowledge, but also for his attitude of conducting research. He often educated his students that sometimes people may not care how good your works are, but they do care your attitude. This concept influences me to have a positive attitude towards my life.

I would like to thank my thesis committee members, Dr. C. David Cooper and Dr. Scott C. Hagen. From Dr. Cooper I learned the spirit of being an engineer you should know where you are, where you want to go, then choose the best way to reach the goal. I would like to express my appreciation to Dr. Hagen for providing me with the office in my first semester of graduate study and treating me like his students.

I want to thank Dr. Bill Burgos and his student, Morgan Minyard, for providing the experimental data for my graduate research. I would like to thank Mr. Thomas Kimble for carefully revising my thesis and my officemate, Dr. Fan Zhang, for her enthusiastic assistance in the project. Finally, I want to convey my love to my girlfriend, Min-Chun Tsai, for encouraging me all the time.

TABLE OF CONTENTS

LIST OF TABLES

LIST OF FIGURES

CHAPTER 1: INTRODUCTION

Hematite (Fe_2O_3) is the most important ore of iron on earth and deposited as sediment from streams and rivers (see Figure 1.1); however, the biogeochemistry of microbial Fe(III) reduction and of associated contaminant interactions is very complicated. Under anaerobic conditions, hematite is the principle electron acceptor, and bacteria will reduce both crystalline (Roden and Phillips, 1996) and non-crystalline (Lovley and Zachara, 1986) ferric oxides producing Fe(II). In addition, the secondary reactions of bioreduction (biological reduction) of hematite may contain aqueous complexation (Roden et al., 1999; Zachara et al., 1999), surface complexation to the residual ferric oxides, precipitation of ferrous minerals (e.g. $FeCO_3$) (Fredrickson et al., 1998), and re-oxidation.

Our study was to analyze the bioreduction of natural hematite and to determine the rate formulations and parameters of the reaction network via modeling. Two kinds of simulations were conducted: a reaction-based biogeochemical (batch) modeling with BIOGEOCHEM 1.0 (Yeh et al., 2005a) and a reactive biogeochemical transport (column) modeling via HYDROGEOCHEM 4.0 (Yeh et al., 2004). Furthermore, the results of simulations were compared with both batch and column experimental data to see if the employed models could be used to adequately determine the reaction rate formulations/parameters and simulate the biological reduction of hematite. If they do, then, hopefully, they can be used satisfactorily for other chemical reaction networks because the biological reduction of solid-phase ferric oxides is much complicated than other chemical reactions.

Figure 1.1: Mineral Hematite

1.1 Background and Literature Review

The bioreduction of hematite and of associated contaminant interaction is very complicated and difficult to describe because multiple simultaneous reactions often occur under Fe(III)-reducing conditions. For instance, bioreduction of Fe(III) will generate biogenic Fe(II) and secondary reactions of Fe(II) may include sorption/surface complexation to mineral surface, aqueous complexation (if complexants are present) (Urrutia et al., 1999; Zachara et al., 2000), and precipitation of ferrous minerals (Fredrickson et al. 1998). The dissimilatory metal reducing bacteria (DMRB) can be employed to dissolve ferric oxides and the biogenic Fe(II) can then chemically react with other reducible compounds in the biologic-chemical reactions (Burgos et al., 2003). Reducible compounds of concern comprise both organic and inorganic pollutants and can

2

be "directly" (biologic) or "indirectly" (combined biologic-chemical) reduced by DMRB. For example, DMRB will directly reduce benzene and toluene (Lovely et al., 1994), but biogenic Fe(II) will indirectly reduce chlorinated aliphatics (Curtis Reinhard, 1994; Kim and Picardal, 1999) and nitroaromatics (Klausen et al., 1995). Besides, various metal such as Co(III) (Caccavo et al., 1994; Brooks et al., 1999), Cr(VI) (Fendorf and Li, 1996), Tc(VII) (Wildung et al., 2000) and U(VI) (Lovley et al., 1991; Fredrickson et al., 2000) can be directly reduced by DMRB or indirectly reduced by biogenic Fe(II).

Because the reactions of bioreduction of hematite are complicated, an appropriate biogeochemical numerical model is needed to properly evaluate and design the bioreduction system of Fe(III). Early geochemical models classified the chemical reactions into two categories (Rubin, 1983): (1) "sufficiently fast"/equilibrium reaction which was mathematically formulated with the mass action equation or (2) slow/kinetic reaction represented by a rate that was the difference between forward and backward rates. Some models conduct the equilibrium reactions very well and are used extensively such as WATEQ (Truesdell and Jones, 1974), MINEQL (Westall et al., 1976), and PHREEQE (Parkhurst et al., 1980). However, more complicated types of geochemical and biochemical reactions cannot be characterized just via equilibrium chemistry (Friedly and Rubin, 1992); thus, mixed equilibrium chemistry and kinetic chemistry is necessary to describe the complex reactions. Some models such as KEMOD (Yeh et al., 1995), OS3D (Steefel and Yabusaki, 1996), BIOKEMOD (Salvage and Yeh, 1998), and RAFT (Chilakapati et al., 2000) have the capability to deal with the mixed kinetic and

equilibrium reactions; nevertheless, most of them still have many limitations in kinetic or equilibrium reactions.

"Qualitative geochemical and biochemical processes must be conceptualized quantitatively as a reaction network" (Yeh et al., 2001), and the reaction network should be converted into matrix forms, so that the equilibrium and kinetic reactions in the reaction network can be decoupled via Gauss-Jordan elimination (Steefel and Macquarrie, 1996; Chilakapati et al., 1998; Yeh et al., 2001). As a result, a reaction-based biogeochemical model is the most generic approach to deal with mixed equilibrium and kinetic reactions (Fang et al., 2003) because the reaction-based models formulate and simulate the production-consumption rate of chemical species based on both the thermodynamic and chemical kinetic principles. Using both principles, the governing equations can be decomposed into three subsets of equations: mass action equations for equilibrium reaction; kinetic-variable equations; and mass conservation equations (Yeh et al., 2001). So, it can be adequately employed to simulate and predict the complex biogeochemical system (Yeh et al., 2001; Burgos et al., 2002; Fang et al., 2003). For example, the simulations of bioreduction of hematite by the dissimilatory-metal reduction bacterium *Shewanella putrefaciens* strain CN32 under nongrowth condition with H_2 as the electron donor are commendable via using a reaction-based model (Burgos et al., 2002; 2003).

In reactive transport modeling, the decomposition on species transport equations is used instead of the matrix decomposition on species balance equations in the batch system; thus, a reaction-based model is applicable to the reactive transport systems (Fang et al.,

2003). For example, BIOGEOCHEM 1.0 can be operated with any hydrologic transport model. Moreover, in the reactive transport modeling, species reactive transport equations can also be decomposed via Gauss-Jordan column reduction of the reaction network into two sets: nonlinear algebraic equations and transport equations of kinetic-variables to represent the equilibrium reactions and kinetically controlled reaction rates, respectively (Fan et al., 2005). There are many general purpose transport models that can be modified to improve the design capabilities for simulating the mixed equilibrium/kinetic reactions due to this approach of matrix decomposition (Fang and Yeh, 2002). The advantages of the reaction-based models are conspicuous; however, some disadvantages also exist in the reaction-based models. The primary disadvantage of using a reaction-based model is that it is difficult to propose the reaction network and to determine the reaction mechanisms (Steefel and van Cappellen, 1998). Moreover, the minimum measured data needs are another major disadvantage (Yeh et al., 2001).

1.2 Objective of Work

The primary objective of this research is to simulate the bioreduction kinetics of natural hematite-coated sand by dissimilatory metal-reducing bacterium (DMRB), *Shewanella putrefaciens* CN32, under growth conditions with lactate as the electron donor. A reaction-based biogeochemical model BIOGEOCHEM 1.0 (Yeh et al., 2005a) will be employed to determine the rate formulations and parameters of the reaction network of hematite bioreduction, and the results of simulation are simultaneously compared with a series of batch experimental data with different initial conditions. A successful

simulation using BIOGEOCHEM 1.0 would serve to validate the individual rate formulations/parameters and the overall theoretical approach.

In addition, the determined rate formulations and parameters will be systematically tested with the column experimental data by using a reactive biogeochemical transport model Hydrogeochem 4.0 (Yeh et al., 2004) that coupled hydrologic transport and reactive biogeochemistry. The column experiments will focus on transient reactive transport and will be conducted under otherwise identical conditions, except that the flow rates are systematically varied. Furthermore, the assumptions regarding equilibrium reactions will be assessed. We will demonstrate that bioreduction of hematite-coated sand in column system can be simulated reasonably using rate formulation/parameters determined from batch experiments. And, we will test if the mechanistic-based reaction rates of batch system can be scaled up and exported to column system.

1.3 Format and Content

This thesis is composed of four chapters. Chapter 2 focuses on the bioreduction of hematite in batch system; it describes the employed model, modeling approach, and the simulated results. Chapter 3 focuses on the bioreduction of hematite in column system; similar to the batch system, it presents the employed model, modeling approach, and the results of simulation in the column system. Chapter 4 summarizes the work of the thesis and outlines some future work in this field.

CHAPTER 2:

SIMULATION AND EXPERIMENT IN BATCH SYSTEMS

The rate formulations and parameters of the reaction network are the keys to simulate or analyze the chemical reactions. In the past, to determine the rate formulations and parameters extensive experiments in the laboratory are required, but now we can easily conduct that with modeling that requires only a specified set of experiments. This chapter focuses on how to formulate the rates of chemical reaction and how to determine the parameters using a reaction-based biogeochemical model in the batch system. In the following sections, we will describe the model, modeling approach, and the results of the simulations.

2.1 Model Description

A reaction-based biogeochemical model is designed to deal with the mixed equilibrium and kinetic reactions for the complicated reaction networks such as geochemical and biochemical reactions. For our study, we employ BIOGEOCHEM 1.0 to conduct the simulations for determining the formulations/parameters of the bioreduction of hematite in the batch system. The following are this model's unique aspects (Fang et al., 2003):

- facilitate the segregation (isolation) of linearly independent kinetic reactions and thus enable the formulation and parameterization of individual rates one reaction by one reaction when linearly dependent kinetic reactions are absent,

- enable the inclusion of virtually any type of equilibrium expressions and kinetic rates users want to specify,

- reduce problem stiffness by eliminating all fast reactions from the set of ordinary differential equations governing the evolution of kinetic variables,

- perform systematic operations to remove redundant fast reactions and irrelevant kinetic reactions,

- systematically define chemical components and explicitly enforce mass conservation,

- accomplish automation in decoupling fast reactions from slow reactions, and

- increase the robustness of the numerical integration of the governing equations with species switching schemes.

As I know, there is no existing model to comprise these aspects simultaneously. In addition, for making the model applicable to a extensive range of problems, BIOGEOCHEM 1.0 provided multiple reaction types like aqueous complexation, adsorption-desorption, ion exchange, oxidation-reduction, precipitation-dissolution, acid-base reactions, and microbial mediated reactions. From the point of view of reaction rate, this model treats an equilibrium reaction as a reaction with infinite rate governed by a mass action equation (Yeh et al., 2001).

In addition to the equilibrium reaction, several kinetic formulations such as the elementary rate law, multiple Monod kinetics, and n^{th} order empirical formulation are programmed to represent the kinetic reaction rates. The most unique function in

BIOGEOCHEM 1.0 is that user can specify and program the equilibrium and kinetic reaction rate formulations into the code. This function is useful when conducting the mixed equilibrium and kinetic reactions of any complicated reaction network.

In short, BIOGEOCHEM 1.0 is a computer code for modeling the reactive chemicals in the batch systems and designed to be easily coupled with a transport model. BIOGEOCHEM 1.0 is run under the DOS system; thus, it needs some commands (an input files) to execute the program. The input file has to define the reaction network, reaction rate formulations/parameters, time steps, and so on. Table 2.1 presents the required input data for running BIOGEOCHEM 1.0.

2.2 Modeling Approach

Before we employ BIOGEOCHEM 1.0 to determine the rate formulations and parameters of the bioreduction of hematite, we have to propose a reaction network to describe the reaction system, and obtain the experimental data that provide the minimum required number of measured species. The consistency of mass conservation equations must be assessed with the experimental data and the assumptions regarding equilibrium reactions should also be assessed. In addition, we also need another software program such as Mathematica 5.0 (Wolfram Research, Champaign, IL) to help us to solve the mass action and mass conservation equations from the reaction matrix decomposition. Before going through the detailed steps, an overview of procedure is necessary.

Table 2.1: Input Data for Running BIOGEOCHEM 1.0

Data Set	Data Set Name	Command Function
DATA SET 1	TITLE	Array for the title of the problem.
DATA SET 2	NUMBER OF SPECIES AND REACTIONS	Specified the number of species, equilibrium reactions, and kinetic reactions.
DATA SET 3	SPECIES INFORMATION	Defined the species' name, phase, mobility, simulate status, initial concentration, and charge.
DATA SET 3A	ADSORPTION INFORMATION	Selected adsorption model and defined the number of adsorption sites.
DATA SET 3B	ION-EXCHANGE INFORMATION	Additional information for ion-exchanged species.
DATA SET 4	REACTION INFORMATION	Specified the individual reactions.
DATA SET 5	INPUT THE SUSPECIOUS SPECIES	Selected the suspected component and specified the decomposition performance.
DATA SET 6	IPUT ADSORBING SITE INFORMATION	Exit program command.
DATA SET 7	H^+, e^-, AND IONIC STRENGTH CORRECTION INFORMATION	Designated ionic strength and located the H^+ and e^- among global species list.
DATA SET 8	TEMPERATURE, PRESSURE AND EXPECTED pE AND pH	Indicated the temperature and expects the minimum and maximum of pE and pH.
DATA SET 9	BASIC REAL AND INTEGER PARAMETERS	Indicated numeric of the simulation.
DATA SET 10	PRINTER AND AUXILIARY STORAGE CONTROL	Specified which time steps would be printed on the output file or be stored in the storage file.
DATA SET 11	SOURCE PARAMETERS	Designated the source input parameters.

2.2.1 Theory and Mathematical Formulations

A biogeochemical system is completely defined by specifying reaction networks (Yeh et al., 2001), and the production-consumption rate of every species is resulted from all reactions that produce or consume that species. From a mathematical point of view, M

species in a reactive and complete mixed batch system can be presented by a set of M ordinary differential equations that can be written as:

$$\left(\frac{dC_i}{dt}\right) = r_i\big|_N \ , \quad i \in M \tag{2.1}$$

where C_i is the concentration of the i-th chemical species, t is time, $r_i|_N$ is the production-consumption rate of the i-th species due to N biogeochemical reactions, and M is the number of chemical species. For reaction-based modeling, the production-consumption rates are described by:

$$r_i\big|_N = \sum_{k=1}^{N}(\nu_{ik} - \mu_{ik})R_k \qquad \textit{so that} \qquad \frac{dC_i}{dt} = \sum_{k=1}^{N}(\nu_{ik} - \mu_{ik})R_k \ , \quad i \in M \tag{2.2}$$

where N is the number of biogeochemical reactions, ν_{ik} is the reaction stoichiometry of the i-th species in the k-th reaction associated with the products, μ_{ik} is the reaction stoichiometry of the i-th species in the k-th reaction associated with the reactants, and R_k is the rate of the k-th reaction. Equation (2.2) states a mass balance for any species in a reactive system and the concept of any species' rate of mass change is due to all reactions that produce or consume this species simultaneously. Furthermore, for facilitating numerical integration, equation (2.2) can be converted into a matrix form:

$$U\frac{dC}{dt} = \nu R \tag{2.3}$$

where **U** is an unit matrix, **C** is a vector with its components representing M species concentrations, **v** is the reaction stoichiometry matrix (M×N), and **R** is the reaction rate vector with N reaction rates as its components. The reaction matrix decomposition decouples equilibrium (i.e., "fast") reactions from kinetic (i.e., "slow") reactions and enforces mass conservation of chemical components via using Gauss-Jordan elimination.

In addition, the decomposition of equation (2.3) also determines the number of linearly independent reactions (N_I) and selects the mass-conserved chemical components (N_C) where N_C is equal to M minus N_I. According to certain assumptions, the researcher can identify the number of linearly independent equilibrium reactions (N_E). As a result, the decomposition of equation (2.3) reduces a set of M simultaneous ordinary differential equations governing the production-consumption of M species into the following three subsets of equations:

- the first subset contains N_E nonlinear algebraic equations representing mass action laws and/or user-specified algebraic equations for the equilibrium reactions and be defined as:

Mass Action Equations for N_E Equilibrium Reactions

$$\frac{dE_i}{dt} = D_{kk}R_k + \sum_{j \in N_{KD(K)}} D_{ij} R_j; \quad i \in N_E; \quad k \in N_E: \quad R_k = \infty \Rightarrow \frac{dE_i}{dt} \approx D_{KK}R_k, \tag{2.4}$$

which is replaced with a thermodynamically consistent algebraic equation.

- the second subset contains ($N_I - N_E$) simultaneous ordinary differential equations representing the rate of change of the kinetic-variables and be defined as:

Kinetic-Variables Equations for ($N_I - N_E$) Kinetic Reactions

$$\frac{dE_i}{dt} = D_{kk}R_k + \sum_{j \in N_{KD(K)}} D_{ij} R_j; \quad i = N_E + 1, \, N_E + 2 \ldots \ldots, \, N_I - N_E;$$

$$k \in N_{KI} \quad \text{where } E_i = \sum_{j=1}^{M} b_{ij} C_j \tag{2.5}$$

- the third subset contains N_C linear algebraic equations representing mass conservation of the chemical components and be defined as:

Mass Conservation Equations for N_C Chemical Components

$$\frac{dT_i}{dt} = 0; \quad i = 1, 2, \ldots\ldots, N_C \quad \text{where} \quad T_i = \sum_{j=1}^{M} b_{ij} C_j \quad (2.6)$$

where E_i is the i-th kinetic variable, D_{kk} is the diagonal term of the decomposed reaction matrix, $N_{KD(k)}$ is the subset of linearly dependent kinetic reactions, which depends on the k-th reaction, N_{KI} is the number of linearly independent kinetic reactions, b_{ij} is the i-th row and j-th column of the matrix resulting from the Gauss-Jordan decomposition of the unit matrix of size M × M, and T_i is the i-th component.

A thermodynamically consistent algebraic equation can be a mass action equation derived based on the law of mass action or a users' specified equation based on one's understanding of the system. The law of mass action means that the forward reaction rate (r_f) divided by the backward reaction rate (r_b) equals the equilibrium constant (K^e); it can be mathematically expressed as:

$$r_f = K_f[A]^a[B]^b \; ; \; \text{for a reaction as} : aA + bB \Leftrightarrow cC + dD \quad (2.7)$$

$$r_b = K_b[C]^c[D]^d; \; \text{for a reaction as} : aA + bB \Leftrightarrow cC + dD \quad (2.8)$$

$$K^e = \frac{[C]^c[D]^d}{[A]^a[B]^b} = \frac{K_f}{K_b}; \; \text{for a reaction as} : aA + bB \Leftrightarrow cC + dD \quad (2.9)$$

where K_f and K_b are the forward and backward rate constants, respectively.

A kinetic-variable equation represents a linear combination of species concentrations, so that the slope of a kinetic-variable-vs.-time graph can be used to estimate the rate of a kinetic reaction when this kinetic reaction is a linearly independently reaction. On the

13

other hand, if the reaction network involves the parallel kinetic reactions (kinetic reactions that are linearly dependent on at least one other kinetic reaction), the slope can only be used to measure "lumped" reaction rate, not individual rate, (Yeh et al., 2001). However, for equilibrium reactions we just need to deem that all N_E reactions are linearly independent since any equilibrium reaction that is linearly dependent on another equilibrium reaction is redundant. Moreover, the result of decomposition is variant because the selection of chemical components is not unique (Yeh et al., 2001), which could be employed to assess system consistency.

2.2.2 Data Needs

For a reaction-based modeling, a certain number of chemical species (or operational quantities) must be measured in order to adequately analyze the experimental data and further to assess the consistency of mass conservation equations. In general, we can estimate the kinetic suite of reactions if the minimum $(N_I - N_E)$ species were measured. Nevertheless, for a complete assessment of system consistency, as many as $(N_I - N_E + N_C)$ species should be measured. In our study, four species, Fe(II), H^+, lactate, and acetate (incomplete), and one operational quantity, total $[Fe^{2+}] = [Fe^{2+}] + [\equiv FeOOFe(II)^+]$, were measured in batch experiments at Pennsylvania State University. Table 2.2 specifies the initial concentrations of hematite-coated sand, lactate, and cell for our batch simulation. The methods and results of batch experiments are summarized in Appendix A (Morgan's work).

Table 2.2: Initial Concentrations of Hematite-coated Sand, Fe(III), Lactate, and Cell for Individual Experimental Conditions.

Batch Experiment	[Sediment] (g/ml)	[Fe(III)] (mM)	[lactate] (mM)	[cell] (cells/mL)
#1 (DEF)	0.06831	25	37	10^9
#2 (GHIJ)	2	732	10.5	10^8
#3 (KLMN)	0.06234	22.8	3.37	10^8
#4 (OPQ)	0.0682	25	0.69	10^8
#5 (STU)	0.0683	25	3.75	10^9
#6 (VWX)	0.0683	25	3.75	10^7
#7 (AaBbCc)	0.0342	12.5	3.67	10^8
#8 (EeFfGg)	0.00684	2.5	3.65	10^8
#9 (ABC)	0.06831	25	54.5	10^8
#10 (EFG)	0.06831	25	6.5	10^6

2.2.3 Modeling Processes

This section presents how to use BIOGEOCHEM 1.0 to determine the formulations and parameters of the reaction rates for the hematite's bioreduction reactions. Before going through the detailed steps of the modeling procedure, it is necessary to recall the following definitions of terminology in our procedure:

- M: number of chemical species in the reaction network,

- N_E: number of equilibrium reactions,

- N_K: number of kinetic reactions,

- N: total number of biogeochemical reactions in reaction network (where N = N_E + N_K),

- N_I: number of linearly independent reactions, and

- N_C: number of chemical components (where $N_C = M - N_I$).

For employing BIOGEOCHEM 1.0 to conduct the simulation of batch system, we have to propose a reaction network to describe the system. For our case, the proposed reaction network is exhibited in Table 2.3 and illustrated in Figure 2.1. Where the first reaction represents the "bacterial reduction of hematite", second reaction reveals the "surface hydration of hematite", third reaction expresses the "sorption of biogenic ferrous iron, Fe(II), to hematite" (see Figure 2.2), fourth reaction describes the "bacteria growth with lactate as electron donor", and the last one means "PIPES buffering". According to the reaction network, we can conduct the matrix decomposition and further to determine the kinetic formulations and parameters via BIOGEOCHEM 1.0. Generally, the reaction-based modeling includes the following steps:

1. A reaction network of N reactions and M species is proposed to describe the system.

2. This information is turned into an input file for BIOGEOCHEM 1.0.

3. The input file is run through the BIOGEOCHEM 1.0 preprocessor to generate an acceptable reaction matrix decomposition.

4. The mass action and mass conservation equations from the decomposition, and the $(N_I - N_E)$ quantities measured from the experiments are entered into Mathematica (Wolfram) and a simultaneous equation solver routine is used to calculate "all chemical species concentration-vs-time curves". These data are compiled and saved as an Excel (Microsoft) file.

5. The kinetic-variable concentration(s) are summed from the appropriate individual species concentrations. A kinetic-variable concentration is plotted versus time (in

Excel), a trend-line equation is obtained, and the derivative of this equation is the reaction rate equation. The rate equation is used to calculate "the reaction rate-vs-time". This is repeated one reaction at a time for all kinetic-variables.

6. Rate formulations are proposed and tested for the individual kinetic reactions. The species concentration-vs-time obtained in step 4 and the reaction rates-vs-time obtained in step 5 are used to match the rates from experimental measurements with those from proposed rate formulations. The rate parameters for any formulation are obtained by graphical optimization for initial parameter estimation followed by an iterative optimization procedure.

7. The BIOGEOCHEM 1.0 input file is updated with these reaction rate formulations and parameters, and BIOGEOCHEM 1.0 is run to simulate the system and calculate all species concentration-vs-time.

8. Comparisons are made between the BIOGEOCHEM 1.0 model simulations and the experimental measurements.

Table 2.3: Reaction Network of Bioreduction of Hematite

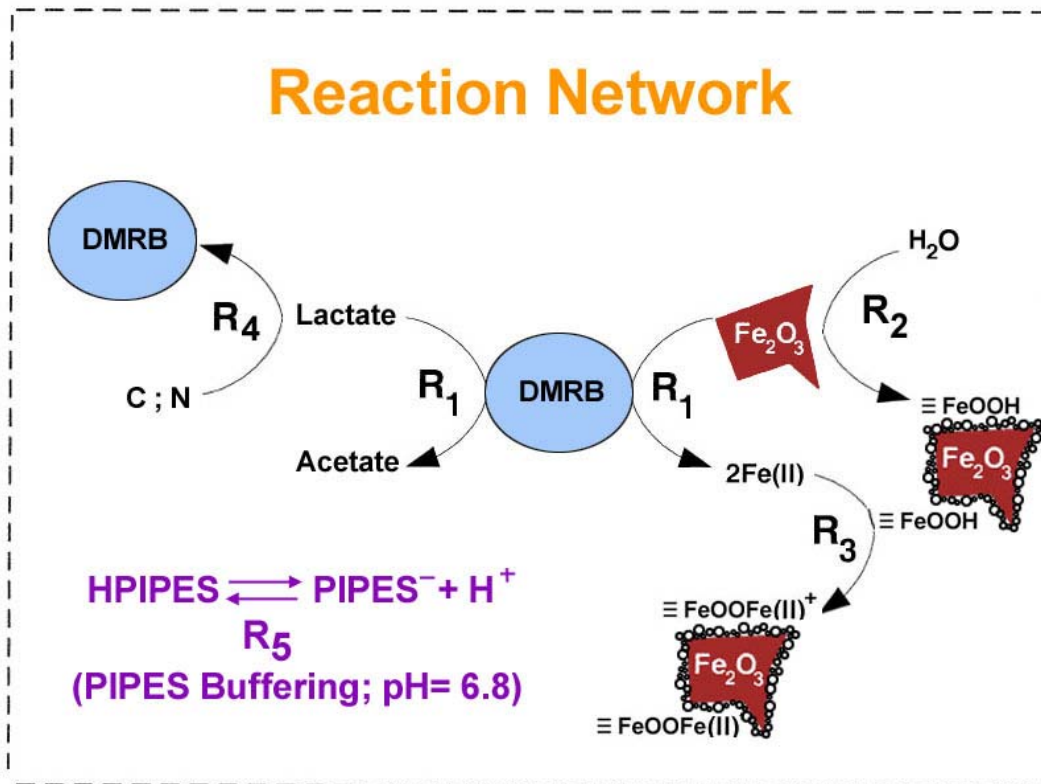| No.	Reaction Network	Type
R1	$2Fe_2O_3 + lactate^- + 7H^+ \rightleftharpoons 4Fe^{2+} + acetate^- + HCO_3^- + 4H_2O$	Kinetic
R2	$Fe_2O_3(bulk) + H_2O \rightleftharpoons 2[\equiv FeOOH](surface)$	Equilibrium
R3	$\equiv FeOOH + Fe^{2+} \rightleftharpoons \equiv FeOOFe(II)^+ + H^+$	Equilibrium
R4	$5lactate^- + 4CO_2 + H_2O + NH_4^+ \rightleftharpoons DMRB + 5acetate^- + 4HCO_3^- + 5H^+$	Kinetic
R5	$HPIPES \rightleftharpoons PIPES^- + H^+$	Equilibrium

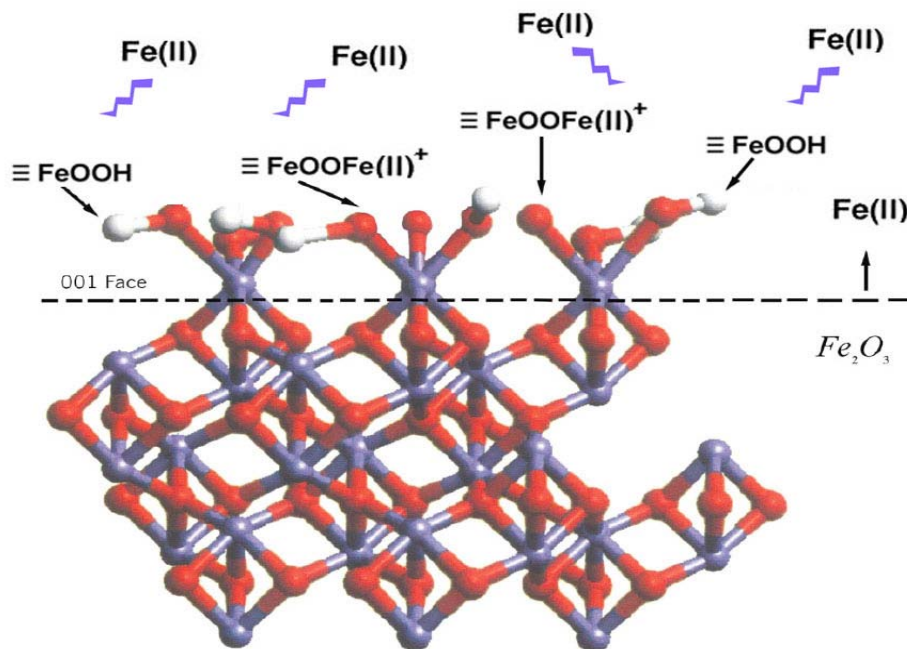Figure 2.1: Reaction Network of Bioreduction of Hematite

Figure 2.2: Sorption of Fe(II) to Hematite

18

Once the reaction network is decided, the N reactions and M species should be numbered and arranged in any order. Typically, the most important chemical reaction is listed first followed by others, and species order depends on the sequence of each species' appearance. We do not usually include H_2O as a species because we assume its activity is one. In addition, we need to select N_C chemical component among the M species in order to identify the mass conserved equations; nevertheless, the selection of chemical components is not unique and can be one of the most difficult aspects of these kinds of problems. For instance, the reaction matrix decomposition may result in a set of components that does not make physical sense to the eye of geochemists, yet they are completely correct from a mathematical standpoint of view and may be used to assess system consistency. The crucial consequences of the reaction decomposition are to select chemical components that yield the most important kinetic-variable equation (i.e., central process under investigation). This outcome is used to formulate a rate equation for the kinetic reactions.

In addition, before we propose and justify the rate formulations and parameters for the individual kinetic reactions, we should clearly comprehend that a reaction rate is estimated by a kinetic-variable equation, not by a time-variant species concentration. Although in some simple systems a kinetic-variable may only consist of a single species. Based on the kinetic-variable equations, we can formulate the rate equation and solve the rate parameters; however, to propose an adequate rate formulation for a kinetic reaction is the most difficult and complicated step of the reaction-based modeling. First, we have to study the reaction network and to estimate which species may influence and be involved

in a particular kinetic reaction rate and then try to formulate the rate equation with these species. For example, R1 of our reaction network expresses the reduction of Fe^{3+} to Fe^{2+}, so we reasonably think that the R1 rate should be relative to Fe_2O_3; however, physical evidence indicates that microbes must be in contact with the hematite surfaces to catalyze the reduction reaction. Therefore, we estimate the R1 rate is proportional to $\equiv FeOOH$ even though R1 doesn't involve in the species $\equiv FeOOH$.

After formulating the rate equation and solving the parameters, we conducted the simulation with the determined formulations/parameters and to compare the results with experimental data in order to justify our proposed formulations and estimated parameters. Generally, for obtaining the most satisfactory rate formulations, we should propose several rate formulations such as the elementary rate, Monod kinetic, and empirical formulations to compare with experimental data.

2.3 Results of Batch Simulation

In our study, we apply BIOGEOCHEM 1.0 to conduct the simulations of bioreduction of hematite. This model is employed to yield the reaction matrix decomposition and to formulate the kinetic reaction rates of the reaction network in batch system. Following sections will represent the results after running BIOGEOCHEM 1.0.

2.3.1 Reaction Matrix Decomposition

According to Table 2.3, the reaction network of bioreduction of hematite contains 13 species (M = 13) except for H_2O, and 5 reactions (N = 5). Experimental evidence

suggested R2, R3, and R5 were equilibrium reactions; thus, $N_E = 3$, so that $N_K = N - N_E = 2$. Furthermore, there is no kinetic reaction that is dependent on the other kinetic reactions; therefore, all reactions are linearly independently reactions ($N_I = N = 5$), so the required number of chemical components is eight ($N_C = M - N_I = 8$). In our case, the solution of thirteen species concentration-vs-time will required thirteen equations, so equation (2.3) can be written in matrix form as:

$$
\begin{bmatrix}
1&0&0&0&0&0&0&0&0&0&0&0&0\\
0&1&0&0&0&0&0&0&0&0&0&0&0\\
0&0&1&0&0&0&0&0&0&0&0&0&0\\
0&0&0&1&0&0&0&0&0&0&0&0&0\\
0&0&0&0&1&0&0&0&0&0&0&0&0\\
0&0&0&0&0&1&0&0&0&0&0&0&0\\
0&0&0&0&0&0&1&0&0&0&0&0&0\\
0&0&0&0&0&0&0&1&0&0&0&0&0\\
0&0&0&0&0&0&0&0&1&0&0&0&0\\
0&0&0&0&0&0&0&0&0&1&0&0&0\\
0&0&0&0&0&0&0&0&0&0&1&0&0\\
0&0&0&0&0&0&0&0&0&0&0&1&0\\
0&0&0&0&0&0&0&0&0&0&0&0&1
\end{bmatrix}
\times
\begin{Bmatrix}
d[Fe_2O_3]/dt\\
d[lactate^-]/dt\\
d[H^+]/dt\\
d[Fe^{2+}]/dt\\
d[acetate^-]/dt\\
d[HCO3^-]/dt\\
d[\equiv FeOOH]/dt\\
d[\equiv FeOOFe]/dt\\
d[CO_2]/dt\\
d[NH_4^+]/dt\\
d[DMRB]/dt\\
d[HPIPES]/dt\\
d[PIPES^-]/dt
\end{Bmatrix}
=
\begin{bmatrix}
-2&-1&0&0&0\\
-1&0&0&-5&0\\
-7&0&+1&+5&+1\\
+4&0&-1&0&0\\
+1&0&0&+5&0\\
+1&0&0&+4&0\\
0&+2&-1&0&0\\
0&0&+1&0&0\\
0&0&0&-4&0\\
0&0&0&-1&0\\
0&0&0&+1&0\\
0&0&0&0&-1\\
0&0&0&0&+1
\end{bmatrix}
\times
\begin{Bmatrix}
R_1\\R_2\\R_3\\R_4\\R_5
\end{Bmatrix}
\quad (2.10)
$$

After matrix decomposition, the selected eight components out of the thirteen species have to yield the kinetic-variable equation for R1 (the most important reaction) since to evaluate the rate of iron reduction is our main objective. In addition, the matrix decomposition also must produce at least one mass conservation equation in terms of species. The matrix decomposition is displayed in Table 2.4. Before calculating the concentration of all species, the equations for equilibrium equations must be determined. Generally, the literature references or preliminary experiments were employed to determine the equilibrium reaction constants. In our study, we have defined or assumed the "surface hydration of hematite" (R2), "sorption of Fe(II) to hematite" (R3), and

Table 2.4: Reaction Matrix Decomposition

(N_I – N_E) Kinetic-variable Equations:

$$\frac{d([Fe^{2+}] + [\equiv FeOOFe(II)^+])}{dt} = 4R_1 \tag{2.11}$$

$$\frac{d[DMRB]}{dt} = R_4 \tag{2.12}$$

N_C Mass Conservation Equations:

$$TOT[Fe_2O_3] = [Fe_2O_3] + 0.5\,[Fe^{2+}] + 0.5\,[\equiv FeOOH] + [\equiv FeOOFe^+] \tag{2.13}$$

$$TOT[lactate^-] = [lactate^-] + 0.25\,[Fe^{2+}] + 0.25\,[\equiv FeOOFe^+] + 5\,[DMRB] \tag{2.14}$$

$$TOT[H^+] = [H^+] + 1.75\,[Fe^{2+}] + 0.75\,[\equiv FeOOFe^+] - 5\,[DMRB] - [PIPES^-] \tag{2.15}$$

$$TOT[acetate^-] = -0.25\,[Fe^{2+}] + [acetate^-] - 0.25\,[\equiv FeOOFe^+] - 5\,[DMRB] \tag{2.16}$$

$$TOT[HCO_3^-] = -0.25\,[Fe^{2+}] + [HCO_3^-] - 0.25\,[\equiv FeOOFe^+] - 4\,[DMRB] \tag{2.17}$$

$$TOT[CO_2] = [CO_2] + 4\,[DMRB] \tag{2.18}$$

$$TOT[NH_4^+] = [NH_4^+] + [DMRB] \tag{2.19}$$

$$TOT[HPIPES] = [HPIPES] + [PIPES^-] \tag{2.20}$$

N_E Mass Action Equations:

$$\frac{d[\equiv FeOOH]}{dt} = R_2 - R_3; \quad R_2 = \infty \quad \Rightarrow \quad \frac{[\equiv FeOOH]^2}{[Fe_2O_3]} = K_2^e \tag{2.21}$$

$$\frac{d[\equiv FeOOFe]}{dt} = R_3; \quad R_3 = \infty \quad \Rightarrow \quad \frac{[\equiv FeOOFe][H^+]}{[\equiv FeOOH][Fe^{2+}]} = K_3^e \tag{2.22}$$

$$\frac{d[PIPES^-]}{dt} = R_5; \quad R_5 = \infty \quad \Rightarrow \quad \frac{[PIPES^-][H^+]}{[HPIPES]} = K_5^e \tag{2.23}$$

TOT[species] means the total concentration of this species; K_2^e; K_3^e; and K_5^e are the equilibrium constants.

"PIPES buffering" (R5) are equilibrium reactions. Furthermore, based on the reference (Burgos et al., 2002), R2 is relative to certain crystalline oxide surfaces, so the mass action equation (2.21) in Table 2.4 cannot adequately describe the formulation for R2 in our modeling because the stoichiometry of R2 is not probably maintained for all hematite surface atoms. Therefore, a "user-specify" formulation for R2, which is based on the concept of surface site species' concentration corresponding to the mineral suspension concentration (Stumm and Morgan, 1996), is proposed to distinguish between the bulk and surface species. In our case, we employed the following equation to substitute for equation (2.21).

$$[\equiv FeOOH]_T = [\equiv FeOOH] + [\equiv FeOOFe(II)^+] = K_{TSS}^e[Fe_2O_3]$$
$$\text{where } K_{TSS}^e = \frac{S_A N_S}{N_A} MW_{Fe_2O_3} \tag{2.24}$$

where $[\equiv FeOOH]_T$ is the total hematite surface site concentration (mol sites L^{-1}), K_{TSS}^e is the "lumped" equilibrium constant for the total surface sites, $[Fe_2O_3]$ is the hematite activity concentration (assumed to equal 1 mole site L^{-1} for crystalline solid), S_A is the hematite unit surface area ($m^2 \ g^{-1}$), N_S is the surface site density (sites m^{-2}), N_A is Avagadro's number (sites mol^{-1}), and $MW_{Fe_2O_3}$ is the molecular weight of hematite (160 g mol^{-1}). In our case, we have assumed a site density of 52 sites nm^{-2} (Cornell and Schwertmann, 1996; Jeon et al., 2001). Using the estimated N_S value of 52 sites nm^{-2} and the measured surface area of 9.04 $m^2 \ g^{-1}$ (Burgos et al., 2002); thus, K_{TSS}^e for equation (2.24) is then calculated as:

$$K_{TSS}^e = \frac{9.04 \, (m^2/g) \times \frac{52 \, (site)}{10^{-18} \, (m^2)}}{6.02 \times 10^{23} \, (site/mole)} \times 160 \, (g/mole) = 0.125 \Rightarrow \log K_{TSS}^e = -0.9 \tag{2.25}$$

Similarly, the maximum amount of adsorption is proportional to the amount of surface area; however, not all of the area is accessible to aqueous adsorbates (Water Quality & Treatment, Fifth Edition). Therefore, the mass action equation (2.22) in Table 2.4 was not used to represent the reaction of "sorption of Fe(II) to hematite" in our simulation. For R3, a "user-specify" formulation based on the concept of the attachment of the material to be adsorbed to adsorbent at an available adsorption site (Snoeyink and Summers, 1999) is proposed to substitute for equation (2.22). In our case, we chose "Freundlich equation" instead and it is described as:

$$q_e = KC_e^n \qquad (2.26)$$

where q_e (mass adsorbate/mass adsorbent) and C_e (moles/volumn) are the equilibrium adsorbate and adsorbent concentrations, respectively. K is the Freundlich capacity factor (the units of K are determined by the units of q_e and C_e), and n is the Freundlich intensity parameter (unitless). Therefore, the sorption of Fe(II) to hematite in R3 can be expressed as:

$$[\equiv FeOOFe(II)^+] = K[Fe^{2+}]^n \qquad (2.27)$$

Freundlich equation is an empirical equation and it is very useful to describe many adsorption data accurately. For our study, because both Fe^{2+} and total $[Fe^{2+}] = [Fe^{2+}] + [\equiv FeOOFe(II)^+]$ were measured, the parameters, K and n, can be determined, independent of other rate equations, via the "best fit" equation using a spreadsheet. Finally, for the last mass action equation (2.23), the logarithm equilibrium constant for PIPES buffering ($\log K_5^e$) is equal to -6.8 according to the product information (Sigma-Aldrich, St. Louis, MO).

2.3.2 Formulations and Parameters for Kinetic Reactions

Based on N_C mass conservation equations (equations 2.13~2.20), N_E equilibrium equations (equations 2.23~2.24, and 2.27), and ($N_I - N_E$) species measured data, we can compute all 13 species concentration-versus-time via using Mathematica software. However, before calculating the concentration of all species, the unit of concentration must be converted into the same units. For our case, the unit of concentration for all species is mole per liter; thus, the unit of cells/mL for bacteria, DMRB, has to be converted into mole per liter. For instance, the 10^{-8} cells/mL is approximated to equal 5×10^{-3} mole L^{-1} based on the bacterium's molecular formula which was assumed as $C_5H_7O_2N$ and thus each cell has 5×10^{-12} g. The accurate value for [DMRB] is 4.4×10^{-3} mole L^{-1}; nevertheless, the approximated value of 5×10^{-3} mole L^{-1} is used due to the assumptions involved (Burgos et al., 2002).

The most important work in the batch system simulation is to determine the rate formulations and parameters for the kinetic reactions. Three rate formulations for R1 will be tested: (1) a physically-based formulation proposed to be first-order with respect to "free" hematite surface sites, $\equiv$FeOOH, (equation 2.28), (2) a dual Monod kinetic rate formulation with respect to the concentrations of lactate and $\equiv$FeOOH (equation 2.29), and (3) a dual Monod kinetic with inhibition rate formulation with respect to the concentrations of lactate, $\equiv$FeOOH, and Fe^{2+} (equation 2.30). In addition, a formal bacteria growth kinetic with cell decay was used to describe R4 (equation 2.31; Metcalf and Eddy, 2003).

$$R_1 = K_{fss}[\equiv FeOOH] \tag{2.28}$$

$$R_1 = U_{max} \frac{[lactate]}{(k_L + [lactate])} \times \frac{[\equiv FeOOH]}{(K_F + [\equiv FeOOH])} \tag{2.29}$$

$$R_1 = V_{max} \frac{[lactate]}{(k_{La} + [lactate])} \times \frac{[\equiv FeOOH]}{\{[\equiv FeOOH] + K_{Fe}(1 + \frac{[Fe^{2+}]}{K_I})\}} \tag{2.30}$$

$$R_4 = \frac{B_{max}}{Y_s} \frac{[lactate]}{(K_b + [lactate])} \times [DMRB] - K_d[DMRB] \tag{2.31}$$

where K_{fss} is the rate constant (hr^{-1}) for R1 in equation (2.28); U_{max} and V_{max} are the maximum specific reaction rate (M hr^{-1}) for R1 in equation (2.29) and (2.30), respectively; K_L, K_F, K_{La} and K_{Fe} are the half-velocity constant (M) for R1 in equation (2.28), (2.29), and (2.30), respectively; K_I is the inhibition coefficient (M) for R1 in equation (2.30); B_{max} is the maximum specific growth rate of DMRB (M new cells/M cells-day); Y_s is the substrate (lactate) consumed coefficient (mol biomass/mol substrate); K_b is the half-velocity constant of bacteria growth rate (M); K_d is the endogenous decay coefficient (M substrate/M substrate-day).

As mentioned above, after the matrix decomposition, we can compute all 13 species concentration-versus-time with the measured data; however, according to the results of standard deviation, we only chose the best three experimental data (Exp. 4~6) with different initial concentrations of DMRB from the ten experiments to conduct our batch simulation. In the following, we employ the data of experiment #4 to interpret how we determine the parameters for each "kinetic" rate formulation; however, before conducting that, the parameters of "equilibrium" formulations should be defined first. In last section,

we have determined the value of K^e_{TSS} and K^e_5 for R2 and R5, respectively; thus, now we need to determine the parameters, K and n, of equilibrium equation (2.27) for R3 via plotting $[Fe^{2+}]$ versus $[\equiv FeOOFe(II)^+]$ and fitting the curve with a power equation as a function of $[Fe^{2+}]$. From Figure 2.3 we can obtain the approximate values of 0.036 and 0.51 for K and n, respectively. After evaluating all of the parameters for the equilibrium reaction, the species concentration-versus-time can be calculated with the experimental data via software Mathematica. Table 2.5 shows the partial (important) species concentration-versus-time for experiment #4.

Table 2.5: Partial Species Concentration-versus-Time for Experiment #4

| Time (hr)	$[Fe_2O_3]$ (M)	$[lactate^-]$ (M)	$[Fe^{2+}]$ (M)	$[\equiv FeOOH]$ (M)	$[\equiv FeOOFe^+]$ (M)	[DMRB] (M)
0	0.0125	0.00069	0	0	0	0.005
0.17	0.0117439	0.000660112	9.09E-07	0.00144554	3.29E-05	0.00501283
1	0.0117281	0.000644779	3.64E-06	0.00141286	6.36E-05	0.00501701
2	0.0117099	0.000645773	0.00001033	0.0013786	9.56E-05	0.00501063
4	0.0116791	0.000617633	0.00002256	0.0013213	0.000149	0.00501765
8	0.0116309	0.000562214	0.00004982	0.0012402	0.000224	0.00503552
12.25	0.0115849	0.000530732	0.00007337	0.00116009	0.000298	0.00503972
20.58	0.0115364	0.000469803	0.000119883	0.00109749	0.000355	0.00506078
24	0.0115111	0.000432746	0.000136954	0.00105757	0.000392	0.00507492
36.3	0.0114579	0.000321781	0.000190584	0.00099135	0.000451	0.00512443
48	0.0113879	0.000267134	0.000235627	0.000878829	0.000555	0.00513488
72.1	0.0113124	0.000171555	0.000321838	0.000794906	0.000629	0.00516807
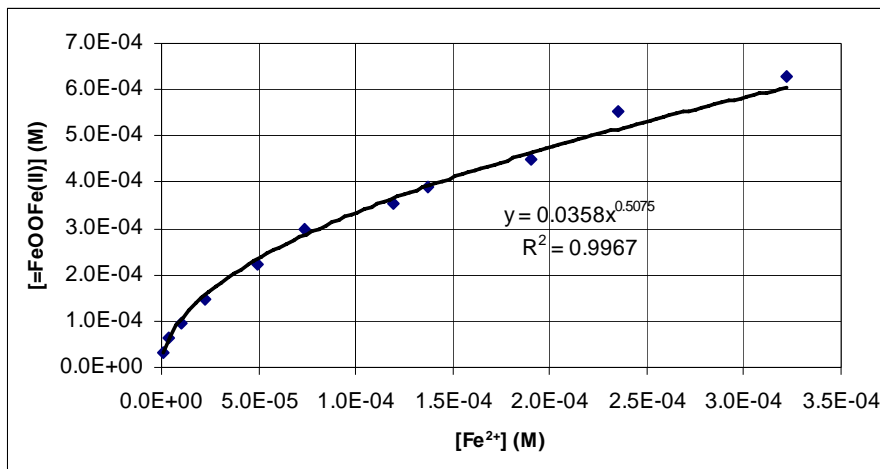
Figure 2.3: Curve of the Empirical Freundlich Equation (R3) for Exp. #4

As the first step in determining the parameters of kinetic rate formulations, we use the kinetic-variable Equation (2.11) and (2.12) to plot the kinetic-variable concentration-vs-time and fit the curve with an equation as a function of time (see Figure 2.4). Second, the time derivative of this equation divided by the rate factor is then equal to the reaction rate. For example, the "best fit" equation in Figure 2.4 for $([Fe^{2+}] + [\equiv FeOOFe(II)^+])$-vs-time is:

$$([Fe^{2+}] + [\equiv FeOOFe(II)^+])\,(M) = -1.39 \times 10^{-7} t^2 + 2.2 \times 10^{-5} t + 7.09 \times 10^{-5} \qquad (2.32)$$

so $\dfrac{d([Fe^{2+}] + [\equiv FeOOFe(II)^+])}{dt}\,(M/hr) = 4R1 = -2.78 \times 10^{-7} t + 2.2 \times 10^{-5} \qquad (2.33)$
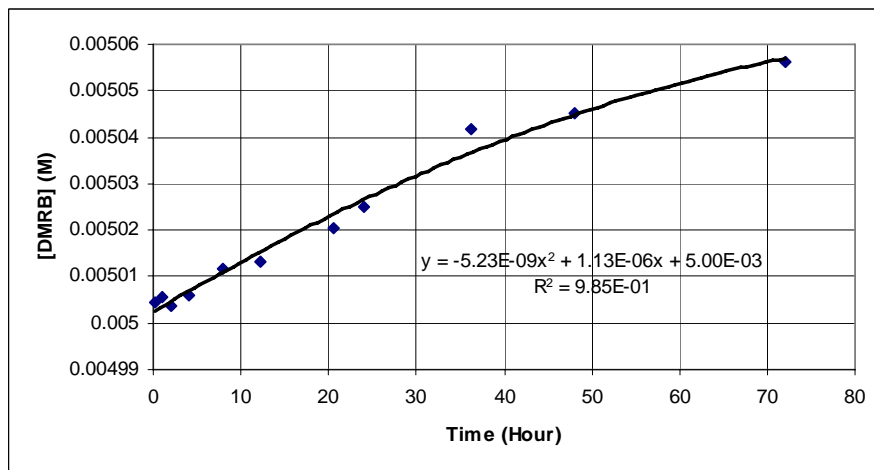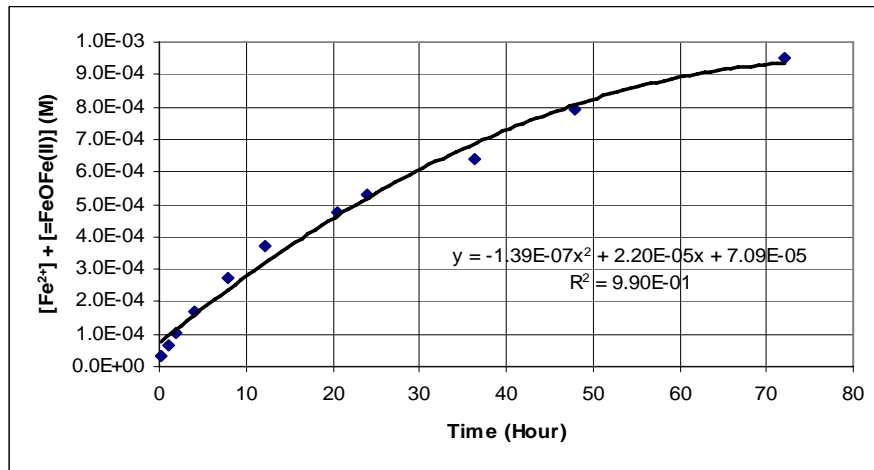

Figure 2.4: The Kinetic-Variable Concentration-vs-Time for Exp. #4

28

Third, we can use equation (2.33) to generate R_1 as a function of time; therefore, the rate formulations and parameters can be tested and determined with all species concentration-vs-time and the reaction rate-vs-time. For instance, equation (2.28), first proposed R1 rate formulation, can be plotted as R_1 versus $\equiv$FeOOH and the K_{fss} then can be determined from the slope. From Figure 2.5 we obtain the rate constant, K_{fss}, of 0.0038 M/hr. For the second proposed R1 rate formulation, we should rearrange the dual Monod kinetic rate formulation (equation 2.29) as:

$$R_1 = \frac{U_{max}}{(\frac{k_L}{[lactate]} + 1)} \times \frac{[\equiv FeOOH]}{(K_F + [\equiv FeOOH])} \qquad (2.34)$$

$$\text{assuming } U_{max\text{-}app} = \frac{U_{max}}{(\frac{k_L}{[lactate]} + 1)}; \text{ thus, } R_1 = U_{max\text{-}app} \times \frac{[\equiv FeOOH]}{(K_F + [\equiv FeOOH])} \qquad (2.35)$$

$$\text{so } \frac{1}{R_1} = (\frac{K_F}{U_{max\text{-}app}})\frac{1}{[\equiv FeOOH]} + \frac{1}{U_{max\text{-}app}} \qquad (2.36)$$

where $U_{max\text{-}app}$ is an approach maximum specific reaction rate (M hr^{-1}) for R1, so the dual Monod kinetic form can be represented by a "single" Monod kinetic form (equation 2.35), and Equation (2.36) then can be plotted as $1/R_1$ versus $1/[\equiv FeOOH]$ to determine the value of K_F (from 1/y-intercept multiplies the slope). From Figure 2.6 we can obtain the half-velocity constant, K_F, of 4.26×10^{-3} M. Then, we rearrange equation (2.29) as:

$$\frac{1}{R_1 \times \{1 + \frac{K_F}{[\equiv FeOOH]}\}} = (\frac{K_L}{U_{max}})\frac{1}{[lactate]} + \frac{1}{U_{max}} \qquad (2.37)$$
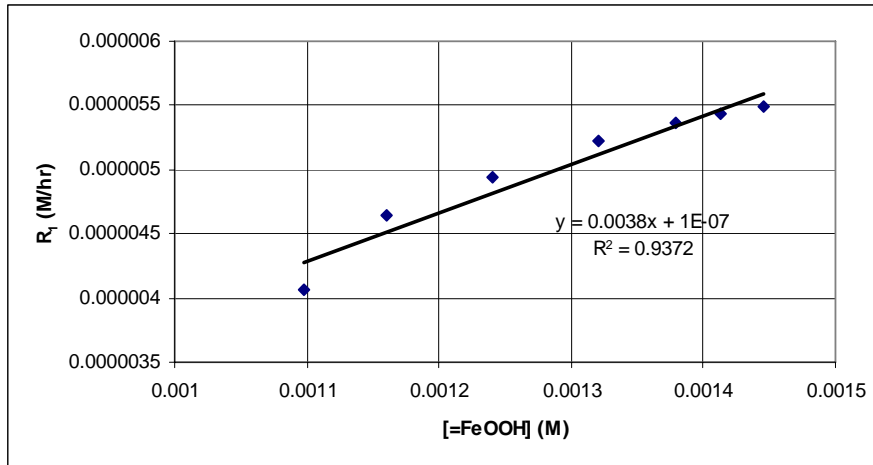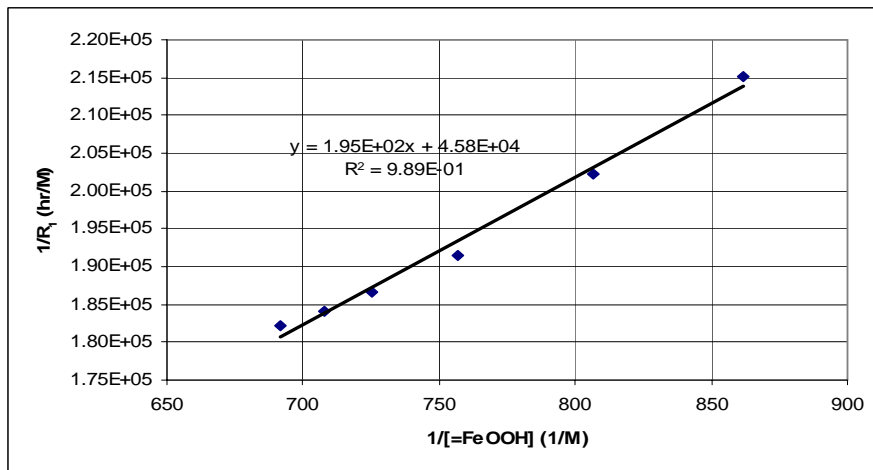
Figure 2.5: R_1 versus $[\equiv FeOOH]$ for Exp. #4

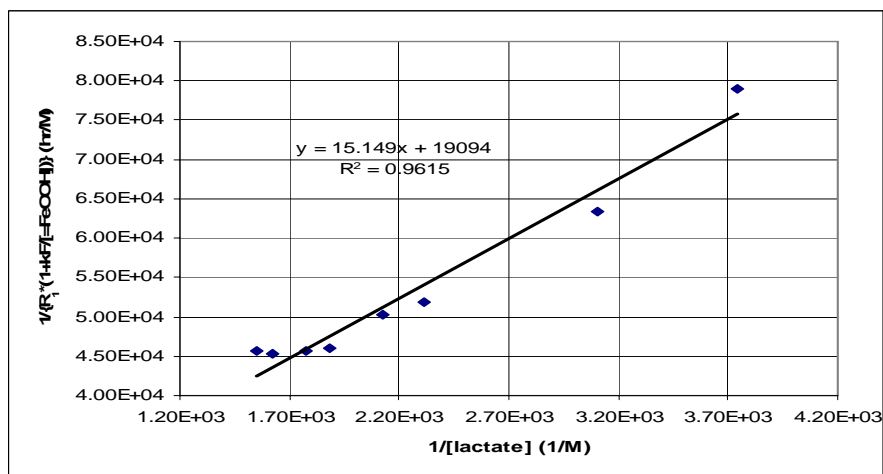Figure 2.6: $1/R_1$ versus $1/[\equiv FeOOH]$ for Exp. #4

Figure 2.7: $1/\{R_1 \times (1+K_F/[\equiv FeOOH])\}$ versus $1/[lactate]$ for Exp. #4

30

After inputting the determined value of K_F into equation (2.37), we can plot $1/\{R_1 \times (1+K_F/[\equiv FeOOH])\}$ versus 1/[lactate] to find out the values of K_L/U_{max} (from the slope) and $1/U_{max}$ (from the y-intersect). From Figure 2.7 we can acquire the half-velocity constant, K_L, of 7.93×10^{-4} M and the maximum specific reaction rate, U_{max}, of 5.24×10^{-5} M/hr, respectively.

In addition, we utilize the iterative optimization procedure to predict our third proposed R1 (where R1 denotes Reaction No. 1) rate formulation. In the beginning, we plot the R_1 (where R_1 denotes rate of R1) versus time via Excel and set up this rate formulation into Excel. Then, we adjust each parameters of this formulation with the involved species concentration-vs-time to fit the curve of R_1-versus-time. After achieving the "best fit" (Figure 2.8), we can obtain each specific value for each parameter. The parameters in equation (2.30) were estimated as 8.5×10^{-5} M/hr, 9.0×10^{-3} M, 3.5×10^{-5} and 6.0×10^{-4} for V_{max}, K_{La}, $K_{Fe,}$ and K_I, respectively.

For evaluating the bacteria growth kinetic rate formulation (R4), we should consider the substrate, lactate, utilization first. According to the reaction network, R1 and R4 both consume the lactate; hence, the lactate utilization for DMRB will be the initial lactate amount minus the consumption of lactate in R1. The consumption of lactate in R1 will generate four times of total Fe^{2+} (total $[Fe^{2+}] = [Fe^{2+}] + [\equiv FeOOFe(II)^+]$); therefore, the lactate utilization in R4 is equal to the initial lactate amount minus one fourth amount of Fe^{2+} and $\equiv FeOOFe(II)^+$. So, we can plot the lactate consumption-vs-time of R4 and fit the curve with an equation as a function of time (Figure 2.9) and the time derivative of
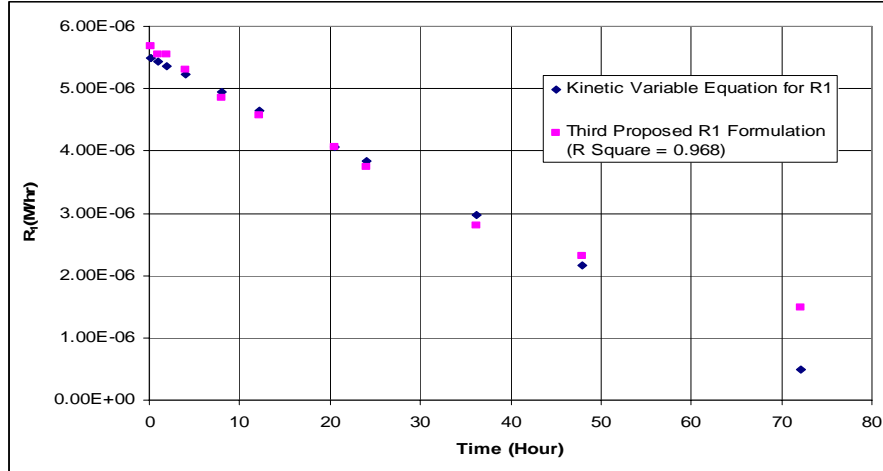
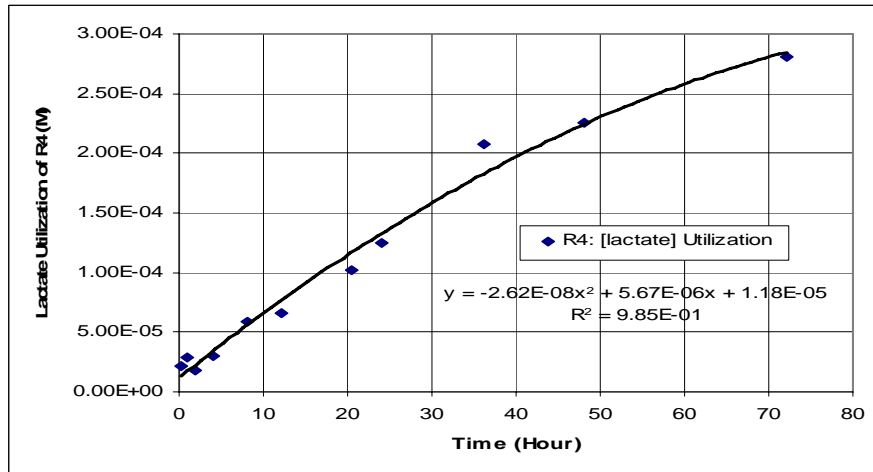Figure 2.8: Optimization Curve of the Third Proposed R1 Formulation for Exp. #4

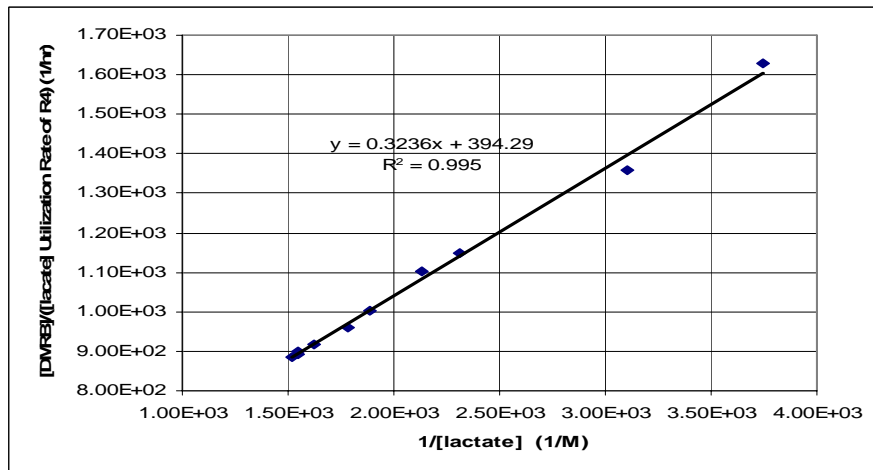Figure 2.9: Lactate Utilization in R4 for Exp. #4

Figure 2.10: [DMRB]/ (R4 [lactate] Utilization Rate) versus 1/ [lactate] for Exp. #4

this equation is then equal to the lactate utilization rate in R4. Based on Figure 2.9 we can calculate the lactate utilization rate of R4 for each specific time point and we also know the lactate utilization rate formulation of R4 as (Metcalf and Eddy, 2003):

$$\text{Lactate Utilization Rate of R4} = B_{max} \frac{[\text{Lactate}]}{K_b + [\text{lactate}]} \times [\text{DMRB}] \tag{2.38}$$

$$\Rightarrow \frac{[\text{DMRB}]}{\text{Lactate Utilization Rate of R4}} = (\frac{K_b}{B_{max}}) \frac{1}{[\text{lactate}]} + \frac{1}{B_{max}} \tag{2.39}$$

Therefore, equation (2.39) can be plotted as [DMRB]/(R4 [lactate] Utilization Rate) versus 1/[lactate] in order to determine the values of B_{max} and K_b. According to Figure 2.10, the values of B_{max} and K_b are 2.54×10^{-3} M new cells/M cells-day and 8.21×10^{-4} M, respectively. However, two more parameters, Y_s and K_d, need to be found out for the bacteria growth kinetic rate formulation (equation 2.31). There, Y_s is the lactate consumed coefficient, so based on the fourth reaction of our reaction network Y_s is equal to 5 mol DMRB/mol lactate. Furthermore, we employ the iterative optimization procedure to determine K_d (Figure 2.11); the determined value of K_d is then equal to 1×10^{-6} M substrate/M substrate-day.
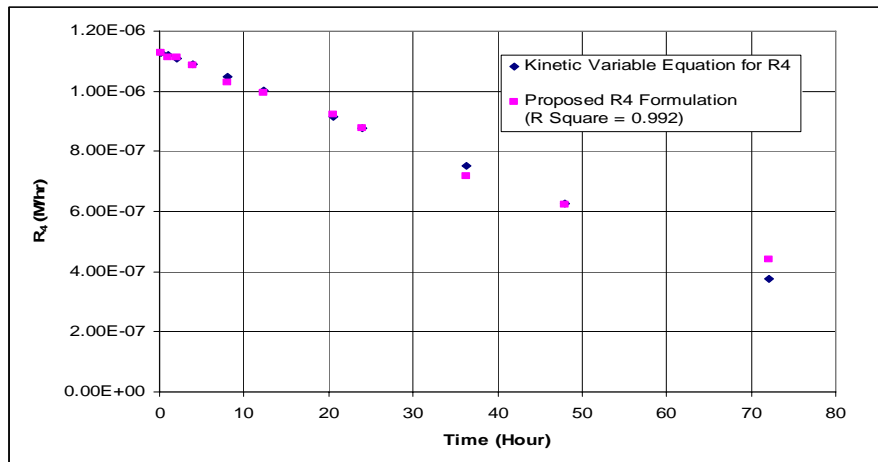

Figure 2.11: Optimization Curve of the Proposed R4 Formulation for Exp. #4

2.3.3 The Simulation Results

In the same way, we repeated the procedures of determining parameters of experiment #4 to find out the parameters of rate formulations for the other experiments. As a result, we can obtain each parameter represented in Table 2.6 (without the units) for each experiment. Moreover, before using BIOGEOCHEN 1.0 to conduct the simulations, we should update the input files with these proposed rate formulations and determined parameters. After running BIOGEOCHEN 1.0, we then can acquire all of the species' concentration at the specific time points that we would like to compare with the batch experimental data. The following figures display the results of simulation contrasted with the batch experimental data simultaneously.

Table 2.6: Input Parameters for the Reaction Rate Formulations

Parameters	Exp. #4	Exp. #5	Exp. #6
K_{fss}	3.8×10^{-3}	9.5×10^{-3}	4.2×10^{-3}
U_{max}	5.24×10^{-5}	5.5×10^{-5}	2.2×10^{-5}
V_{max}	8.5×10^{-5}	3.2×10^{-5}	1.8×10^{-5}
B_{max}	2.54×10^{-3}	3.3×10^{-4}	2.55×10^{-2}
K_L	7.93×10^{-4}	7.0×10^{-4}	5.5×10^{-4}
K_F	4.26×10^{-3}	4.0×10^{-3}	3.3×10^{-3}
K_{La}	9.0×10^{-3}	9.8×10^{-3}	9.6×10^{-3}
K_b	8.21×10^{-4}	2.52×10^{-3}	1.1×10^{-5}
K_{Fe}	3.5×10^{-5}	6.0×10^{-6}	2.0×10^{-3}
K_I	6.0×10^{-4}	1.0×10^{-5}	1.5×10^{-5}
Y_s	5	5	5
K_d	1.0×10^{-6}	1.0×10^{-6}	1.0×10^{-6}
K	3.6×10^{-2}	1.35×10^{-1}	1.5×10^{-2}
n	0.51	0.624	0.4

Figure 2.12: Simulation Results of the First Proposed R1 Formulation for Exp. #4

Figure 2.13: Simulation Results of the Second Proposed R1 Formulation for Exp. #4

Figure 2.14: Simulation Results of the Third Proposed R1 Formulation for Exp. #4

Figure 2.15: Simulation Results of the First Proposed R1 Formulation for Exp. #5
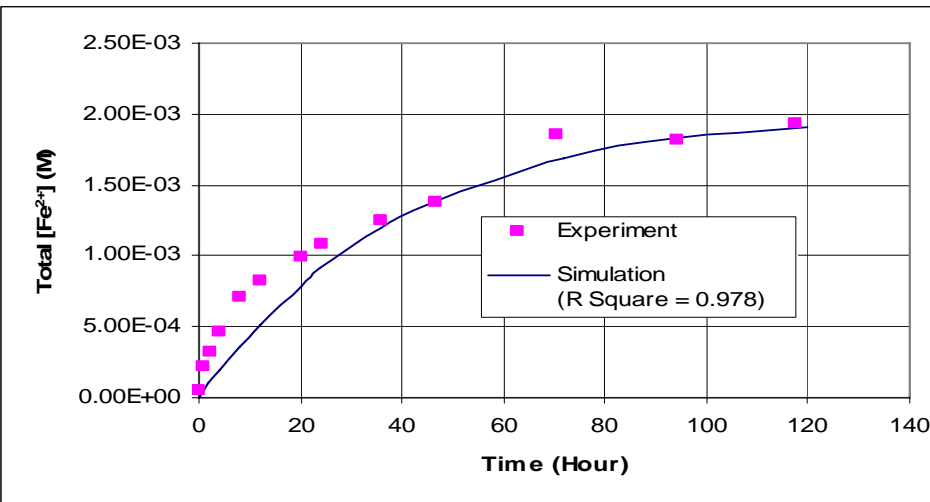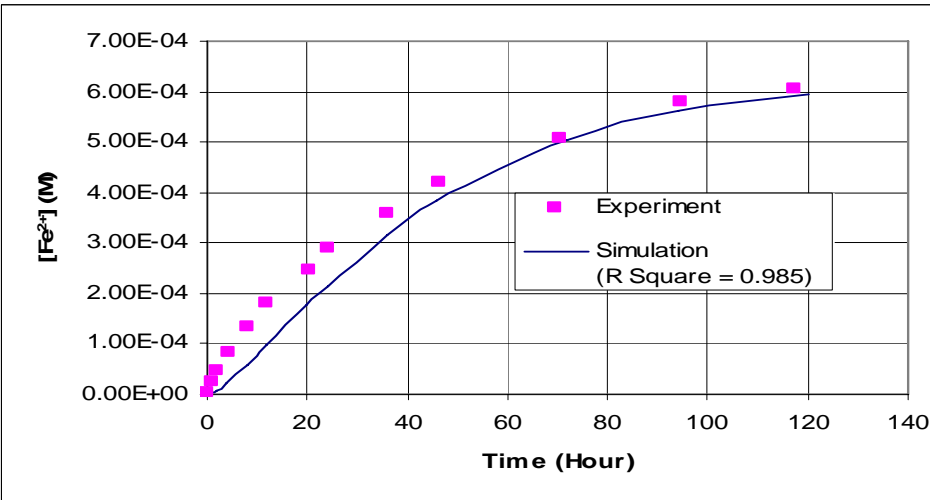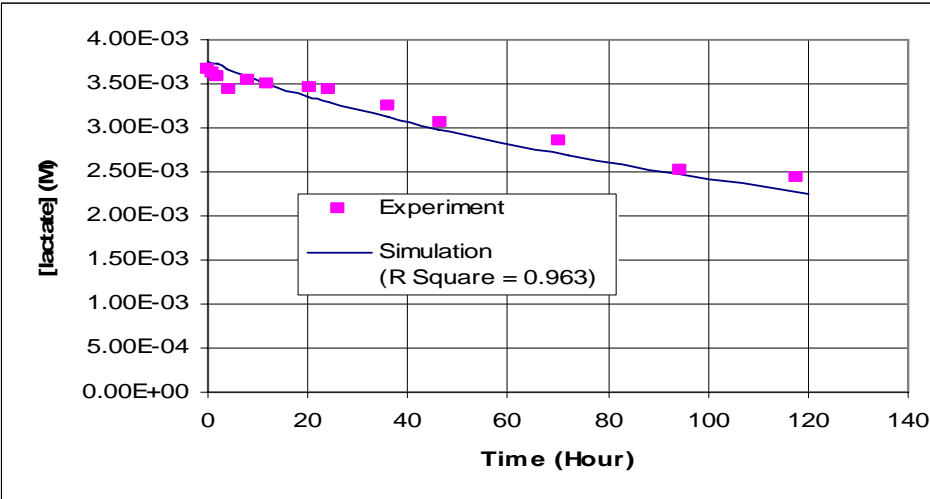
Figure 2.16: Simulation Results of the Second Proposed R1 Formulation for Exp. #5
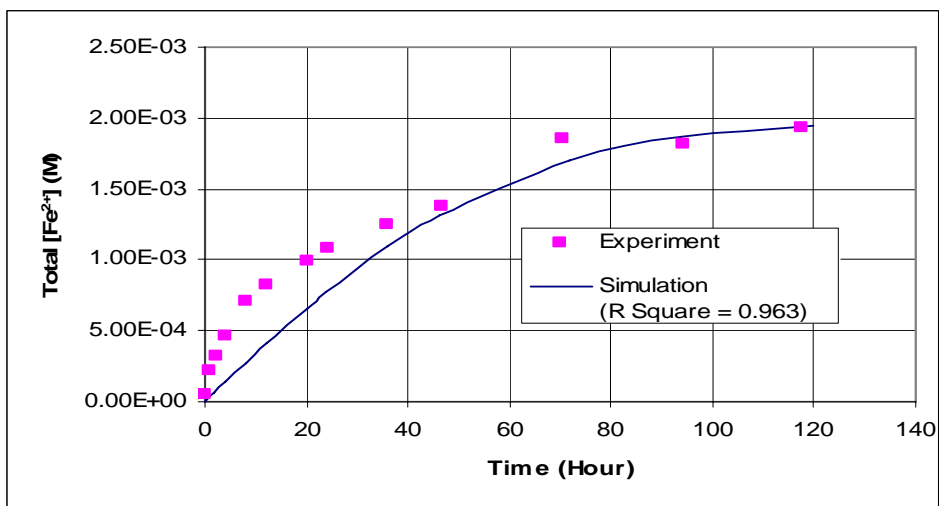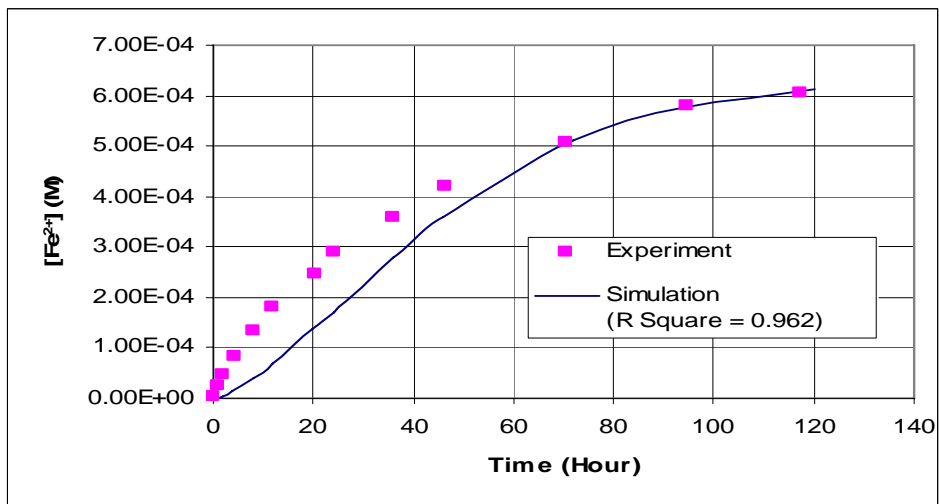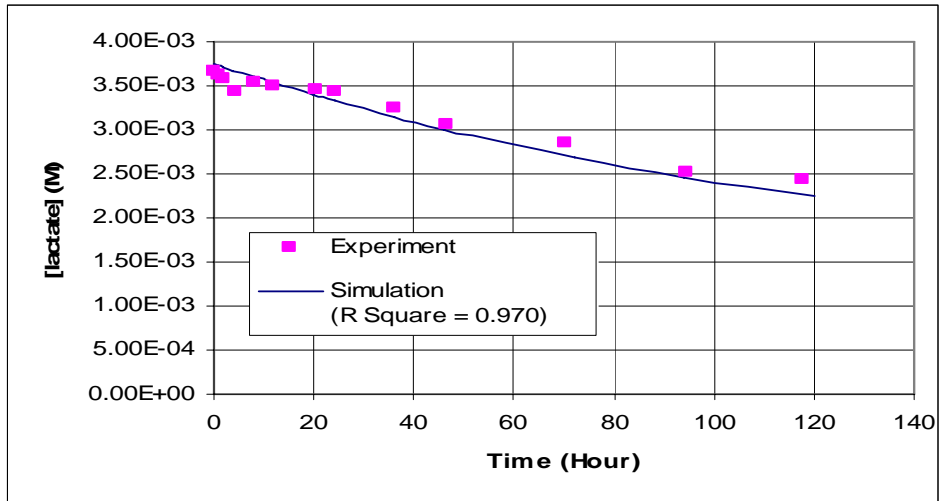
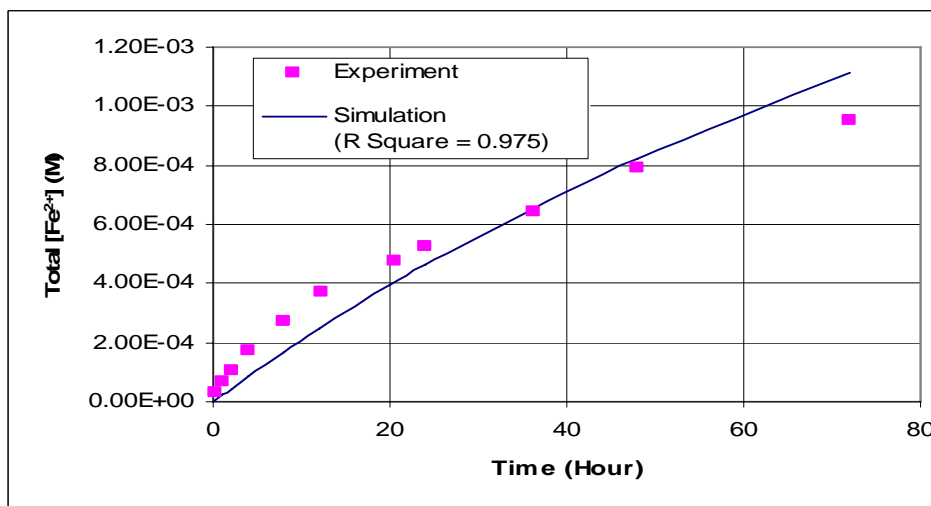Figure 2.17: Simulation Results of the Third Proposed R1 Formulation for Exp. #5
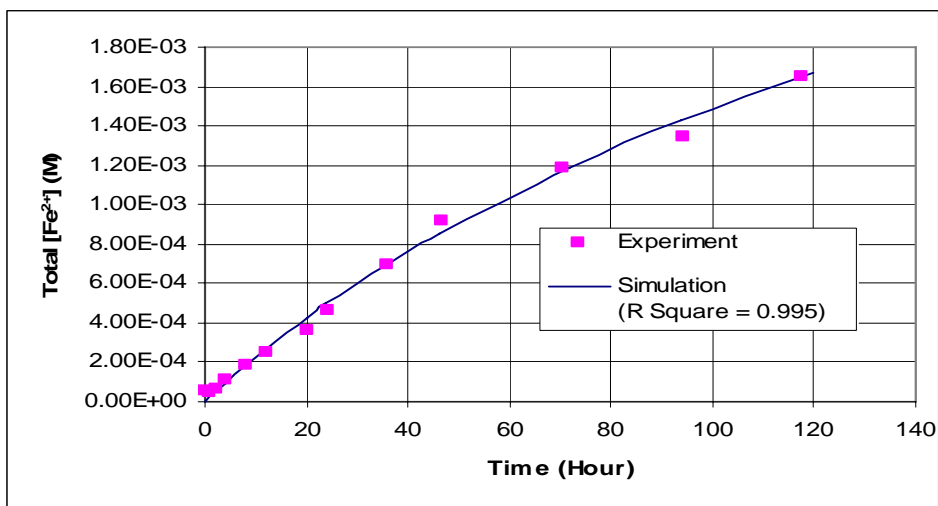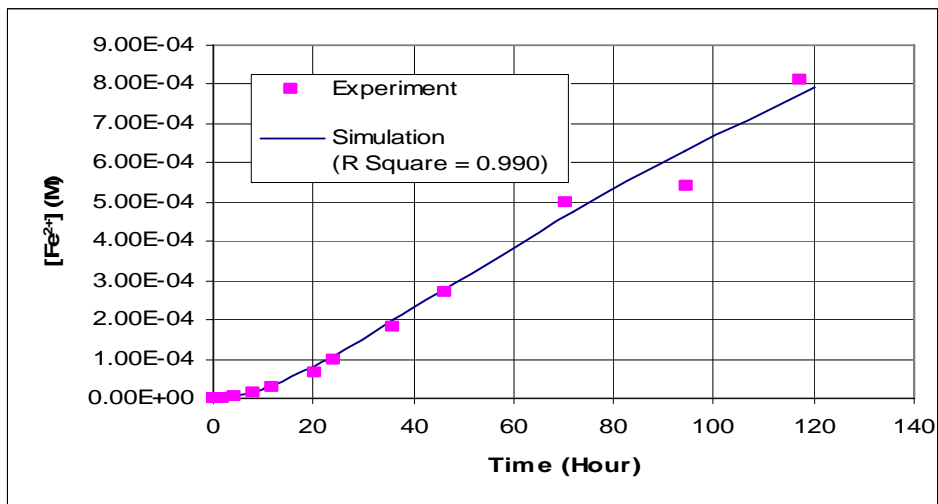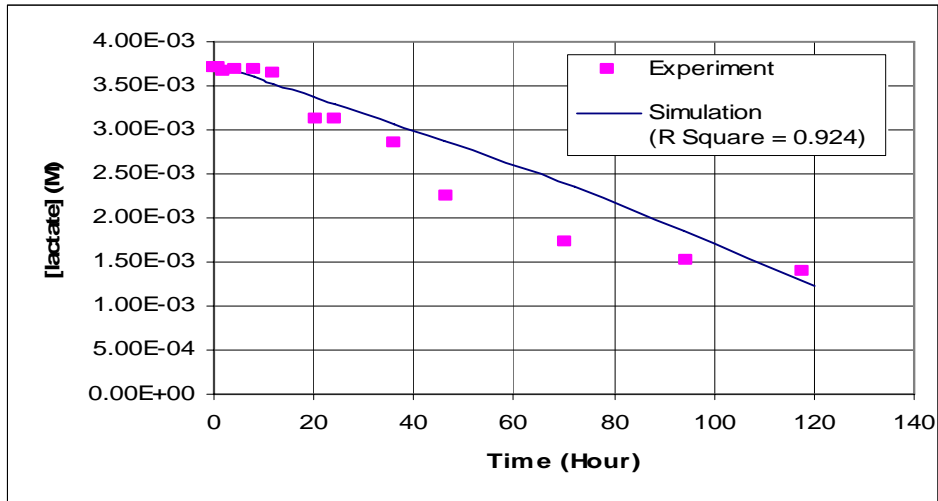
Figure 2.18: Simulation Results of the First Proposed R1 Formulation for Exp. #6

41
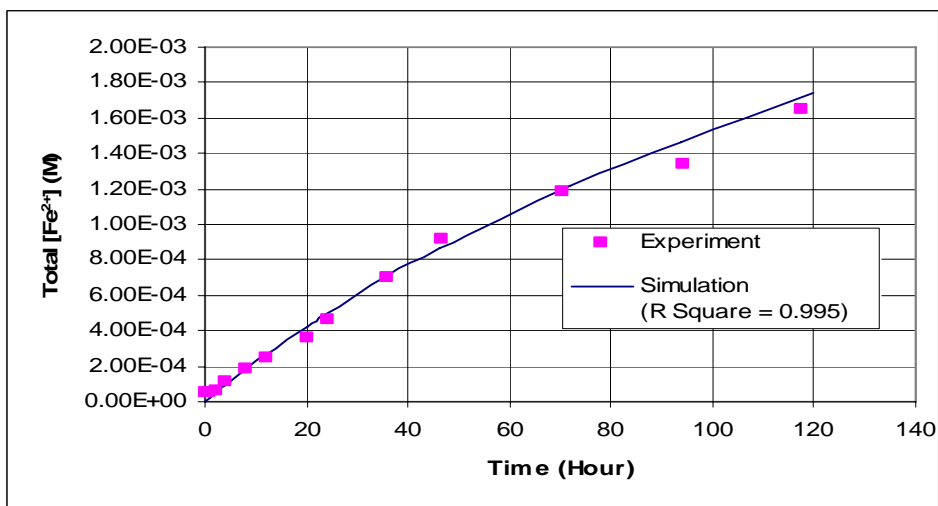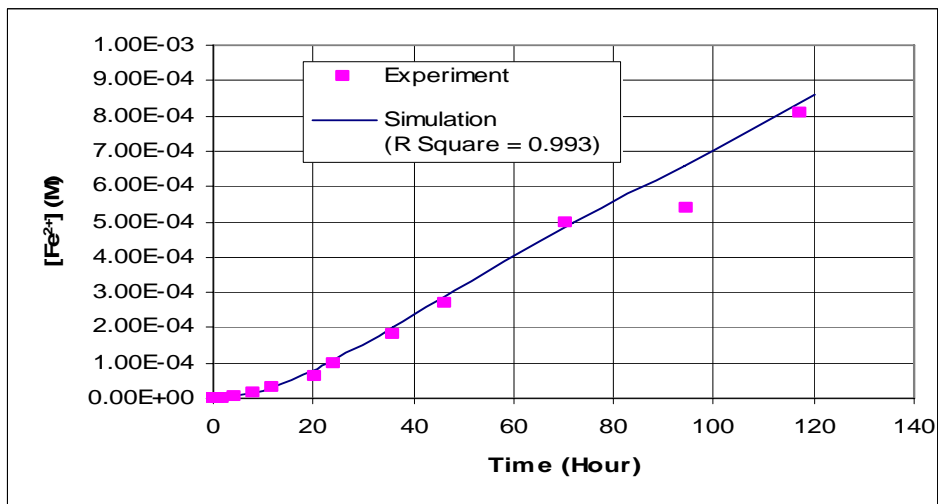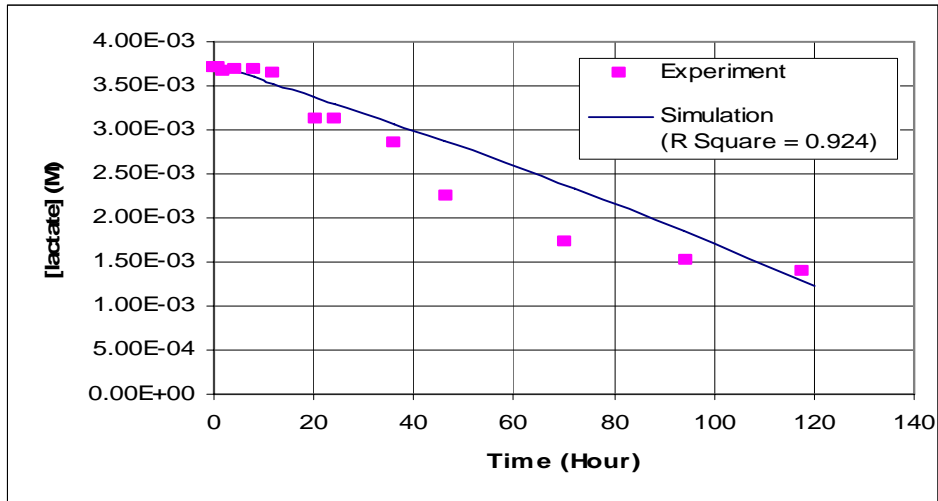
Figure 2.19: Simulation Results of the Second Proposed R1 Formulation for Exp. #6
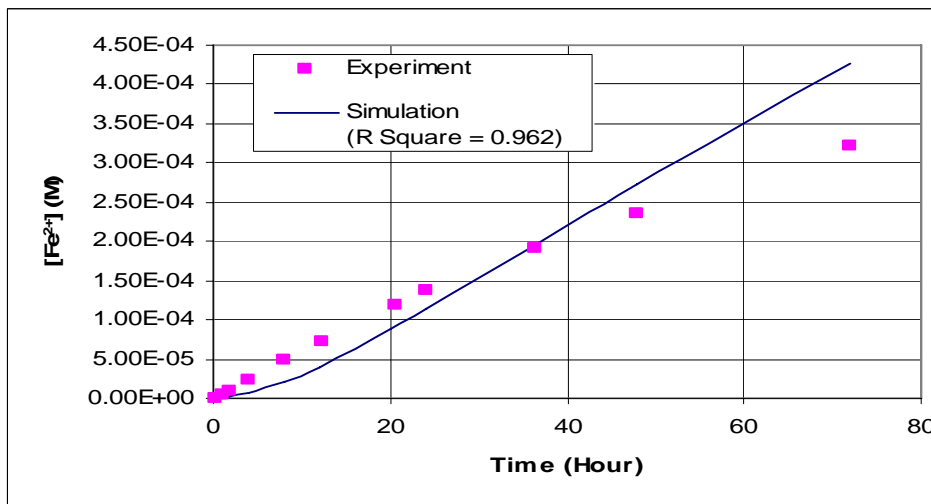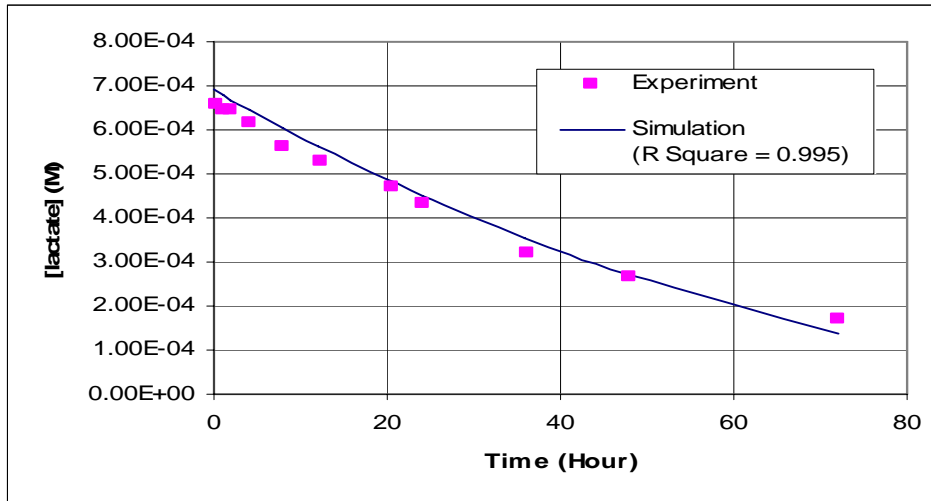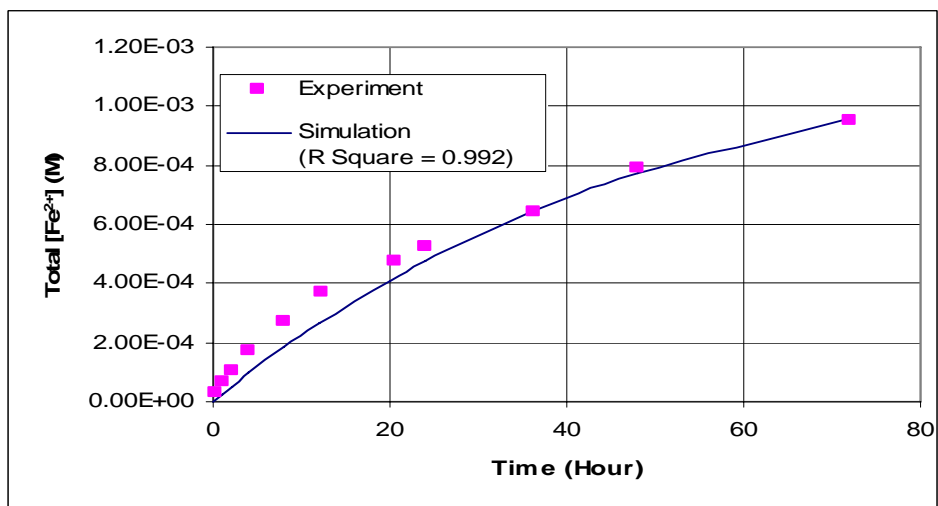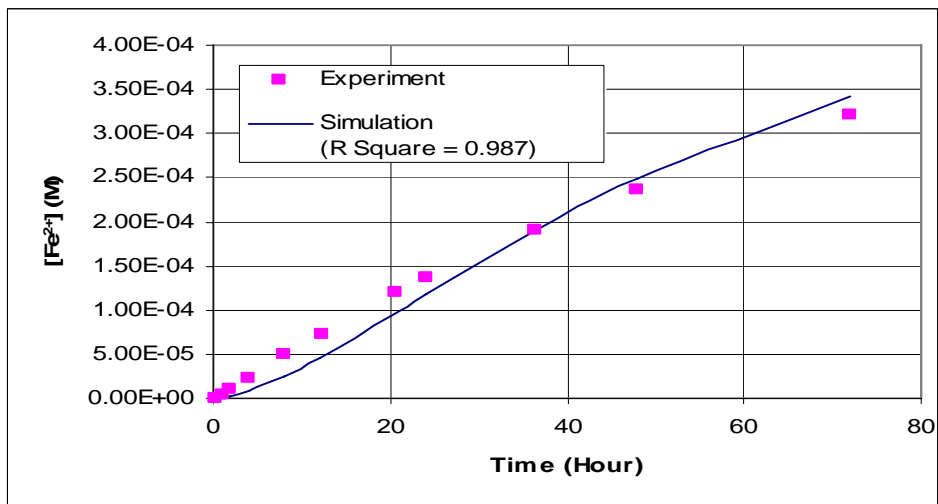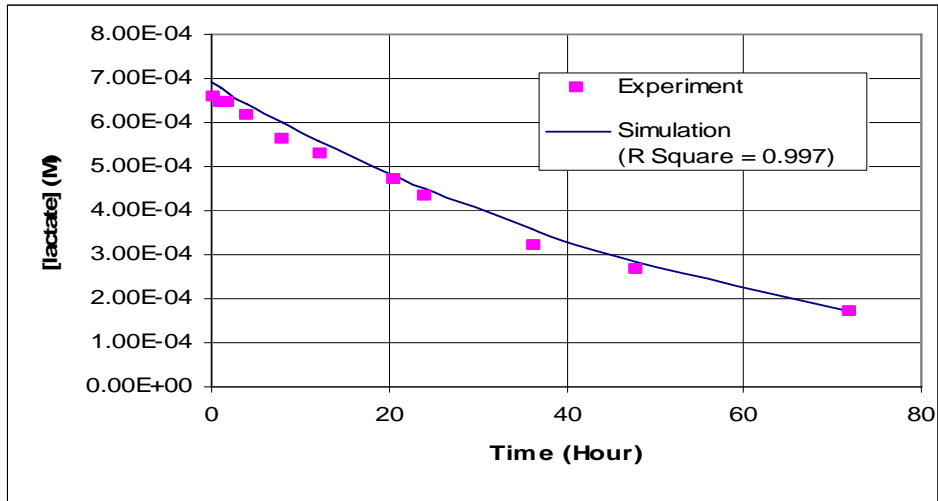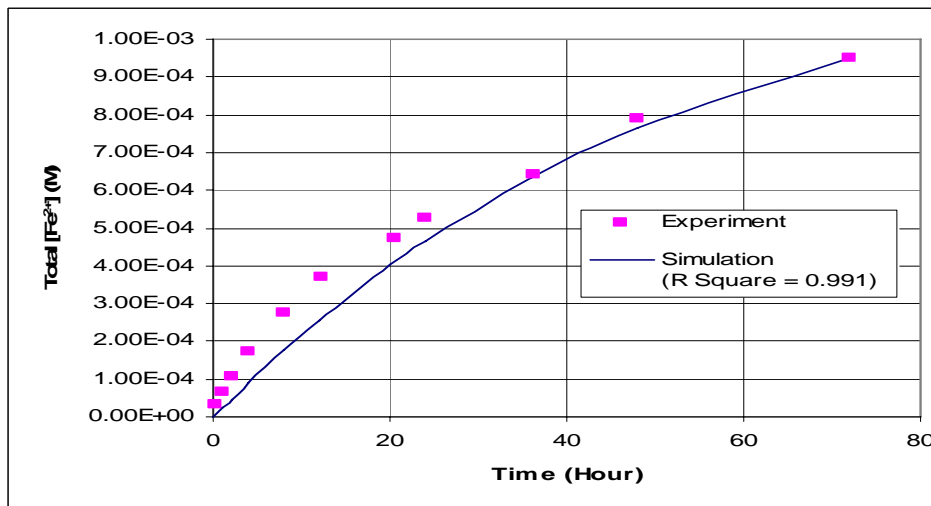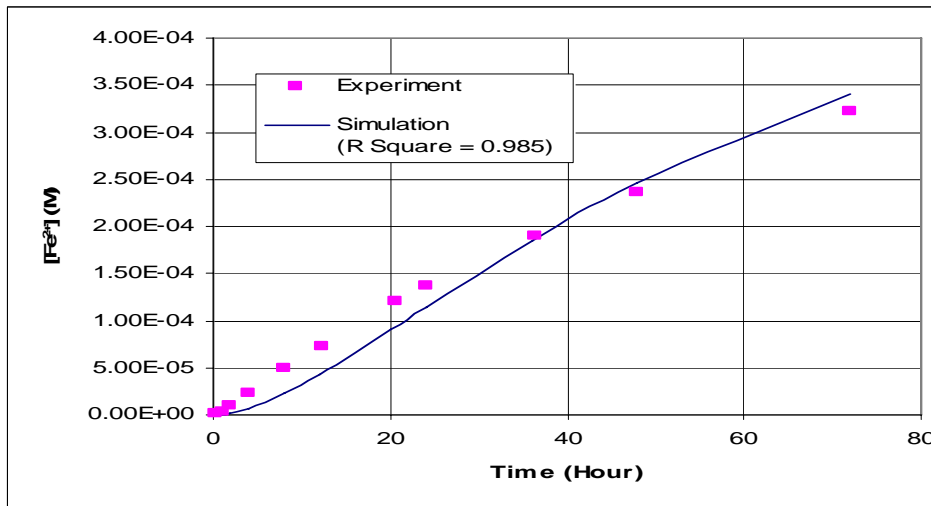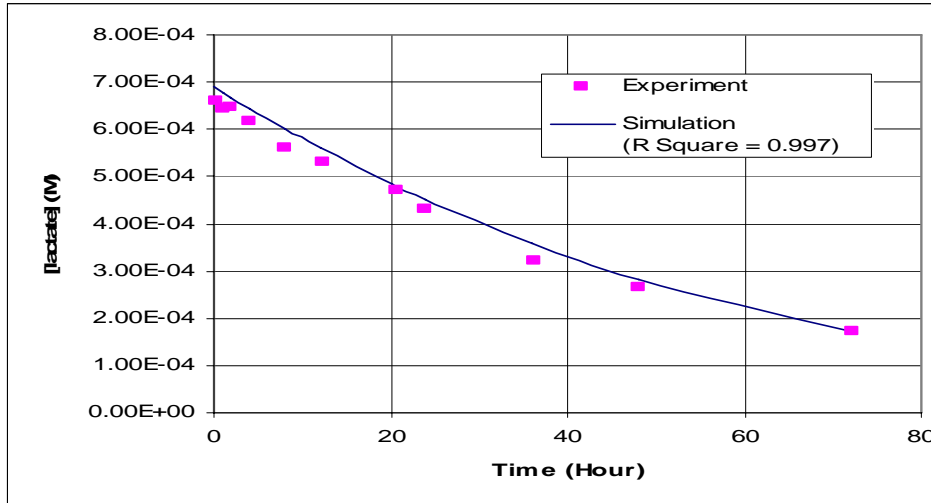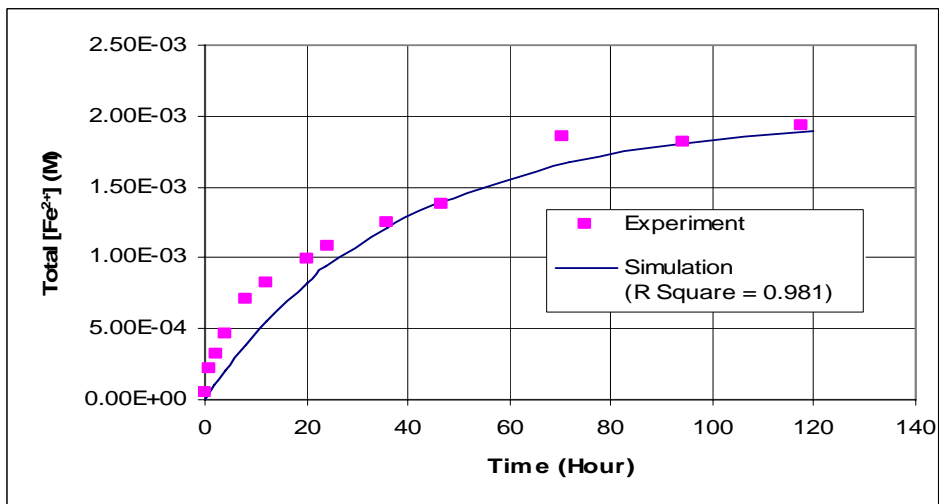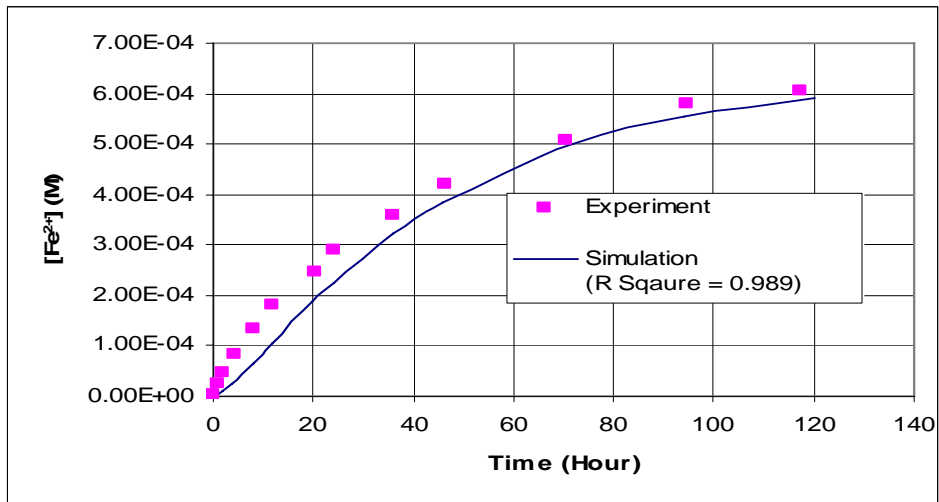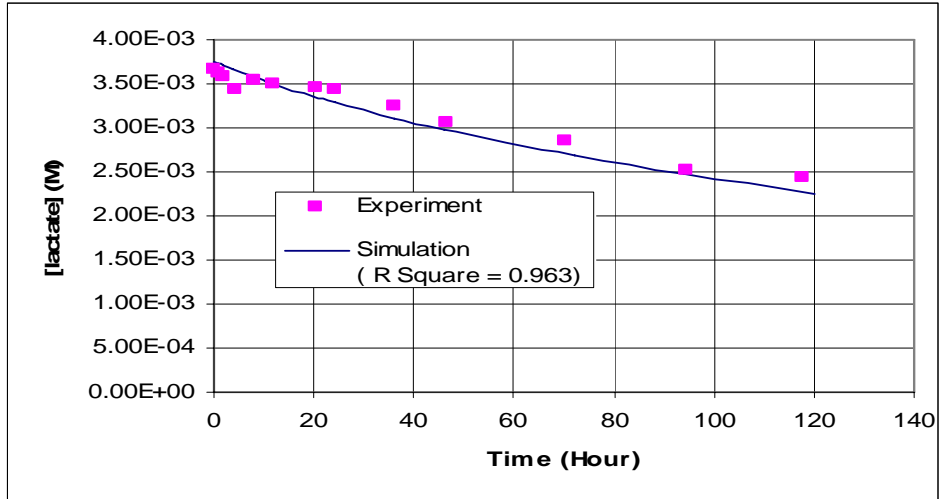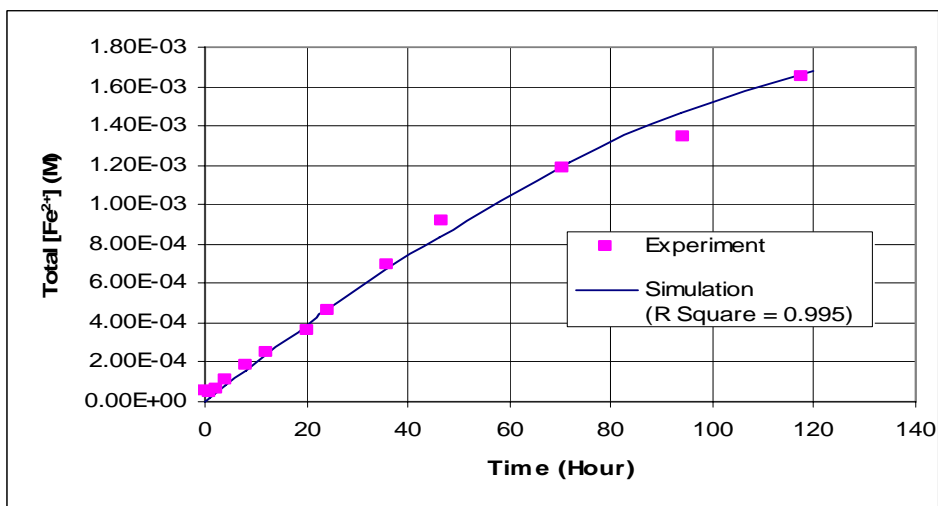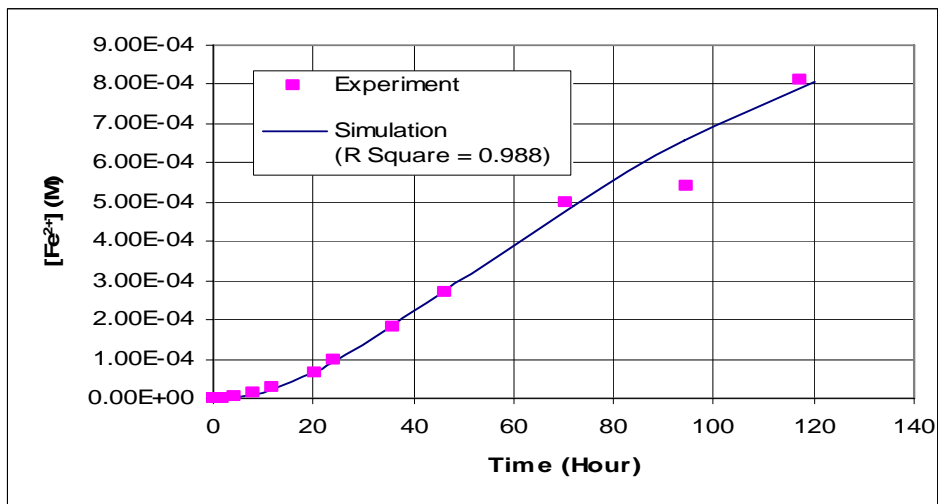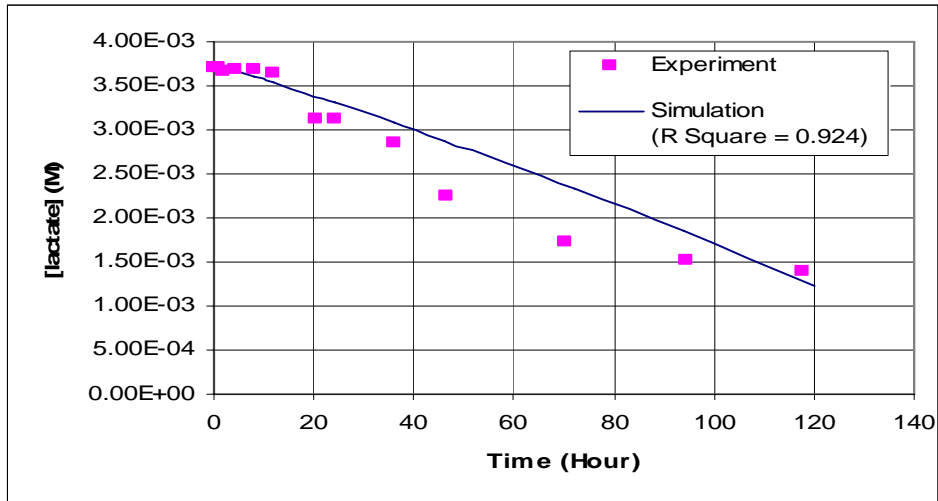
Figure 2.20: Simulation Results of the Third Proposed R1 Formulation for Exp. #6

2.4 Conclusion and Discussion

The biogeochemistry of microbial Fe(III) reduction and of associated contaminant interactions is very complicated, so an appropriate biogeochemical numerical model is needed to properly evaluate and design the bioreduction system of Fe(III); furthermore, using a model to determine the rate formulations and parameters of the reaction network is more convenient and economic than the statistical method because it is not necessary to measure all of the chemical species for using a reaction-based model.

Our primary objective of batch system is using a reaction-based biogeochemical model BIOGEOCHEM 1.0 to simulate the bioreduction kinetics of natural hematite-coated sand by dissimilatory metal-reducing bacterium (DMRB), *Shewanella putrefaciens* CN32, under growth conditions with lactate as the electron donor. This reactive system can be completely defined by a specifying reaction network (Yeh et al., 2001); therefore, we proposed a reaction network on Table 2.3 to describe the hematite bioreduction for our study, and further converted this reaction network into a matrix form. As a result, the equilibrium and kinetic reactions in the reaction network can be decoupled via Gauss-Jordan elimination into three subsets of equations: mass action equations for equilibrium reaction, kinetic-variable equations for kinetic reaction, and mass conservation equations. After the matrix decomposition, we can calculate all species' concentration with the experimental data; however, a "reliable" experimental data is extremely important because dispersive data will result in a bad fit of the reaction rate via fitting the curve of the kinetic-variable concentration-vs-time. Moreover, the experiments have to be carefully designed to satisfy minimum data need.

The most important task of the batch system simulation is to identify the rate formulations and parameters of the "bacterial reduction of hematite" (R1). Therefore, we proposed three possible rate formulations to describe the bioreduction rate of hematite and systemically determined each parameter for each rate formulation. These rate formulations and parameters were verified by comparing the results between simulation and experiment. A successful simulation using BIOGEOCHEM 1.0 would serve to validate the individual rate formulations and parameters and the overall theoretical approach. From Figure 2.12 to Figure 2.20, we can know that our proposed formulations with the determined parameters are reasonably good to express the R1 rate. However, the determined rate formulations and parameters should be also systematically tested with the column experiments by using a reactive biogeochemical transport model in order to further demonstrate these formulations/parameters and the hypothesis that mechanistic-based reaction rates of batch system can be scaled up and exported to column system.

CHAPTER 3:

SIMULATION AND EXPERIMENT IN COLUMN SYSTEMS

An important part of this research is to determine the reliability of batch simulations. We will do this by comparing the results from our batch simulations with column experiments. This chapter will describe the model, modeling approach, and the results of the column simulations.

3.1 Model Description

HYDROGEOCHEM 4.0 is an evolution of HYDROGEOCHEM 3.0 (Personal Communication). The major modifications of HYDROGEOCHEM 3.0 are the reformulation of the reactive chemistry calculations and the addition of a heat transfer module. HYDROGEOCHEM 4.0 is modified for generic application to reactive transport problems controlled by both kinetic and equilibrium reactions in subsurface media and incorporates heat transfer. As a result, HYDROGEOCHEM 4.0 is a comprehensive simulator of coupled fluid flow, hydrologic transport, heat transfer, and biogeochemical transport under variably saturated conditions in two dimensions.

In short, HYDROGEOCHEM 4.0 is a hydrologic transport model coupled with a reaction-based model, BIOGEOCHEM 2.0 (Yeh et al., 2005b). It is noted that BIOGEOCHEM 1.0 was designed for batch modeling while BIOGEOCHEM 2.0 was developed for coupling with hydrologic transport. The two versions are identical in theory and numerical approximations. They differ only in the code structure to facilitate

the coupling of BIOGEOCHEM 2.0 with hydrologic transport, so HYDROGEOCHEM 4.0 also includes the unique function that user can specify and program the reaction rate formulations into the code. Furthermore, this model can simulate complexation reactions, adsorption/desorption reactions, ion-exchange reactions, precipitation/dissolution reactions, reduction/oxidation, volatilization reactions, diffusion reactions, and sedimentation reactions.

HYDROGEOCHEM 4.0 runs on the DOS operating system and it requires two kinds of inputs: the run-stream input file names and the input data file. The input data file includes the geometry of the system, the spatial distribution of finite elements and nodes, the properties of the medium, reaction network, and the initial and boundary conditions. The program output includes the spatial distribution of pressure head, total head, velocity fields, moisture contents, temperature, and chemical concentrations as a function of time as well as the distribution of all chemical species at user-specified nodes.

Furthermore, the units of measure are: decimeter (dm) for length, mole for the mass for any chemical species, kg/dm^3 (kg/liter) for density, equivalents/mass for the ion-exchange capacity, kelvin (K) for temperature, and any units of time may be used as long as the time unit is consistent throughout the input file. Furthermore, the corresponding concentration unit of all species (aqueous, sorbed, and precipitated species) and the corresponding unit for the sorption distribution coefficient are mole/liter of fluid (Molar) and dm^3/kg (=ml/g), respectively.

3.2 Modeling Approach

HYDROGEOCHEM 4.0 is an accurate, efficient, and robust tool for solving the governing equation of fluid flow and reactive chemical transport; thus, using a reactive transport model is an easier and convenient way to demonstrate the hypothesis that mechanistic-based reaction rates of batch system can be scaled up and exported to a column system. Before using HYDROGEOCHEM 4.0 to simulate the reactive chemical transport, the formulations and parameters of the kinetic reactions must be given or determined via a reaction-based model. Also, the consistency of mass conservation equations and the assumptions regarding equilibrium reactions were assessed.

3.2.1 Theory and Mathematical Formulations

Finite difference method and finite element method are the most two common numerical methods used to reduce partial differential equations into the most basic form of the governing equations. HYDROGEOCHEM 4.0 uses the finite element method to solve the partial differential equations; the advantages and details of the finite element method can be found elsewhere (Yeh, 1999, 2000).

As mentioned in Chapter 2, a biogeochemical system is completely defined by specifying reaction networks, and the production-consumption rate of every species is out of the entire reactions which produce or consume that species. Therefore, the ordinary differential equations (equation 2.2 and 2.3) in a reactive batch system can be extended to the reactive transport system via replacing the ordinary equations with the transport equation as shown by Fan et al (2003):

$$\theta \frac{\partial C_i}{\partial t} - L(C_i) + QC_i = \theta \, r_i|_N = \sum_{k=1}^{N}(v_{ik} - \mu_{ik})R_k, \quad i \in M; \quad \text{where} \quad L(C_i) = \frac{\partial}{\partial x}(\theta D \frac{\partial C_i}{\partial X}) - v \frac{\partial C_i}{\partial x} \quad (3.1)$$

where θ is the effective moisture content, $r_i|_N$ is the production-consumption rate of the i-th species due to N biogeochemical reactions, C_i is the concentration of the i-th chemical species, t is time, L is the advection-dispersion/diffusion operator, Q is the flow rate, N is the number of biogeochemical reactions, v_{ik} is the reaction stoichiometry of the i-th species in the k-th reaction associated with the products, μ_{ik} is the reaction stoichiometry of the i-th species in the k-th reaction associated with the reactants, R_k is the rate of the k-th reaction, M is the number of chemical species, D is the hydrodynamic dispersion coefficient, x is the distance, and v is the velocity. Equation (3.1) is a statement of mass balance for any species in a transport system and can be converted into a matrix form for decomposing the reaction network.

3.2.2 Data Needs

The column experiments were conducted at Pennsylvania State University as well and focused on transient reactive transport under otherwise identical conditions, except that the flow rate was systematically varied. The specific flow rates and initial conditions for each column experiment are shown in Table 3.1, and the details and results are summarized in Appendix A (Morgan's work).

Table 3.1: Column Experimental Parameters

Columns	Average Flow Rate (ml/day)	Average Sand Weight (grams)	Initial Cell Concentration (cells/mL)
A-D	10.6	9.069	10^8
G-J	1.6	9.007	10^8
K-N	5.9	9.009	10^8

3.2.3 Modeling Processes

This section describes how to utilize HYDROGEOCHEM 4.0 to conduct the simulation for the transport of bioreduction of hematite and to test the determined rate formulations and parameters from the batch system. Before going through the detailed steps of the modeling procedure, an overview of procedure represented below is useful for understanding the column modeling.

1. Rate formulations and parameters of the reaction network were determined by the batch system via running BIOGEOCHEM 1.0.

2. The domain of interest of column is defined and divided into an appropriate amount of elements and nodes.

3. The basic characteristics (bulk density, pore volume, porosity et al.) of the porous medium are estimated from the column experimental setup and the tracer experimental data.

4. HYDROGEOCHEM 4.0 is employed to determine the longitudinal dispersivity of material via fitting the breakthrough curve of the tracer.

5. After obtaining all of the needed information, the combined information from batch and column system is then transferred into an input file for HYDROGEOCHEM 4.0 to model the concentration of each species at any node and time point that we would like to compare with experimental data.

6. Comparisons are made between the HYDROGEOCHEM 4.0 model simulations and the column experimental measurements.

Before conducting the column simulation, we have to define the domain of interest. According to the column experimental setup, the domain of interest has an inner diameter of 1 cm and 7.5 cm long. This region is packed with a concentration of bacteria of 10^8 cells/mL and 9 g of iron coated sand as shown in Figure 3.1. The bulk density of this region is 1.53 g/cm^3. We divided the domain into 30 equal size elements (0.25 cm long x 1 cm diameter each) corresponding 62 nodes revealed in Figure 3.1 as well.
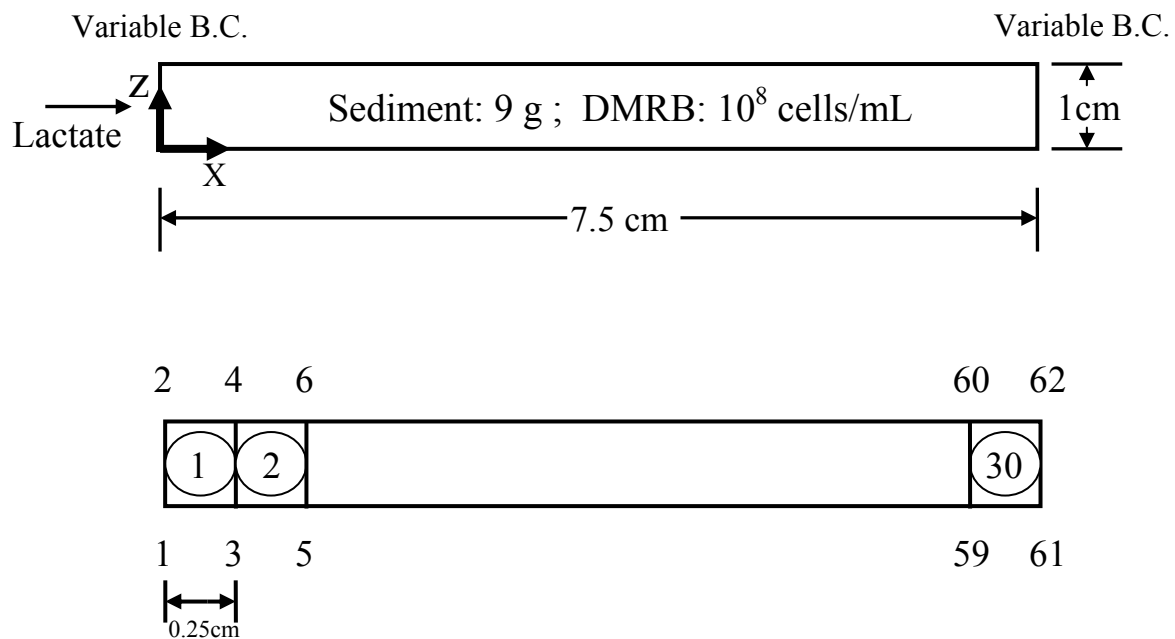
Figure 3.1: The Domain of Interest with the Initial Conditions (top) and the Discretization for the Domain (bottom)

From the breakthrough curve of tracer (Figure 3.2), we measured the pore volume of 4 mL and the porosity of 0.68 pore volume mL/bulk volume mL (at effluent concentration/influent concentration = 0.5), respectively. For determining the longitudinal dispersivity (Ld), the best approach is to plot the entire data set and the

theoretical breakthrough curve for a range of values of longitudinal dispersivity by modeling and then select the value that provides the best overall fit with the tracer experiment data. From Figure 3.2, we selected the value of 0.01 cm for the longitudinal dispersivity of the porous medium.
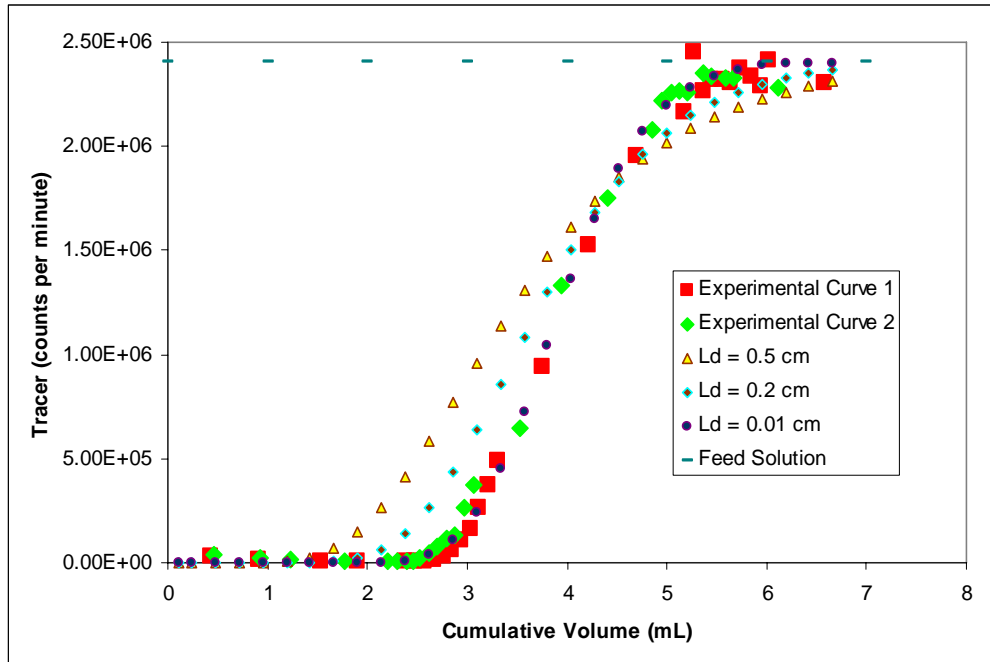
Figure 3.2: Fitting the Experimental Breakthrough Curve with Different Longitudinal Dispersivities

After obtaining the basic characteristics of the medium, we then create an input file including all information from batch and column system to model the hematite bioreduction transport. However, creating an input file for running HYDROGEOCHEM 4.0 is much more complicated than for BIOGEOCHEM 1.0. This is due to the consideration of chemical transport. The input data file for HYDROGEOCHEM 4.0 should indicate the geometry of the system, the spatial distribution of finite elements and

nodes, the properties of the media, reaction network, the initial condition, and the boundary conditions. Table 3.2 shows the important input parameters for our column simulation. After executing HYDROGEOCHEM 4.0 with the input file, the output file will automatically provide the concentration of each species at the specific nodes and time points that we would like to know. Finally, the results of simulation are compared with the experimental data to see if our determined formulations and parameters from batch system are reliable.

Table 3.2: Input Parameters for HYDROGEOCHEM 4.0

Parameter's Name	Value/Type
Number of time steps	5200
Time step size (hr)	0.1
Longitudinal dispersivity (dm)	0.001
Bulk density (kg/dm^3)	1.53
Moisture content (dimensionless)	0.68
Number of nodes	62
Number of elements	30
Number of species	13
Number of equilibrium reactions	2
Number of kinetic reactions	3
Absolute temperature (K)	293
Inflow velocity (dm/hr)	0.056; 0.0085; and 0.032
Boundary condition type	Variable boundary

3.3 Results of Column Simulation

In column simulation, we apply the formulations and parameters determined from batch system to HYDROGEOCHEM 4.0 to simulate the bioreduction of hematite with different flow rates. The reaction network of hematite bioreduction is also the same with batch system. The results of column simulation will be represented in the following sections.

3.3.1 Formulations and Parameters for Column Simulation

Before dealing with the column simulation, we need to identify the formulations and parameters for the chemical reaction rates. In batch system, we defined R1 and R4 as kinetic reactions and defined R2, R3, and R5 as equilibrium reactions; however, in column system we have to change the second reaction, surface hydration of hematite, into a kinetic reaction. The reason is that in column system not all of the hematite surface sites react with water at the same time. In other words, the surface sites of hematite picked in the column do not contact with the influent solution simultaneously because the influent solution does not permeate throughout the entire column immediately. Therefore, the equation (2.24) for R2 is modified as:

$$R_2 = K_{fw}[Fe_2O_3] - K_{bw}([\equiv FeOOH] + [\equiv FeOOFe(II)^+]); \text{ where } \frac{K_{fw}}{K_{bw}} = K_{TSS}^e \qquad (3.2)$$

$$K_{TSS}^e[Fe_2O_3] = [\equiv FeOOH] + [\equiv FeOOFe(II)^+] \qquad (2.24)$$

where K_{fw} is the forward rate constant, K_{bw} is the backward rate constant, and K_{TSS}^e is the "lumped" equilibrium constant for the total surface sites. The forward rate constant divided by the backward rate constant must equal the equilibrium constant. Therefore, in the column system the rate of R2 eventually will reach the identical equilibrium situation with batch system. In Chapter 2 we calculated the value of 0.125 for K_{TSS}^e; thus, in column simulation the quotient of the forward rate constant to the backward rate constant should equal 0.125.

The main purpose of column simulation is to examine the formulations and parameters determined from batch system. With the exception of the formulation of R2, the rate

formulations are the same as the batch simulation. In addition, the parameters arranged in Table 2.6 for individual batch experiment have to be identically input into the column simulation in order to inspect the accuracy of the resolved parameters and our proposed rate formulations.

3.3.2 Reaction Matrix Decomposition

The reaction network can be converted into a matrix form by HYDROGEOCHEM 4.0, decoupling the equilibrium and kinetic reactions of the reaction network. After the matrix decomposition, we obtain eleven kinetic-variable equations and two equilibrium equations. The kinetic-variable equations are represented as follows:

$$\frac{d\left(\left[Fe_2O_3\right]\right)}{dt} = -2R_1 - R_2 \tag{3.3}$$

$$\frac{d\left(\left[lacetate^-\right]\right)}{dt} = -R_1 - 5R_4 \tag{3.4}$$

$$\frac{d\left(\left[H^+\right] + [Fe^{2+}] - [PIPES^-]\right)}{dt} = -3R_1 + 5R_4 \tag{3.5}$$

$$\frac{d\left(\left[acetate^-\right]\right)}{dt} = R_1 + 5R_4 \tag{3.6}$$

$$\frac{d\left(\left[HCO_3^-\right]\right)}{dt} = R_1 + 4R_4 \tag{3.7}$$

$$\frac{d\left(-[Fe^{2+}] + [\equiv FeOOH]\right)}{dt} = -4R_1 + 2R_2 \tag{3.8}$$

$$\frac{d\left([Fe^{2+}] + [\equiv FeOOFe(II)^+]\right)}{dt} = 4R_1 \tag{3.9}$$

$$\frac{d([CO_2])}{dt} = -4R_4 \qquad (3.10)$$

$$\frac{d([NH_4^+])}{dt} = -R_4 \qquad (3.11)$$

$$\frac{d([DMRB])}{dt} = R_4 \qquad (3.12)$$

$$\frac{d([HPIPES]+[PIPES^-])}{dt} = 0 \qquad (3.13)$$

In addition, one mass action equation and one user specified rate formulation were used to describe the equilibrium equations. The user specified formulation is the same as equation (2.27), and the mass action equation is identical to equation (2.23); they are represented as follows:

$$\frac{[PIPES^-][H^+]}{[HPIPES]} = K_5^e = 10^{-6.8} \qquad (2.23)$$

$$[\equiv FeOOFe(II)^+] = K[Fe^{2+}]^n \qquad (2.27)$$

3.3.3 The Simulation Results

Column simulations were assigned to further demonstrate the reliability of formulations and parameters determined from the batch system. Three proposed rate formulations for R1 in batch simulation were tested under the same condition to see which one could provided the best overall fit with the experimental data: (1) a physically-based formulation proposed to be first-order with respect to "free" hematite surface sites, $\equiv$FeOOH (equation 2.28), (2) a dual Monod kinetic rate formulation with respect to the

concentrations of lactate and $\equiv$FeOOH (equation 2.29), and (3) a dual Monod kinetic with inhibition rate formulation relative to the concentrations of lactate, $\equiv$FeOOH, and Fe^{2+} (equation 2.30). In addition, a formal bacteria growth kinetic with cell decay (equation 2.31) described R4 rate formulation was also verified via column simulation. Figure 3.3 to 3.11 display the results of simulation contrasted with the column experimental data simultaneously.

As mentioned above, we changed the R2 rate formulation from an equilibrium to a kinetic reaction (equation 3.2); therefore, we should go back to check if equation 3.2 is applicable to the batch system in order to demonstrate the reliability of our assumption. This iterative examination is a very important procedure to justify the consistency of our entire simulations between batch and column system. We employed the data of batch experiment #4 to make the comparison between equilibrium R2 rate formulation and kinetic R2 rate formulation under the same circumstance. The forward rate constant, K_{fw}, and the backward rate constant, K_{bw}, for equation 3.2 are 0.03 hr^{-1} and 0.24 hr^{-1}, respectively. As a result, the "lumped" equilibrium constant, K_{TSS}^{e}, for the total surface sites in equation 3.2 is the same value (0.125) as the batch system. The compared results are shown in Figure 3.12 to 3.14.
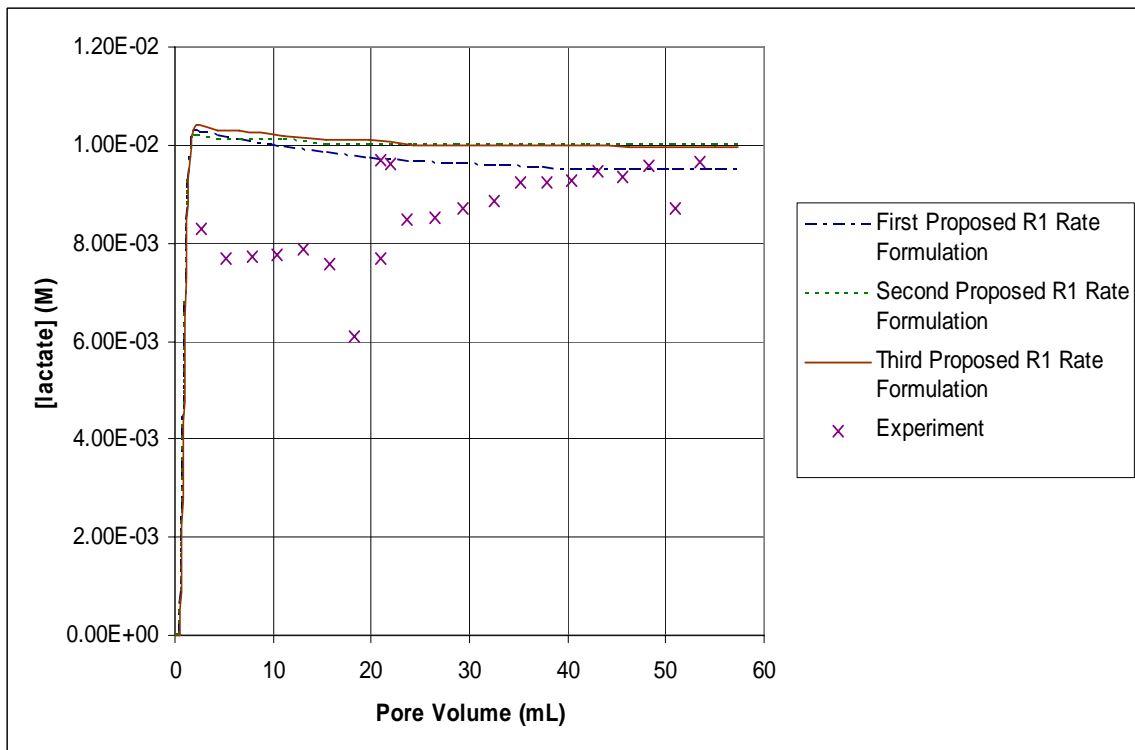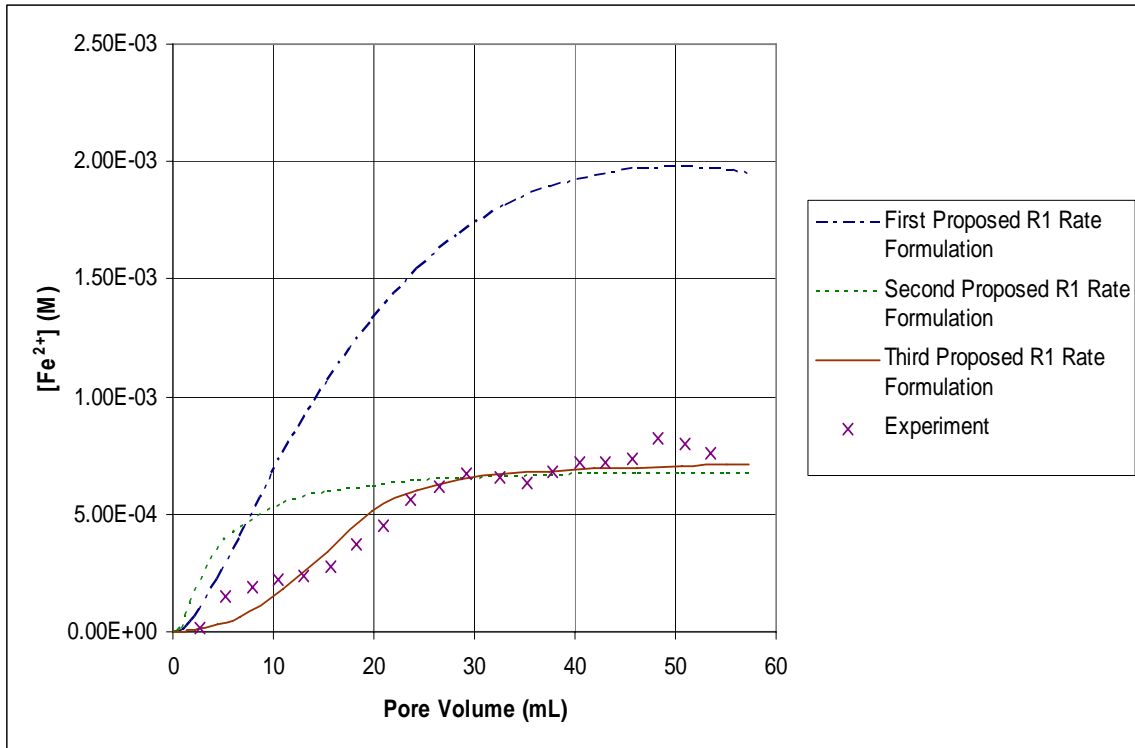
Figure 3.3: Simulation Results for Column A-D (Q=10.6 ml/day) and Parameters
Determined from Batch Experiment #4
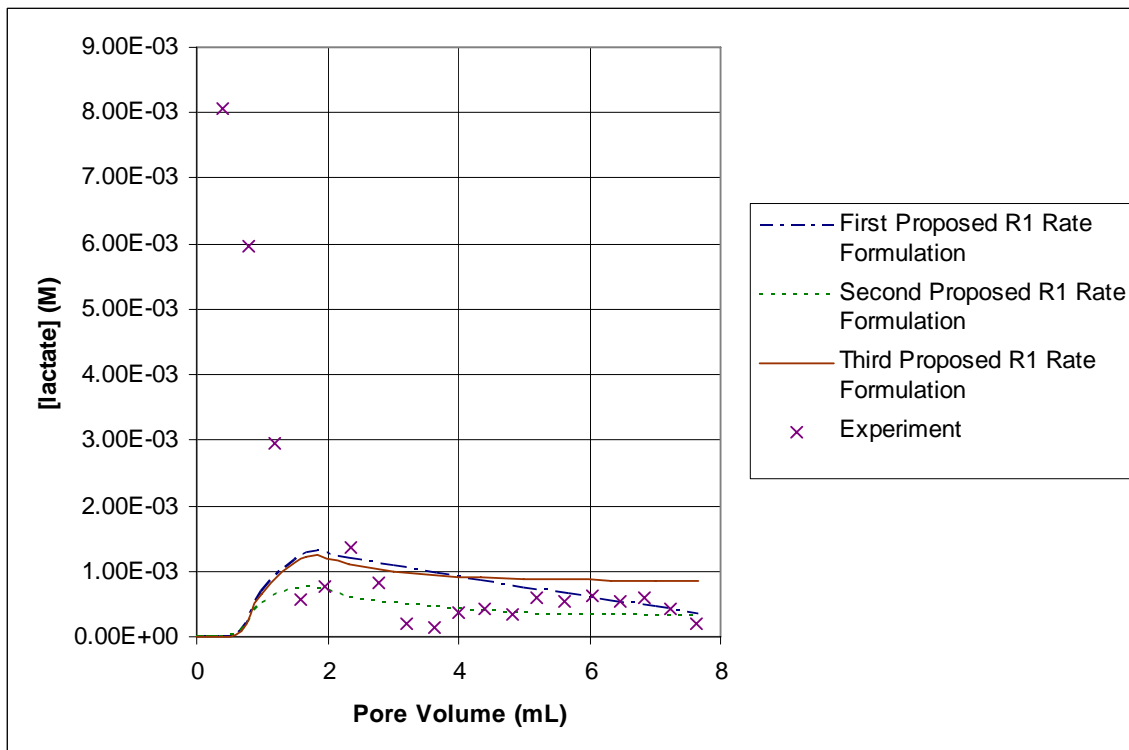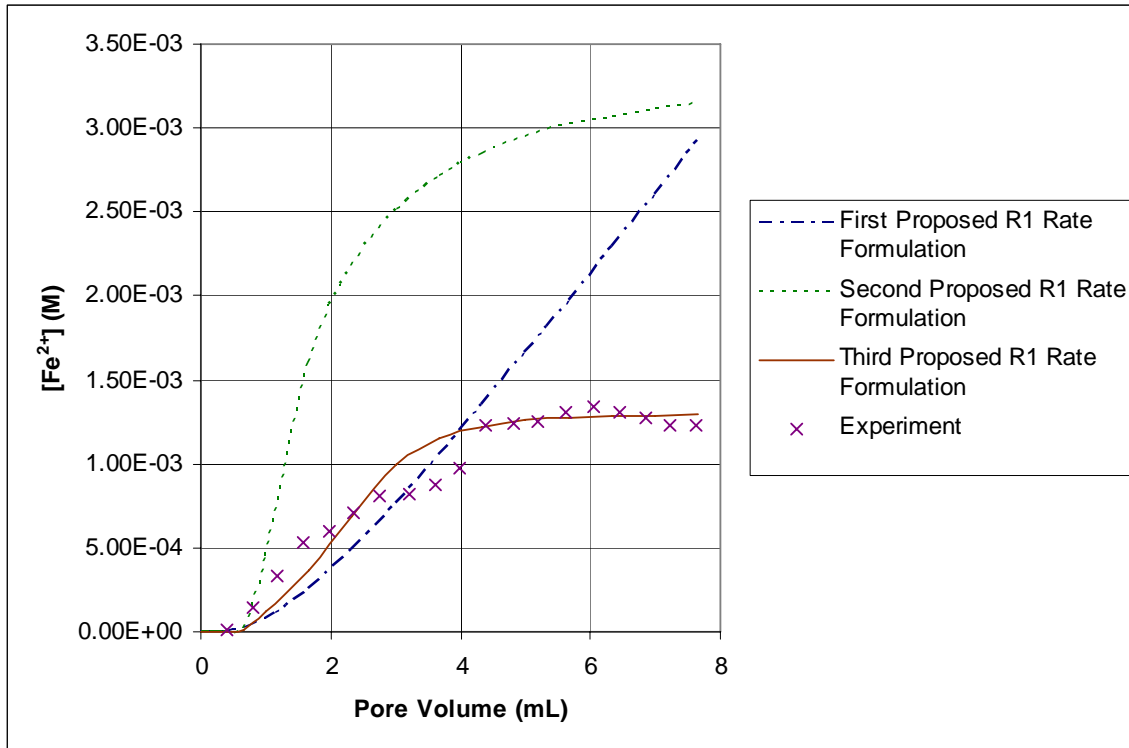
Figure 3.4: Simulation Results for Column G-J (Q=1.6 ml/day) and Parameters
Determined from Batch Experiment #4
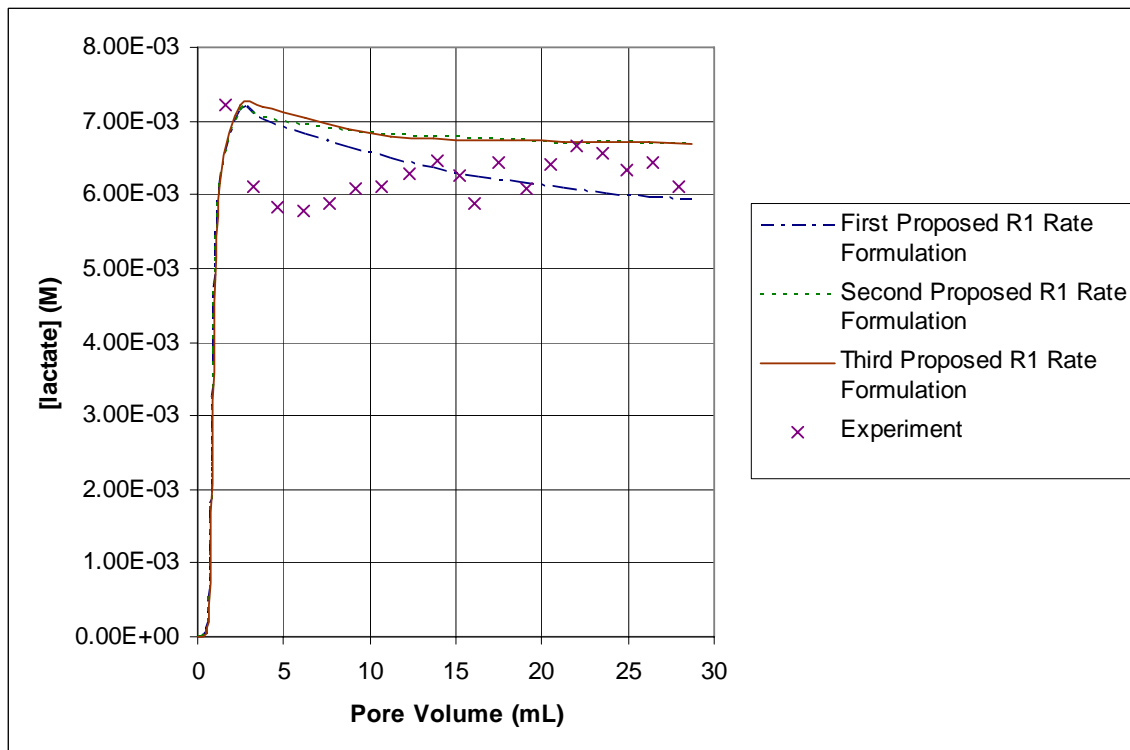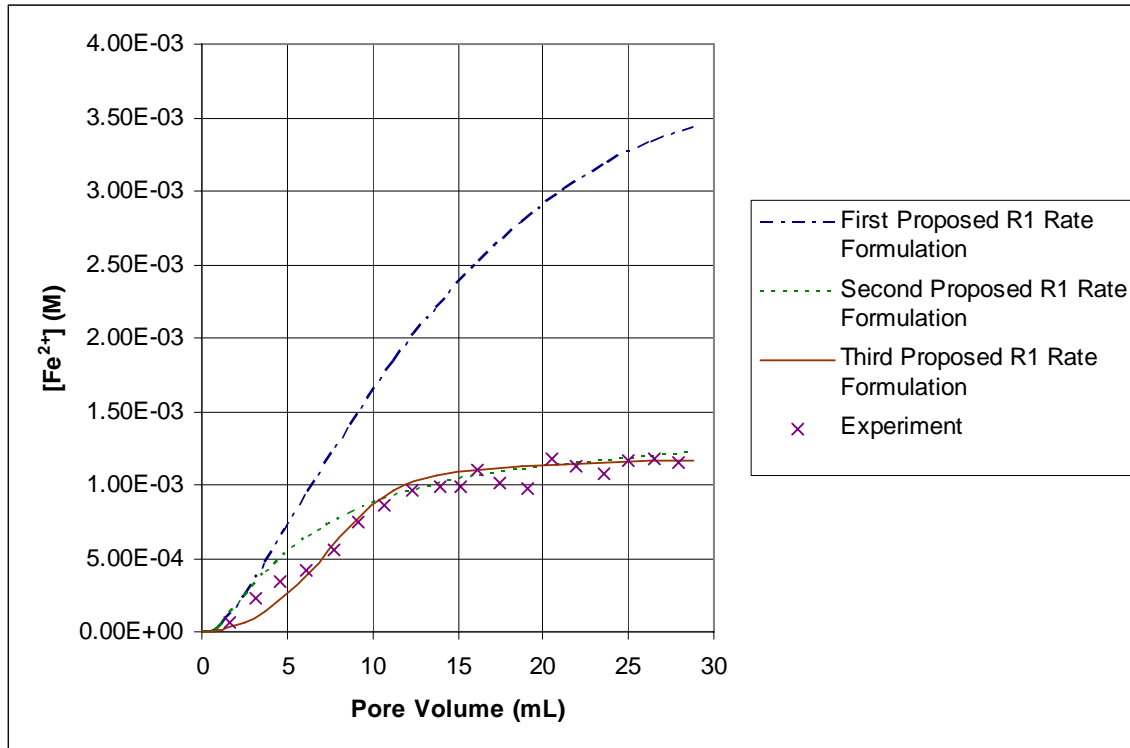
Figure 3.5: Simulation Results for Column K-N (Q=6 ml/day) and Parameters
Determined from Batch Experiment #4

60
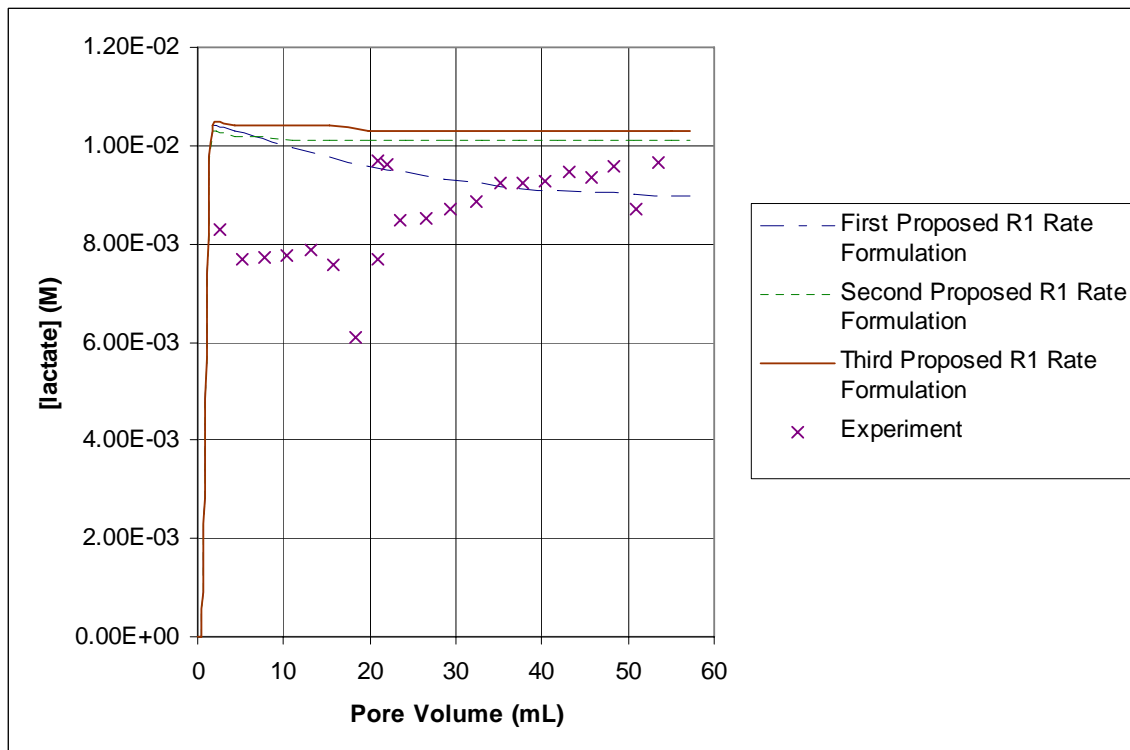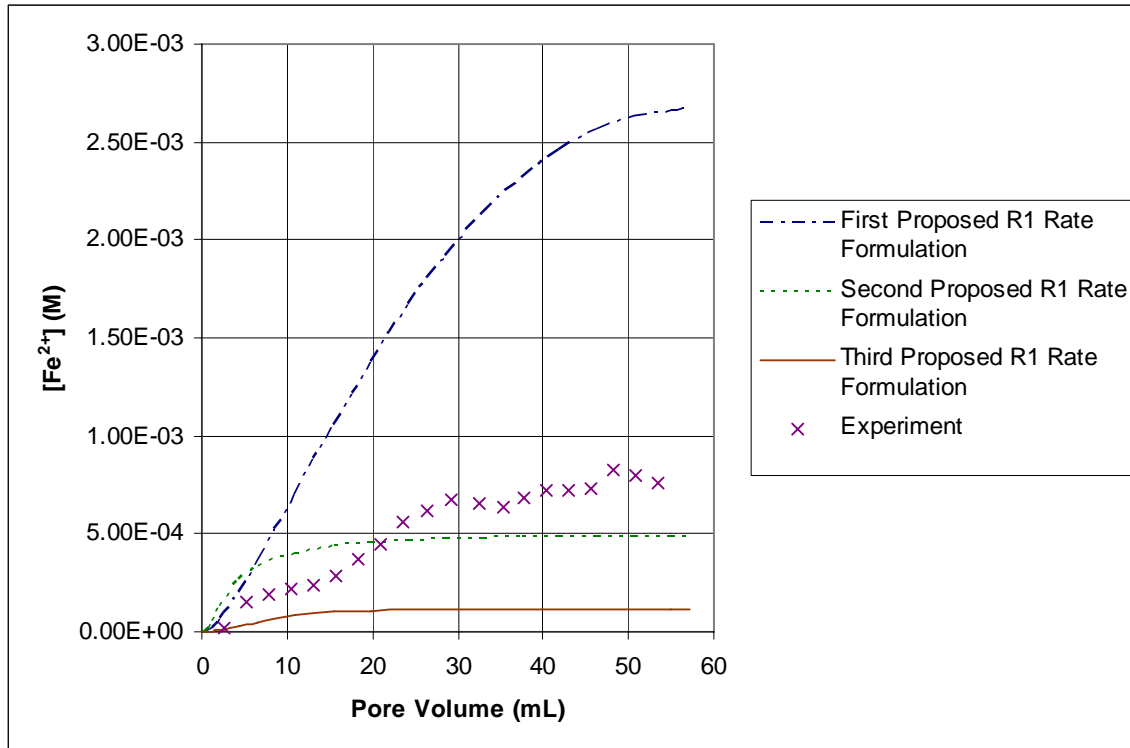
Figure 3.6: Simulation Results for Column A-D (Q=10.6 ml/day) and Parameters
Determined from Batch Experiment #5
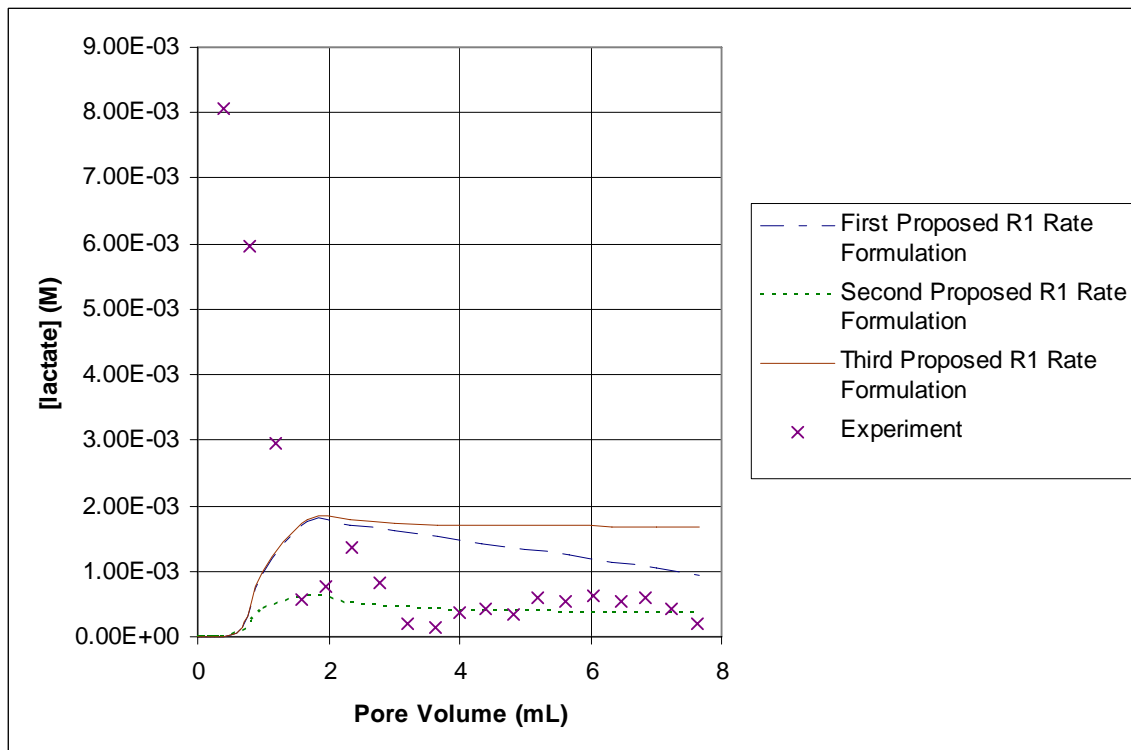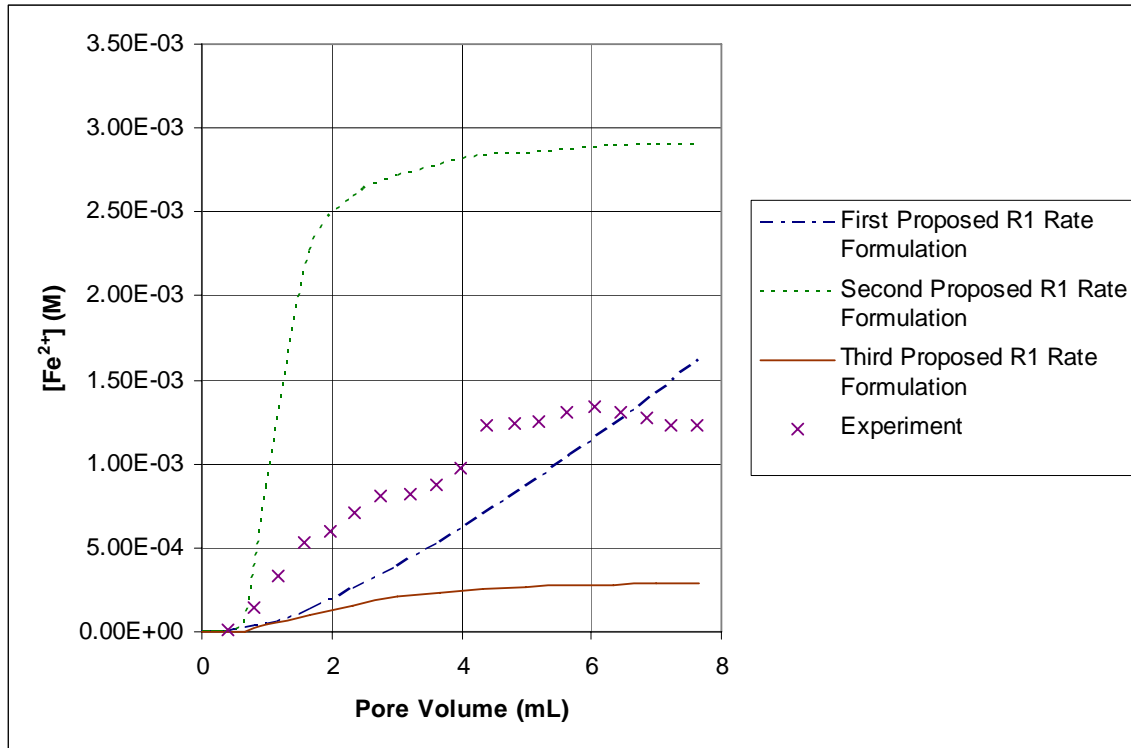
Figure 3.7: Simulation Results for Column G-J (Q=1.6 ml/day) and Parameters
Determined from Batch Experiment #5
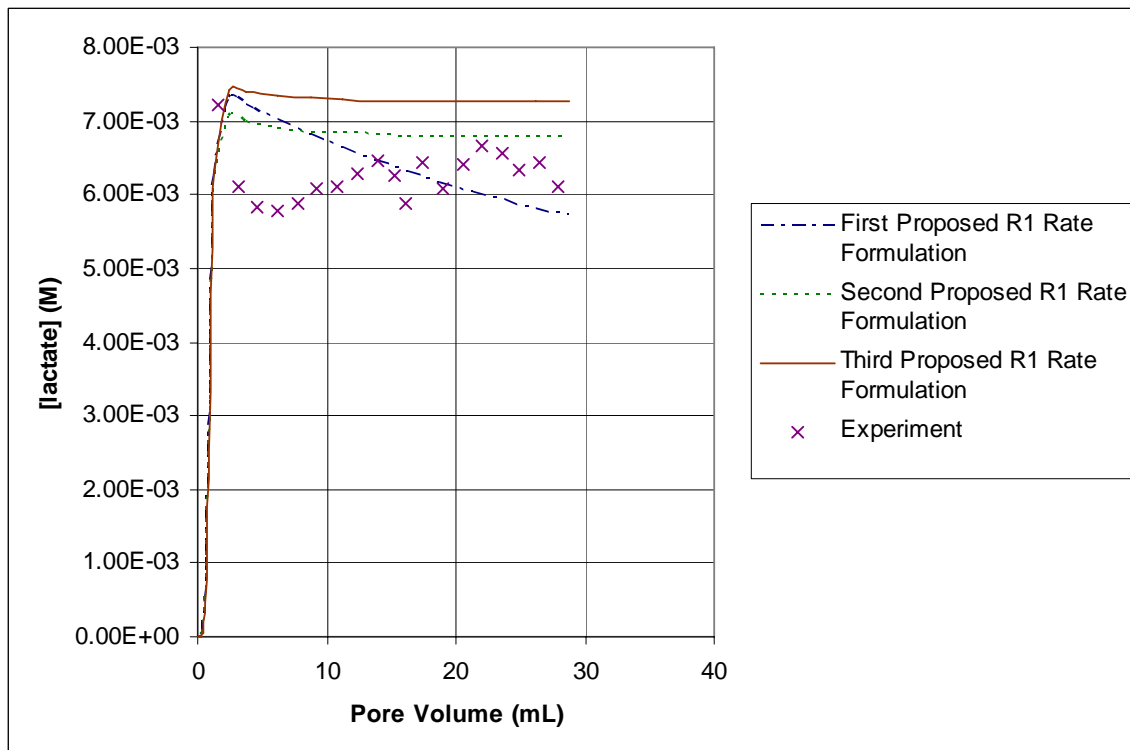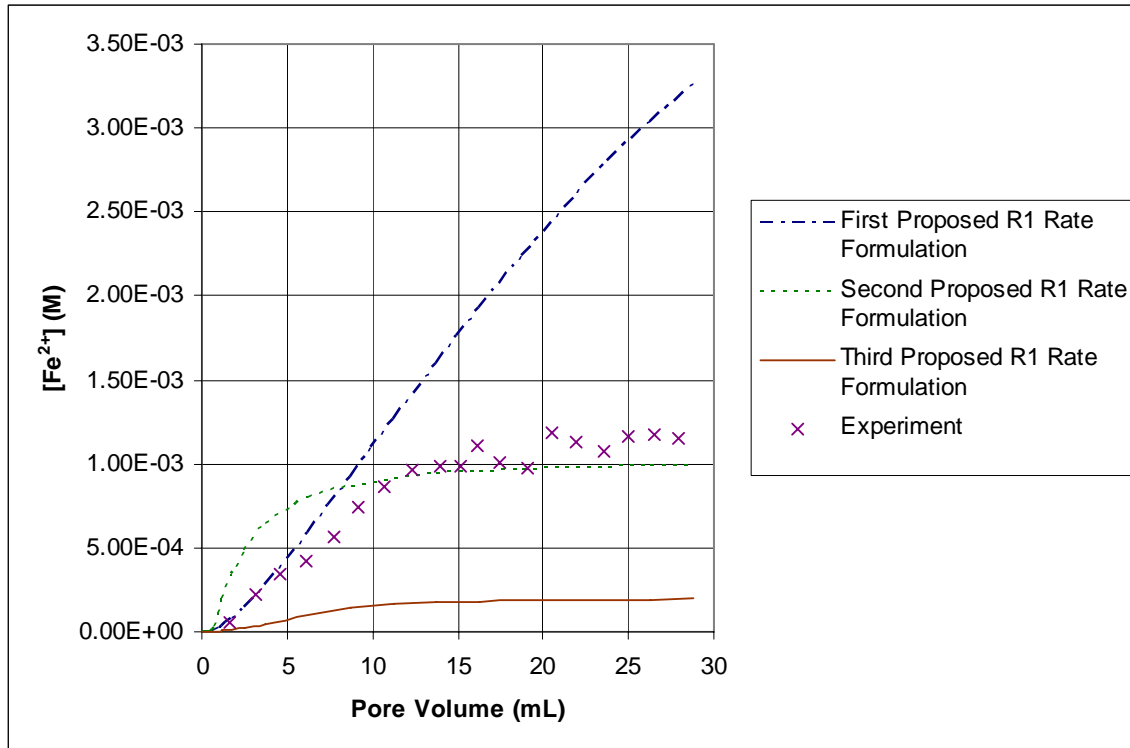
Figure 3.8: Simulation Results for Column K-N (Q=6 ml/day) and Parameters
Determined from Batch Experiment #5
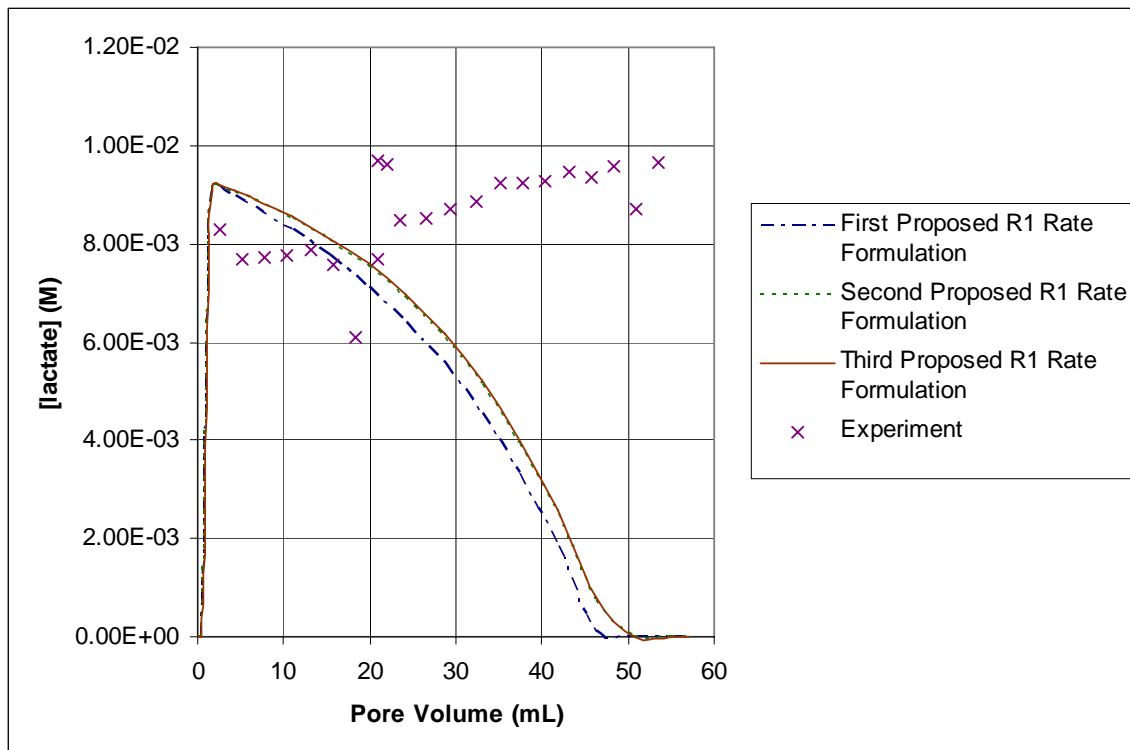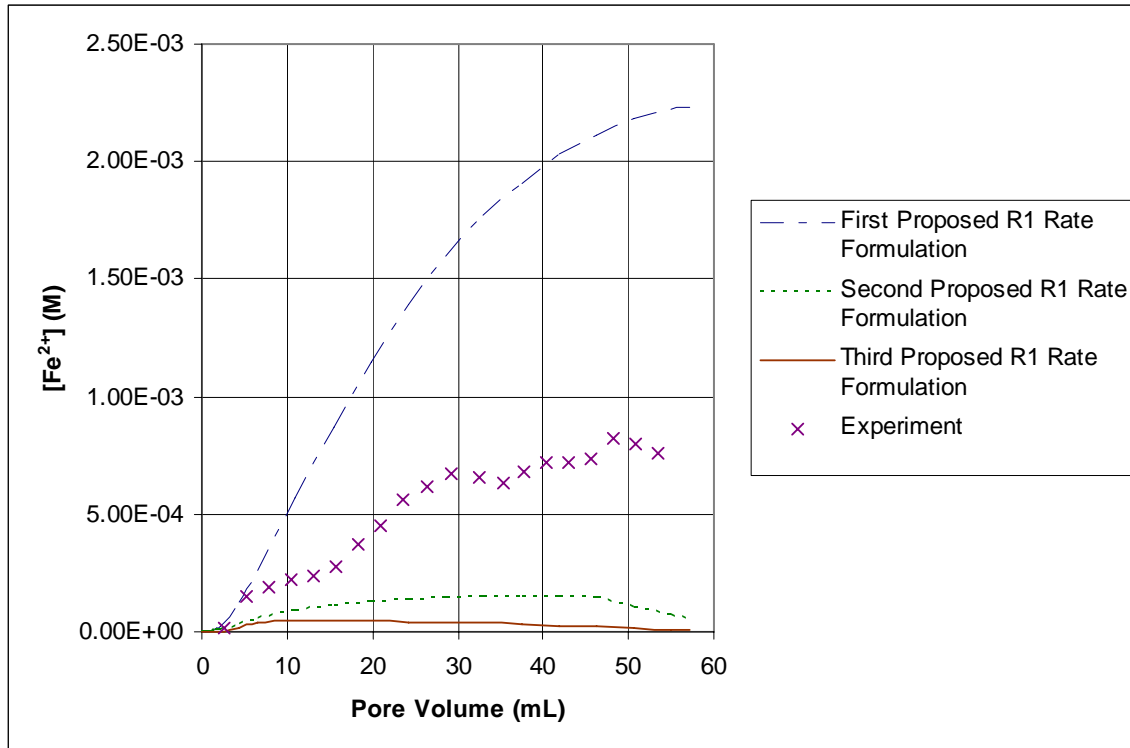
Figure 3.9: Simulation Results for Column A-D (Q=10.6 ml/day) and Parameters
Determined from Batch Experiment #6
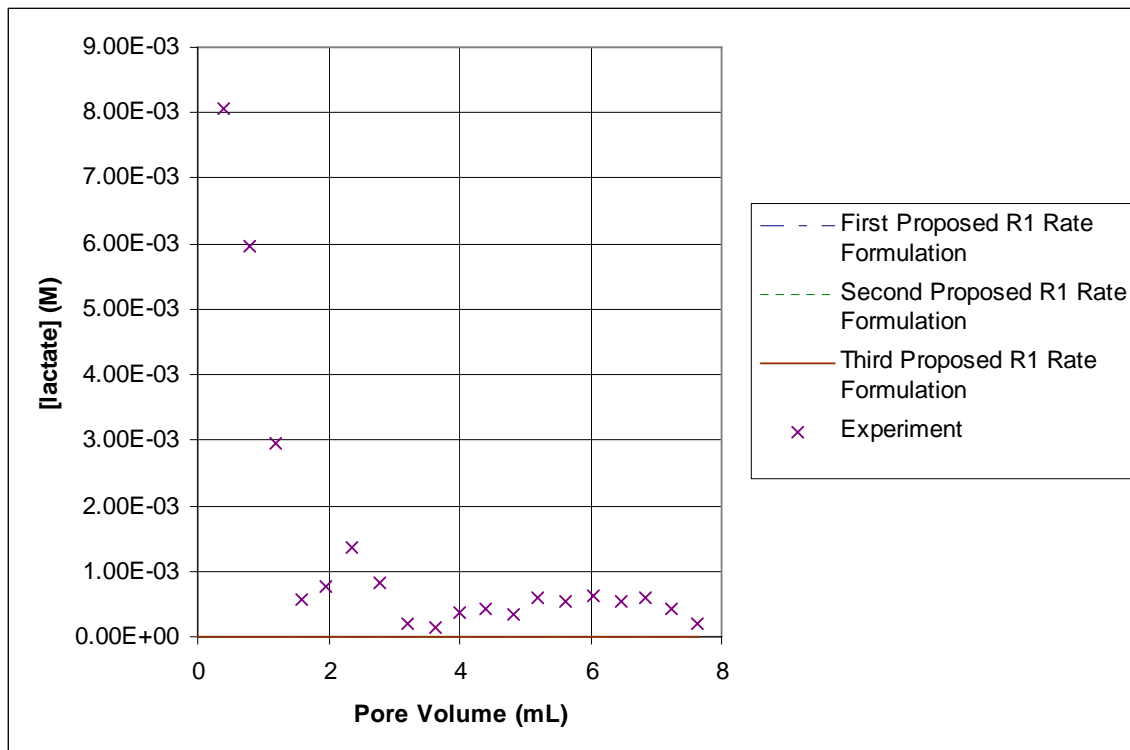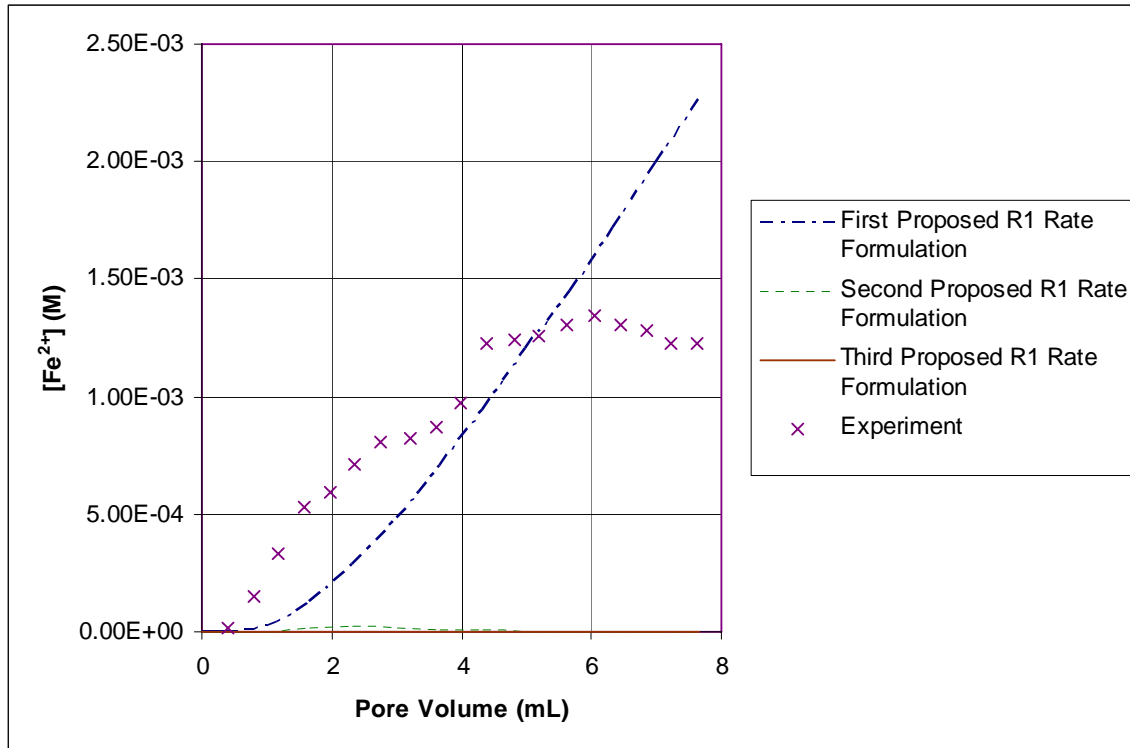
Figure 3.10: Simulation Results for Column G-J (Q=1.6 ml/day) and Parameters Determined from Batch Experiment #6

65
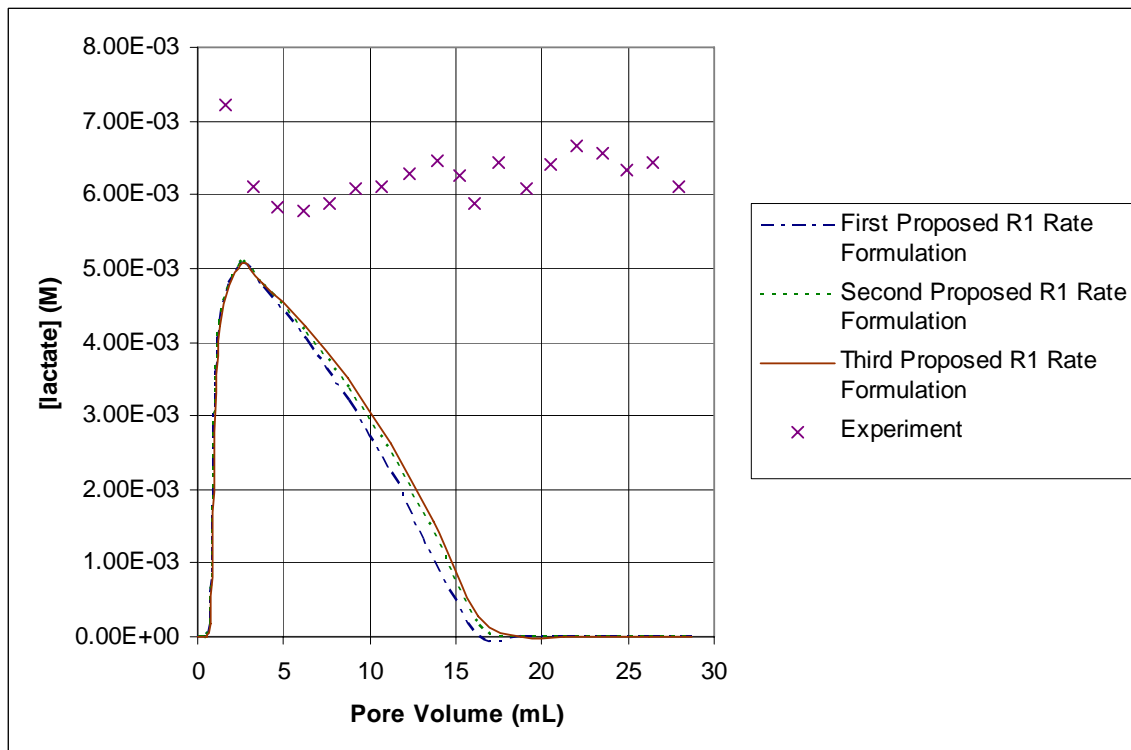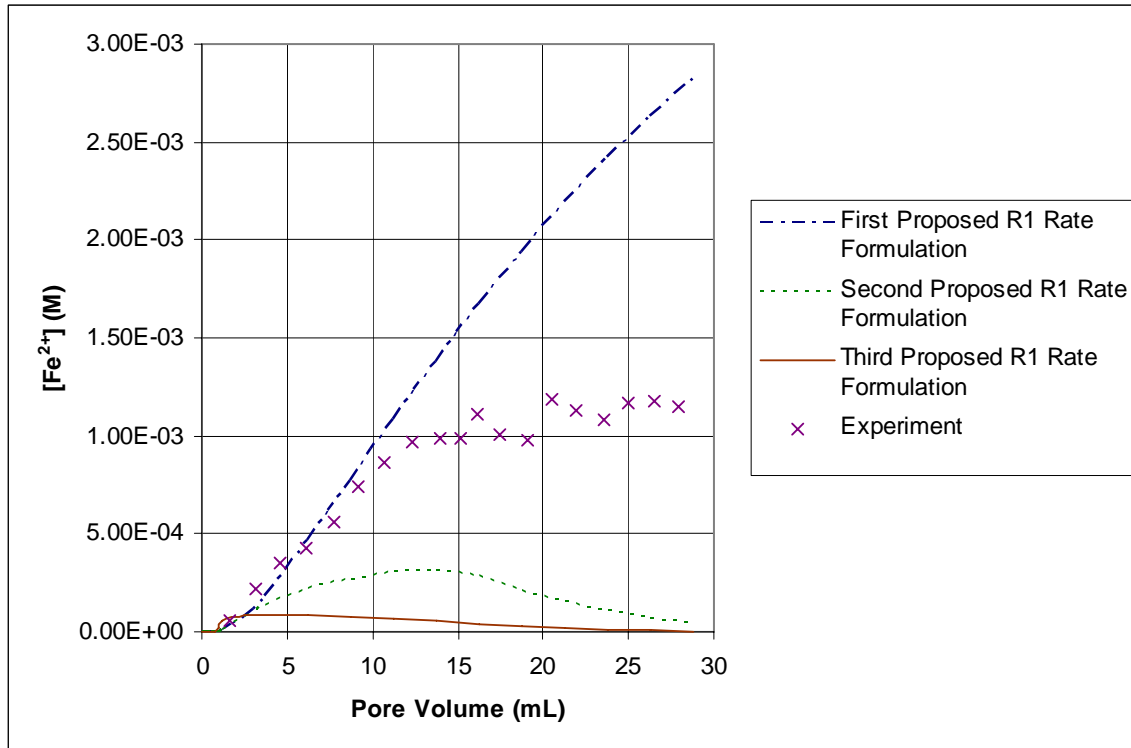
Figure 3.11: Simulation Results for Column K-N (Q=6 ml/day) and Parameters
Determined from Batch experiment #6
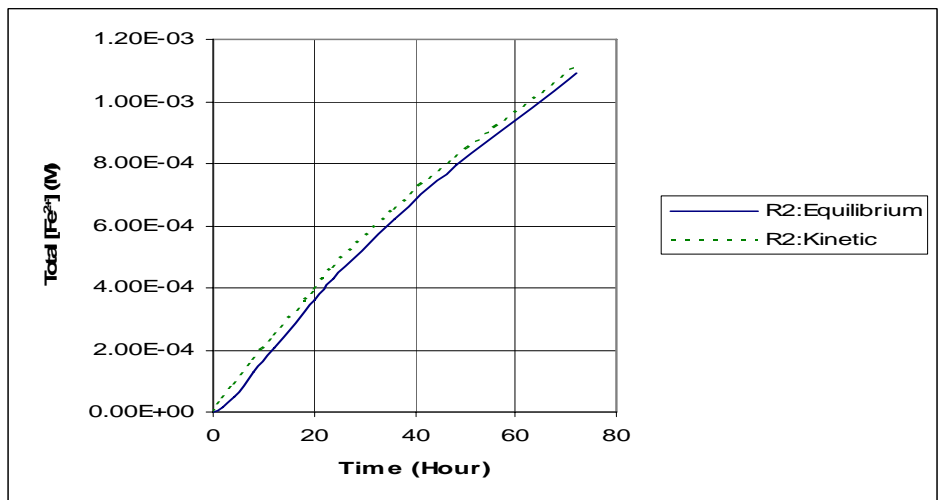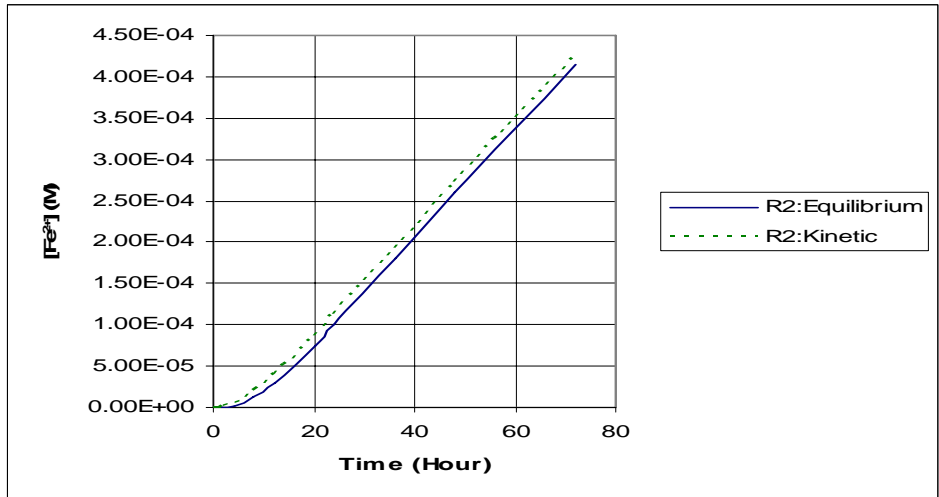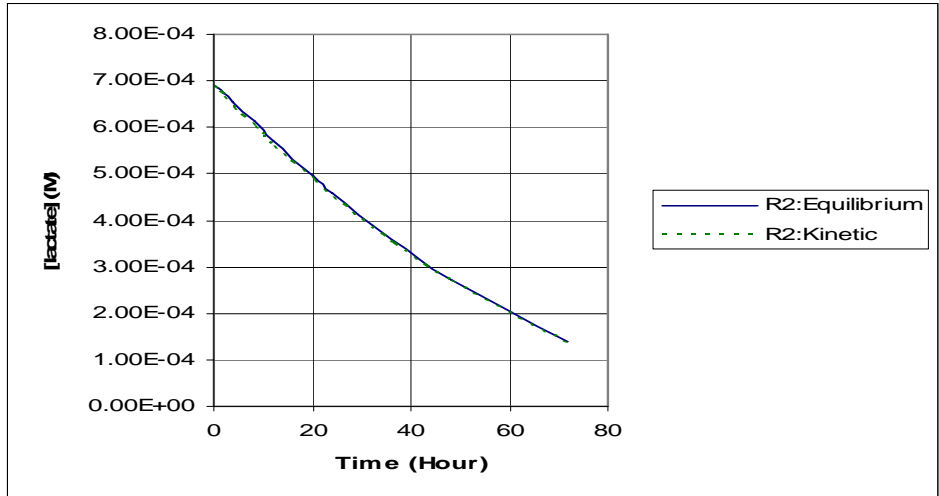
Figure 3.12: Comparison between the Equilibrium and Kinetic R2 Rate Formulation with the First Proposed R1 Formulation
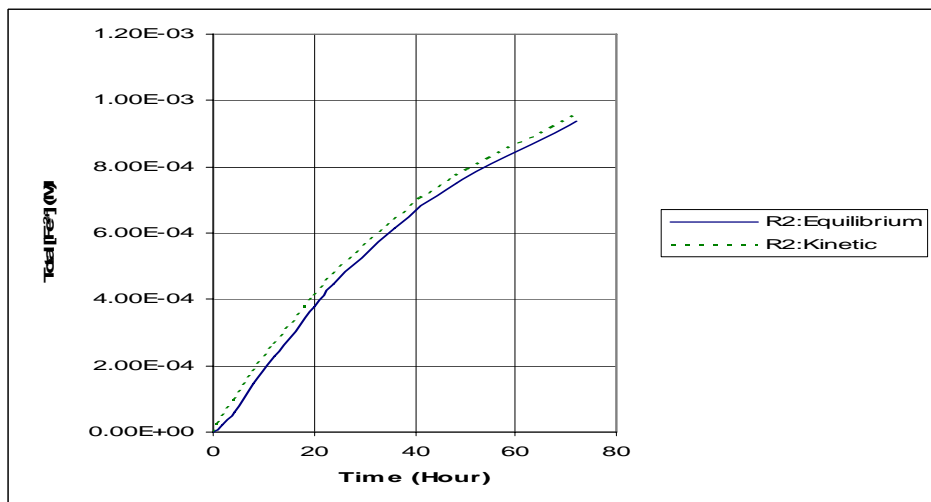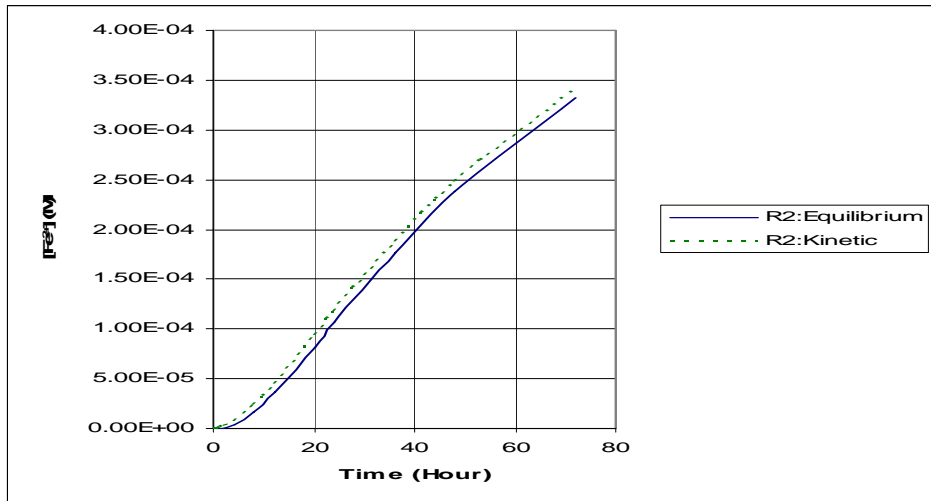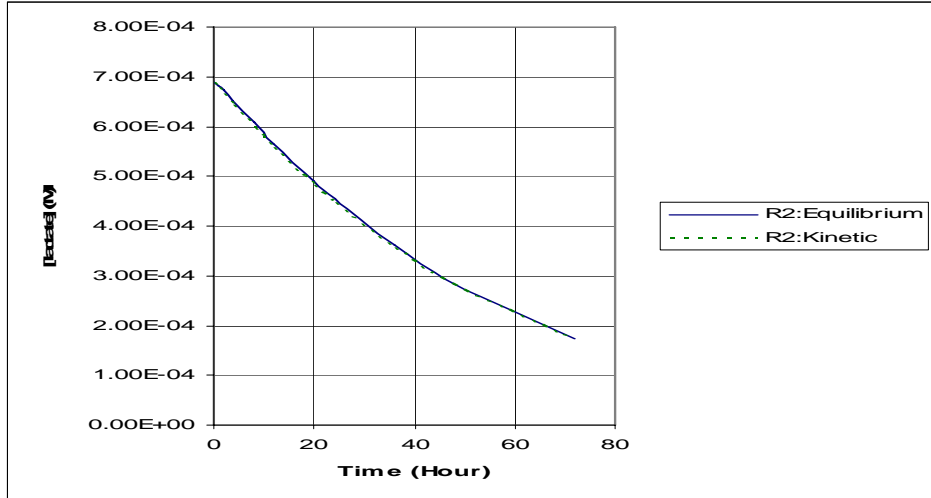
Figure 3.13: Comparison between Equilibrium and Kinetic R2 Rate Formulation with the Second Proposed R1 Formulation
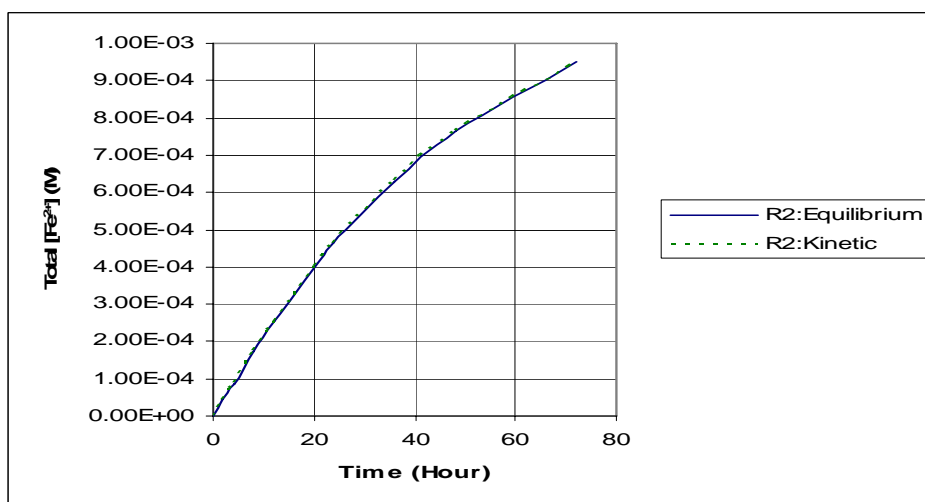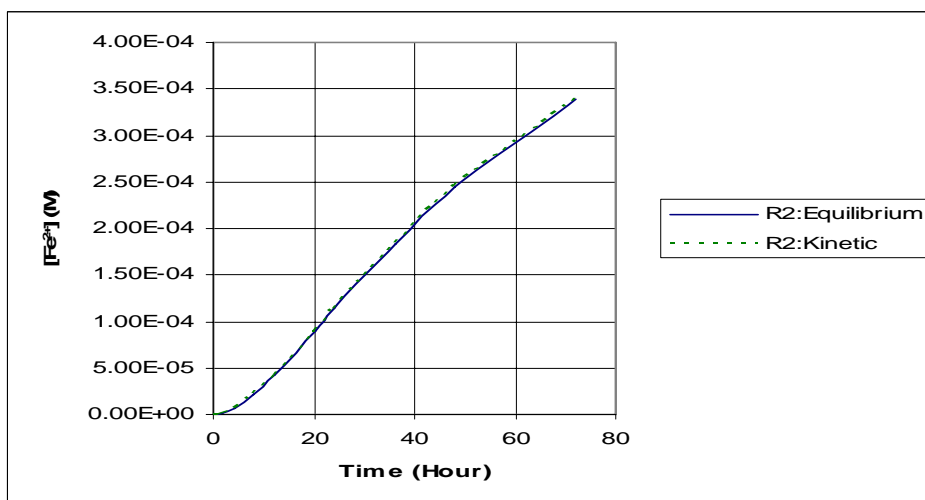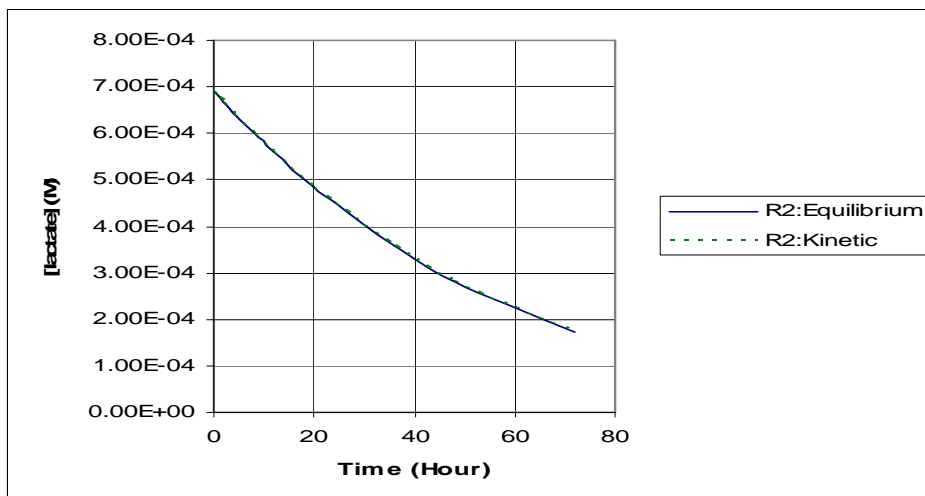
Figure 3.14: Comparison between Equilibrium and Kinetic R2 Rate Formulation with the Third Proposed R1 Formulation

3.4 Conclusion and Discussion

The main purpose of column simulation is to examine the formulations and parameters determined from the batch system. In the batch system, we obtained three groups of parameters (Table 2.6) for each rate formulation from batch experiment #4, #5 and #6, respectively. These three groups of parameters and proposed kinetic rate formulations were systematically tested by a reactive biogeochemical transport model, HYDROGEOCHEM 4.0, with column experimental data in order to find out the "universal" rate formulations with scale-dependent parameters of the bioreduction of hematite.

From Figure 3.3 to Figure 3.11, we found that only the dual Monod kinetic with inhibition rate formulation with respect to the concentrations of lactate, $\equiv$FeOOH, and Fe^{2+}, with the parameters obtained from batch experiment #4 could fit the experimental data well for all flow rates. The reason is the column experiments were conducted under the same initial concentration (10^8cells/mL) of dissimilatory metal-reducing bacterium (DMRB) with the batch experiment #4; therefore, DMRB is believed to affect the reduction of Fe^{3+} to Fe^{2+}. This assumption also can be demonstrated by simply comparing the column simulation results between batch experiment #5 (initial DMRB = 10^9cells/mL) and #6 (initial DMRB = 10^7cells/mL) because these two experiments were conducted under the same condition except the concentration of DMRB.

From Figure 3.6 to Figure 3.11, we determined that the R1 reaction rate of batch experiment #5 is higher than experiment #6; therefore, in the future the third proposed R1

rate formulation should be modified to be proportional to the DMRB and the formulation for the bacterial growth rate (R4) should be the same as R1 except the coefficients. Additionally, the column simulation results of the third proposed R1 rate with the parameters determined from batch experiment #4 (Figure 3.4~3.6) demonstrate the hypothesis that mechanistic-based reaction rates of batch system can be scaled up to and exported to column system. Based on the results of whole column simulation, we recognize that the rate formulations and parameters determined with modeling have to be iteratively tested in order to avoid misjudging the reliability of the proposed formulations and the determined parameters.

Figure 3.12 to Figure 3.14 shows that in the batch system the equilibrium reaction rate for surface hydration of hematite (R2) can be substituted for the kinetic rate formulation (equation 3.2). In the past, most people deemed R2 reaction in the batch system as an equilibrium reaction; however, based on our research R2 can be represented in more than one way. This demonstration could vanquish the issue of the consistency of the R2 rate formulation between our batch and column simulation, and further suggests that many chemical reactions may be expressed by more than one unique rate formulation.

CHAPTER 4: SUMMARY AND FUTURE WORK

4.1 Summary

The biogeochemistry of microbial Fe(III) reduction and of associated contaminant interactions is very complicated; thus, we proposed a reaction network for analyzing the bioreduction of natural hematite-coated sand by dissimilatory metal-reducing bacterium (DMRB), *Shewanella putrefaciens* CN32, under growth conditions with lactate as the electron donor. Furthermore, the rate formulations and parameters of the reaction network were determined and validated by a reaction-based biogeochemical model, BIOGEOCHEM 1.0, and a reactive biogeochemical transport model, HYDROGEOCHEM 4.0, respectively.

The proposed reaction network of hematite bioreduction is comprised of thirteen species and five chemical reactions: (1) the bacterial reduction of hematite, (2) the surface hydration of hematite, (3) the sorption of Fe(II) to hematite, (4) the bacteria growth with lactate as electron donor, and (5) the PIPES buffering. In the batch system we defined the bioreduction of hematite (R1) and microbial growth (R4) as kinetic reactions and defined the hydration (R2), adsorption of ferrous iron (R3), and PIPE buffering (R5) as equilibrium reactions. This reaction network was then decoupled via Gauss-Jordan elimination into three mass action equations for equilibrium reactions, two kinetic-variable equations for kinetic reactions, and eight mass conservation equations. Based on these equations and the batch experimental data, we calculated the concentration of each species to generate the kinetic rate equations as a function of time by fitting the curve of

the kinetic-variable concentration-vs-time for formulating the kinetic reaction rates and determining the parameters.

Our primary objective was to determine the rate formulations and parameters for the bacterial reduction of hematite, R1. We proposed three rate formulations to represent R1: (1) a physically-based formulation proposed to be first-order with respect to "free" hematite surface sites ($\equiv$FeOOH), (2) a dual Monod kinetic rate formulation with respect to the concentrations of lactate and $\equiv$FeOOH, and (3) a dual Monod kinetic with inhibition rate formulation with respect to the concentrations of lactate, $\equiv$FeOOH, and Fe^{2+}. Furthermore, a formal formulation for bacteria growth kinetic with cell decay was used to describe the kinetic bacteria growth rate.

For the equilibrium reactions, two "user-specify" formulations were employed to substitute for the mass action equations of the surface hydration of hematite (R2) and the sorption of Fe(II) to hematite (R3), respectively. The first "user-specify" formulation for R2 was based on the concept of surface site species concentration corresponding to the mineral suspension concentration; thus, in R2 the total surface site ([$\equiv$FeOOH] + [$\equiv$FeOOFe(II)$^+$]) was proportional to the concentration of hematite. The second "user-specify" formulation for R3 was expressed using a empirical Freundlich equation according to the concept of the attachment of the material to be adsorbed to adsorbent at an available adsorption site, so in R3 the concentration of $\equiv$FeOOFe(II)$^+$ was represented by a power equation as a function of [Fe2$^+$]. The last equilibrium reaction, PIPES

buffering, was described by a mass action equation and the logarithm equilibrium constant was equal to – 6.8 according to the product information.

After determining all of the reaction rate formulations, the parameters for each rate formulation were systematically resolved with the batch experiments #4, #5, and #6 data. The determined formulations and parameters were input into BIOGEOCHEM 1.0 to simulate the bioreduction of hematite under the batch system, and individually compared the results with batch experimental data for verifying the individual rate formulations/parameters and the overall theoretical approach. The determined formulations and parameters were compared with the column experiments by using a reactive biogeochemical transport model, HYGROGEOCHEM 4.0.

For the column simulation, we estimated the basic characteristics of the porous medium and determined the domain of interest from the column experimental setup and the tracer experimental data, and then divided the domain of interest of column into 30 elements (0.25 cm x 1 cm each) corresponding to 62 nodes. After obtaining all of the needed information, the combined information from batch and column system was converted into an input file for HYDROGEOCHEM 4.0 to model the transportation of hematite bioreduction. We made comparisons between the simulations and the column experimental data to see which proposed R1 rate formulation with determined parameters could provide the best overall fit with the column experimental data.

Our batch simulations for each batch experiment were reasonably good at predicting the bioreduction of hematite for all proposed R1 rate formulation. In our column simulations, only the dual Monod kinetic with inhibition rate formulation with respect to the concentrations of lactate, $\equiv$FeOOH, and Fe^{2+}, with the parameters obtained from batch experiment #4 could fit the experimental data well for all flow rates. The reason is that the column experiments were conducted under the same initial concentration of DMRB with batch experiment #4; thus, we conclude that the reaction rate of hematite bioreduction is relevant to the concentration of DMRB. Moreover, from the iterative batch and column simulations we conclude that while hydration reaction has been considered fast based on batch experiments and physical reasoning in the literature, the assumption of fast reaction does not hold up in column experiments. We also find that a slow-reaction hypothesis for hydration reaction is valid based on both batch and column experiments.

4.2 Future Work

The rate formulations and parameters of the reaction network are the keys to successfully simulate or analyze the biological reduction of hematite. We found only the third proposed R1 rate formulation under certain concentrations of DMRB was satisfactory. In the future, the R1 rate formulation should be modified to include the initial concentration of DMRB. Furthermore, the column experiment should be carefully designed to measure the influence of different initial DMRB's concentrations. Therefore, if the modified R1 rate formulation with the parameters determined from batch system can fit well with the column experimental data for all flow rates and concentrations of DMRB, the "universal"

rate formulations with scaled-dependent parameters for the bioreduction of hematite can

be established.

APPENDIX A: BATCH AND COLUMN EXPERIMENTAL DATA

A.1 Batch Experimental Approach and Results

For batch experiments, all reactors were managed in 120 mL clear serum bottles with 80

to 90 mL of the background electrolyte solution at a constant temperature of 20 °C. To

each reactor the hematite-coated sand, lactate, and cells were added, then all reactors'

solution volume were increased to 100 mL with the background electrolyte solution. At

times of around 0, 1, 2, 4, 8, 12, 20, 24, 36, 48, 72, 96, and 120 hours, duplicate or

triplicate 5 mL samples were collected to analyze acid-extractable Fe(II), dissolved Fe(II),

total Fe(II), organic acids, and pH.

For analytical techniques, the acid-extractable Fe(II) was measured by adding a 2 mL

collected sample to a vial containing 0.2 ml of 5.5 N HCL in an anaerobic chamber. This

sample was then removed from the anaerobic chamber and placed on the shaker table for

24 hours to extract the Fe(II). After the acid-extraction, a 0.25 μm pore bottletop was

employed to filter the sample and 0.01 to 0.08 mL of the filtered sample was then added

into 2.4 mL of ferrozine reagent solution (1 g/L ferrozine in 50 mM HEPES Buffer, pH =

8.0). The acid-extractable Fe(II) was detected via Shimidzu UV/Vis-1601 Spectrometer

at a wavelength of 562 nm and the concentration was determined based on a Fe(II)

standard curve. Similarly, the dissolved Fe(II) was measured by adding 0.1 to 0.5 mL

collected sample with filtered into 2.4 mL of ferrozine reagent in the anaerobic chamber.

Then, the analytic procedure of dissolved Fe(II) is the same with the acid-extractable Fe(II) analysis.

In addition, the remaining filtrate from the acid-extractable sample was utilized to measure the organic acids, lactate and acetate, via a Water 2695 Separations Module High Performance Liquid Chromatography. The Waters 2996 Photodiode Array Detector at 211 nm was employed to detect the organic acids and the concentrations of lactate and acetate were then determined by comparing with the standard curves. For evaluating the solution pH, the combined remaining filtrate from the experimental reactors in the anaerobic chamber was used to evaluate the pH. Table A.1 to A.3 and Figure A.1 to A.3 show the results of batch experiments.

A.2 Column Experimental Approach and Results

The column experiments were managed in triplicate or quadruple for minimizing the discrepancy of results due to any variation in the pore volume, and the columns used in the experiments have an inner diameter of 1 centimeter and are 10 centimeter long. Before injecting the feed solution, all columns were packed with 9 grams of iron coated sand packed to a bed length of 7.5 cm and a bacteria concentration of 10^8 cells/mL. The feed solution employed in all column experiments was the same background electrolyte solution used in the batch experiments with around 8.8 mM sodium lactate and 0.1 gL^{-1} yeast extract. The feed solution was filtered through a 0.25 pore size filter and then autoclaved at 121 °C for fifteen minutes. While the solution was still warm, the feed solution was purged overnight with nitrogen gas.

After purging the feed solution, the different flow rate of feed solution was then set to push through the columns for individual column experiment. During the period of column experiments (21 days), the column effluent was sampled every 24 hours in a scintillation vial with 1 to 5 mL of 1 N HCl depending on the amount of effluent liquid collected. The collected samples were then weighed, filtered using 0.25 um pore filter, and wrapped with Teflon tape and Parafilm before being stored at 4 °C until analyzed. After 21 days, the columns were deconstructed in an anaerobic chamber and 1 g samples of sand from the influent, middle, and effluent sections of the column were collected in vials containing 5 mL of 0.625 N HCl in order to analyze total Fe(II).

The 1,10-phenanthroline method was employed to evaluate the Fe(II) concentration at a wavelength of 510 nm via the following steps: (1) put 3.2 mL of MilliQ filtered water, 0.5 mL of collected sample and 0.05 mL of concentrated HCL into a scintillation vial. The HCl is needed to keep the pH of solution below 2 to prevent the oxidation of Fe(II) in the sample. (2) Add 0.24 mL of 0.73 M ammonium fluoride and allow to complex with Fe(III) for 2 minutes. (3) Add 0.5 mL of 1,10-phenanthroline and 0.5 mL of 15.5 M ammonium acetate buffer for dyeing the Fe(II). After completely mixing the solution, 1.65 mL of this solution was used to measure the Fe(II) by 1601 Shimidzu UV/Vis Spectroscope at 510 nm. Furthermore, the column analytic procedure of organic acids, lactate and acetate, is the same with the batch system analysis. Table A.4 to A.6 and Figure A.4 shows the result of the column experiments.

Table A.1: Experimental Data for Batch Experiment #4

Time events	hrs	Fe(II) Tot (mol/L)	std dev	Fe(II) aq (mol/L)	std dev	pH	Lactate (mol/L)	Acetate (mol/L)	Cell # (initial)	Control Lactate (mol/L)
0	0.17	3.383E-05	4.356E-06	9.088E-07	2.862E-07	7.02	0.0006601		10^8	0.00067361
1	1.00	6.726E-05	6.081E-06	3.635E-06	2.862E-07	7.09	0.0006448			0.000716734
2	2.00	0.0001059	3.041E-06	1.033E-05	7.572E-07	7.02	0.0006458			0.000733785
3	4.00	0.0001716	8.458E-06	2.256E-05	1.239E-06		0.0006176			0.000746593
4	8.00	0.0002739	1.358E-05	4.982E-05	8.937E-07	7	0.0005622	0.000537		0.000660973
5	12.25	0.0003717	7.08E-06	7.337E-05	3.353E-06	6.95	0.0005307			0.000712192
6	20.58	0.0004747	3.086E-05	0.0001199	7.358E-06	7.08	0.0004698	0.0005251		0.000703179
7	24.00	0.0005286	2.378E-05	0.000137	6.8E-06	7.08	0.0004327	0.0005394		0.000643894
8	36.30	0.0006417	5.025E-05	0.0001906	9.674E-06	6.96	0.0003218	0.0007993		0.000662507
9	48.00	0.0007905	2.501E-05	0.0002356	1.031E-05	7.07	0.0002671	0.0008417		0.000670644
10	72.10	0.0009511	9.546E-05	0.0003218	1.922E-05		0.0001716	0.0010717		0.000645312

Table A.2: Experimental Data for Batch Experiment #5

Time events	hrs	Fe(II) Tot (mol/L)	std dev	Fe(II) aq (mol/L)	std dev	pH	Lactate (mol/L)	Acetate (mol/L)	Cell # initial	Control Lactate (mol/L)
0	0	5.71898E-05	6.081E-06	4.048E-06	3.786E-07		0.0036757		10^9	0.003711036
1	1.05	0.000219093	5.448E-06	2.379E-05	2.516E-06	6.95	0.0036325			0.003723068
2	2.05	0.000322599	2.33E-05	4.767E-05	4.267E-06	7.03	0.0035853			0.003719142
3	4.05	0.00046799	3.119E-05	8.221E-05	3.851E-06	7	0.0034477			0.003750399
4	8.02	0.000710016	1.484E-05	0.0001345	7.194E-06	6.97	0.0035415			0.003796706
5	12.04	0.000819658	5.01E-05	0.0001805	8.758E-06	6.95	0.0035014	0.0003011		0.00370291
6	20.27	0.000989376	2.235E-05	0.0002452	1.845E-05	7.05	0.0034539	0.0003848		0.003756253
7	24.03	0.001078394	9.408E-05	0.0002917	1.134E-05	6.97	0.0034351	0.0005446		0.003869242
8	36	0.001251751	0.0001262	0.0003574	1.085E-05	6.98	0.0032407	0.0005944		0.003767482
9	46.45	0.001377923	7.733E-05	0.0004219	1.867E-05		0.0030547	0.0008132		0.003735046
10	70.45	0.001852099	8.756E-05	0.0005064	3.329E-05	7.02	0.0028505	0.0013537		0.003711036
11	94.4	0.001812893	0.0001501	0.0005805	3.495E-05	7	0.0025294	0.0016827		
12	117.5	0.001936785	0.0002025	0.0006072	5.296E-05	7.06	0.0024446	0.0023792		

Table A.3: Experimental Data for Batch Experiment #6

Time events	hrs	Fe(II) Tot (mol/L)	std dev	Fe(II) aq (mol/L)	std dev	pH	Lactate (mol/L)	Acetate (mol/L)	Cell # initial	Control Lactate (mol/L)
0	0	5.51761E-05	1.719E-05	-2.479E-07			0.0037097		10^7	0.003711036
1	1.05	4.87322E-05	4.243E-06	4.131E-07	1.431E-07	6.92	0.0037056			0.003723068
2	2.05	6.4842E-05	6.976E-06	1.405E-06	1.431E-07	7.04	0.0036669			0.003719142
3	4.05	0.000109547	9.766E-06	4.627E-06	6.238E-07	7.01	0.0036785			0.003750399
4	8.02	0.000182444	1.485E-05	1.429E-05	1.365E-06	6.95	0.0036919			0.003796706
5	12.04	0.000248494	3.079E-05	2.933E-05	2.936E-06	6.98	0.0036471			0.00370291
6	20.27	0.000358846	2.849E-05	6.37E-05	8.161E-06	6.99	0.0031232	0.0007438		0.003756253
7	24.03	0.000466782	3.659E-05	9.634E-05	6.744E-06	6.93	0.0031323	0.0009401		0.003869242
8	36	0.000695944	0.0001064	0.0001813	3.176E-05	6.95	0.0028547	0.0012412		0.003767482
9	46.45	0.000921317	0.0002787	0.0002691	9.064E-05		0.0022553	0.0019292		0.003735046
10	70.45	0.001188451	0.0002039	0.0004979	0.0001153	7.02	0.0017342	0.0026777		
11	94.4	0.001343535	0.0005084	0.0005413	0.0002073		0.0015241	0.0028998		
12	117.5	0.001649795	0.0005166	0.0008098	0.000271	7.07	0.0014041	0.0029902		

Table A.4: Experimental Data for Column A-D

Cul time (hr)	Average Vol (ml)	Cumulative Vol (ml)	Avg Flow (vol/time)	pore volumes	avg [Fe(II)] (umol/L)	avg [lactate] (mM)	avg [acetate] (mM)
17:38:00	10.6508	10.6508		2.6627	18.585	8.287425	0.938047
39:46:00	10.34955	21.00035	10.37	5.250088	152.2225	7.665983	2.567419
65:06:00	10.4488	31.44915	10.42	7.862288	192.16	7.708561	3.164005
87:54:00	10.19555	41.6447	10.42	10.41118	217.6575	7.766583	3.320641
111:39:00	10.61405	52.25875	10.49	13.06469	237.335	7.8882	4.076575
136:12:00	10.4933	62.75205	10.52	15.68801	280.0725	7.571722	3.051879
159:25:00	10.38955	73.1416	10.56	18.2854	373.44	6.106161	2.403189
183:16:00	10.5373	83.6789	10.60	20.91973	448.14	7.690352	2.988933
207:16:00	10.83505	94.51395	10.58	23.62849	559.6775	8.470399	3.282031
232:02:00	11.35955	105.8735	10.65	26.46838	618.0625	8.53105	3.340068
256:52:00	11.2298	117.1033	10.94	29.27583	672.8775	8.713326	2.892662
280:17:00	12.7868	129.8901	11.21	32.47253	656.2175	8.843961	2.755826

Table A.4: Experimental Data for Column A-D (Continued)

Cul time (hr)	Average Vol (ml)	Cumulative Vol ml)	Avg Flow (vol/time)	pore volumes	avg [Fe(II)] (umol/L)	avg [lactate] (mM)	avg [acetate] (mM)
303:29:00	11.06805	140.95815		35.23954	631.8425	9.244578	2.860068
327:08:00	10.3938	151.35195	11.30	37.83799	683.335	9.236756	3.147555
351:16:00	10.3853	161.73725	10.41	40.43431	722.2875	9.277328	3.291137
374:46:00	10.52505	172.2623	10.45	43.06558	723.42	9.462558	3.286523
400:01:00	10.36605	182.62835	10.38	45.65709	732.8425	9.360683	3.446218
422:31:00	10.5333	193.16165	10.45	48.29041	821.6575	9.585822	3.214308
447:55:00	10.5078	203.66945	10.48	50.91736	799.625	8.720175	2.579209
471:15:00	10.2453	213.91475	10.39	53.47869	757.705	9.671496	3.440379
495:15:00	10.25705	224.1718	10.40	56.04295	2749.416	9.692184	3.131141
518:50:00	9.73455	233.90635	10.36	58.47659	443.7547	9.618311	3.183266

Table A.5: Experimental Data for Column G-J

Cul time (hr)	Average Vol (ml)	Cumulative Vol (ml)	Avg Flow (vol/time)	pore volumes	avg [Fe(II)] (umol/L)	avg [lactate] (mM)	avg [acetate] (mM)
14:16:00	1.574883	1.574883		0.393721	12.41268	8.071459	1.87267
38:40:00	1.601217	3.1761	1.57	0.794025	148.7947	5.952218	4.451868
63:23:00	1.567217	4.743317	1.52	1.185829	331.1664	2.966715	7.952379
87:18:00	1.60755	6.350867	1.61	1.587717	531.9365	0.572434	10.7314
111:10:00	1.533217	7.884083	1.54	1.971021	594.3329	0.756687	10.24722
134:23:00	1.572217	9.4563	1.63	2.364075	712.8819	1.361621	9.6675
157:56:00	1.610217	11.06652	1.64	2.766629	805.1674	0.809509	14.93446
183:48:00	1.72955	12.79607	1.60	3.199017	819.206	0.197938	11.00444
208:31:00	1.67255	14.46862	1.62	3.617154	871.7248	0.127819	11.05216
230:36:00	1.511217	15.97983	1.64	3.994958	974.0774	0.355757	10.88266
254:30:00	1.62155	17.60138	1.63	4.400346	1225.042	0.437321	11.15893
279:04:00	1.688883	19.29027	1.65	4.822567	1244.87	0.346192	10.11989

Table A.5: Experimental Data for Column G-J (Continued)

301:34:00	1.50755	20.79782	1.61	5.199454	1256.345	0.602025	10.64884
325:34:00	1.63255	22.43037	1.63	5.607592	1306.881	0.545856	10.54883
351:06:00	1.748883	24.17925	1.64	6.044813	1341.327	0.631908	11.08197
375:43:00	1.672883	25.85213	1.63	6.463033	1303.046	0.53513	10.86043
398:35:00	1.513883	27.36602	1.59	6.841504	1278.637	0.596566	10.83399
422:07:00	1.58255	28.94857	1.61	7.237142	1224.437	0.418007	10.99205
446:07:00	1.587217	30.53578	1.59	7.633946	1225.636	0.204308	11.13087

Table A.6: Experimental Data for Column K-N

| Cul time (hr)	Average Vol (ml)	Cumulative Vol (ml)	Avg Flow (vol/time)	pore volumes	avg [Fe(II)] (umol/L)	avg [lactate] (mM)	avg [acetate] (mM)
20:48:00	6.559883	6.559883		1.639971	59.01998	7.210081	2.584335
45:12:00	6.260217	12.8201	6.15759	3.205025	222.9864	6.105412	5.230403
67:17:00	5.572217	18.39232	6.055843	4.598079	347.764	5.834554	5.201668
91:17:00	6.178217	24.57053	6.178217	6.142633	422.8487	5.772492	5.309075
115:17:00	6.252217	30.82275	6.252217	7.705688	559.9489	5.886197	5.307827
138:58:00	5.88455	36.7073	5.963232	9.176825	740.7919	6.073936	5.37755
163:16:00	6.234883	42.94218	6.157909	10.73555	861.7128	6.099437	5.265167
187:41:00	6.41955	49.36173	6.310001	12.34043	963.612	6.295423	4.810928
211:58:00	6.278883	55.64062	6.205623	13.91015	983.0434	6.459684	4.723364
234:43:00	5.22555	60.86617	5.512668	15.21654	983.6614	6.249638	5.018598
259:12:00	3.632367	64.49853		16.12463	1107.133	5.889626	5.730688
283:00:00	5.29755	69.79608	5.342067	17.44902	1007.944	6.434675	5.358218
308:06:00	6.428217	76.2243	6.146502	19.05608	973.5912	6.080963	5.345572
331:10:00	5.845883	82.07018	6.082422	20.51755	1183.01	6.420761	4.909585
354:07:00	5.801217	87.8714	6.066632	21.96785	1126.813	6.660072	5.26085
379:24:00	6.240217	94.11162	5.923475	23.5279	1079.859	6.572478	5.292567
402:12:00	5.727883	99.8395	6.029351	24.95988	1167.226	6.344265	5.110898
426:20:00	5.99455	105.8341	5.961431	26.45851	1176.423	6.446127	5.482115
450:47:00	6.068217	111.9023	5.956532	27.97557	1148.969	6.10323	5.391081
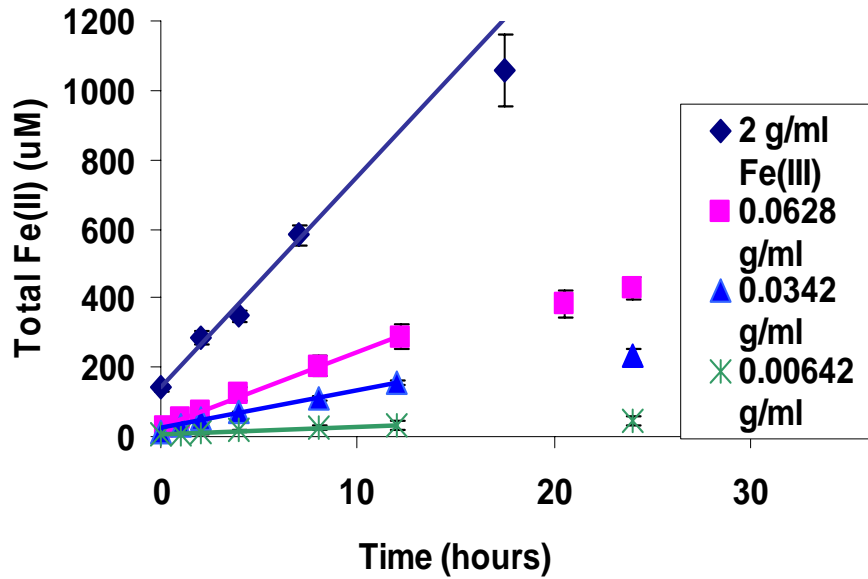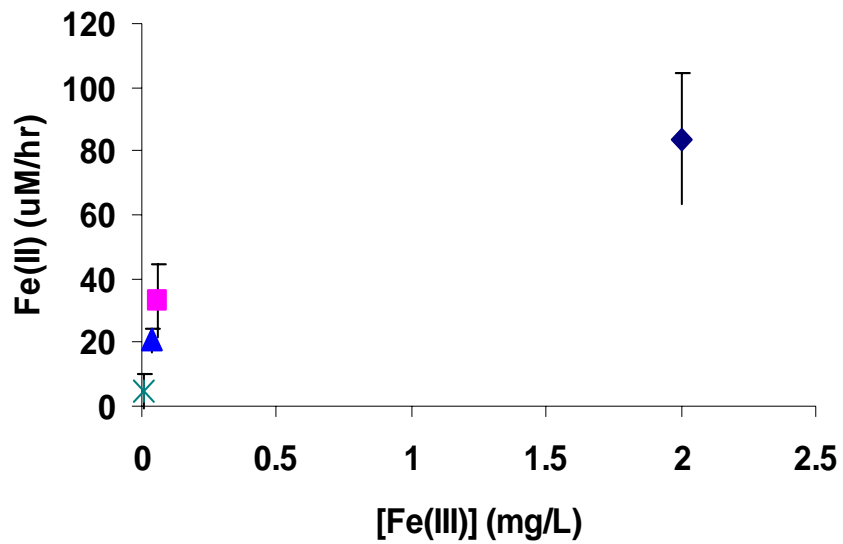
Figure A.1 Varied initial Fe(III) sand concentration batch experimental data. (A) The rate from the first 12 hours of each experiment was based on the amount of total iron produced over time. (B) The rate of each experiment was plotted against the experimental condition in order to determine the order of the reaction.
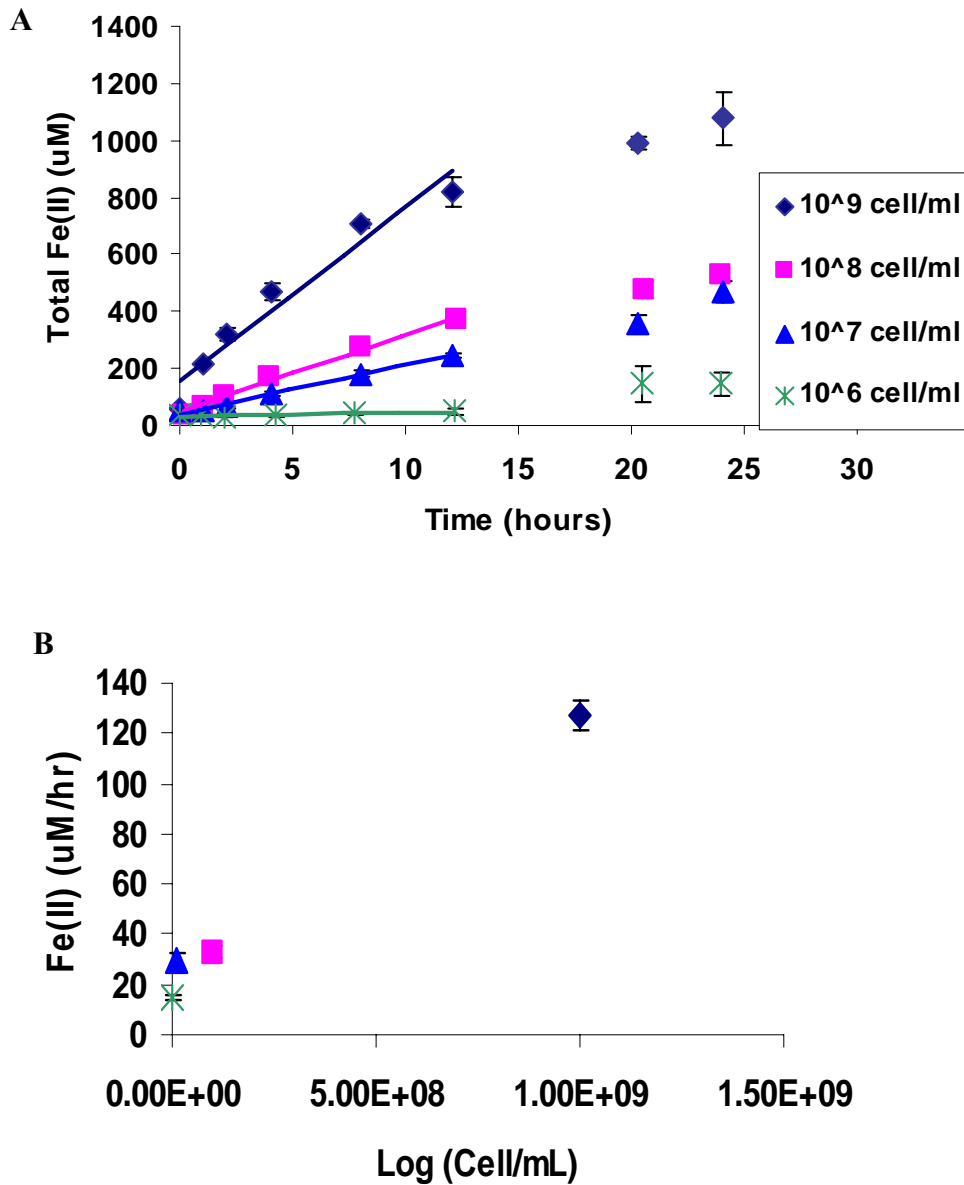
Figure A.2 Varied initial cell concentration as cell/mL. (A) The rate for the first twelve hours of each batch experiment was used to calculate the rate of reduction. (B) The rate plotted against the batch experimental condition in order to determine the order of reaction R1.

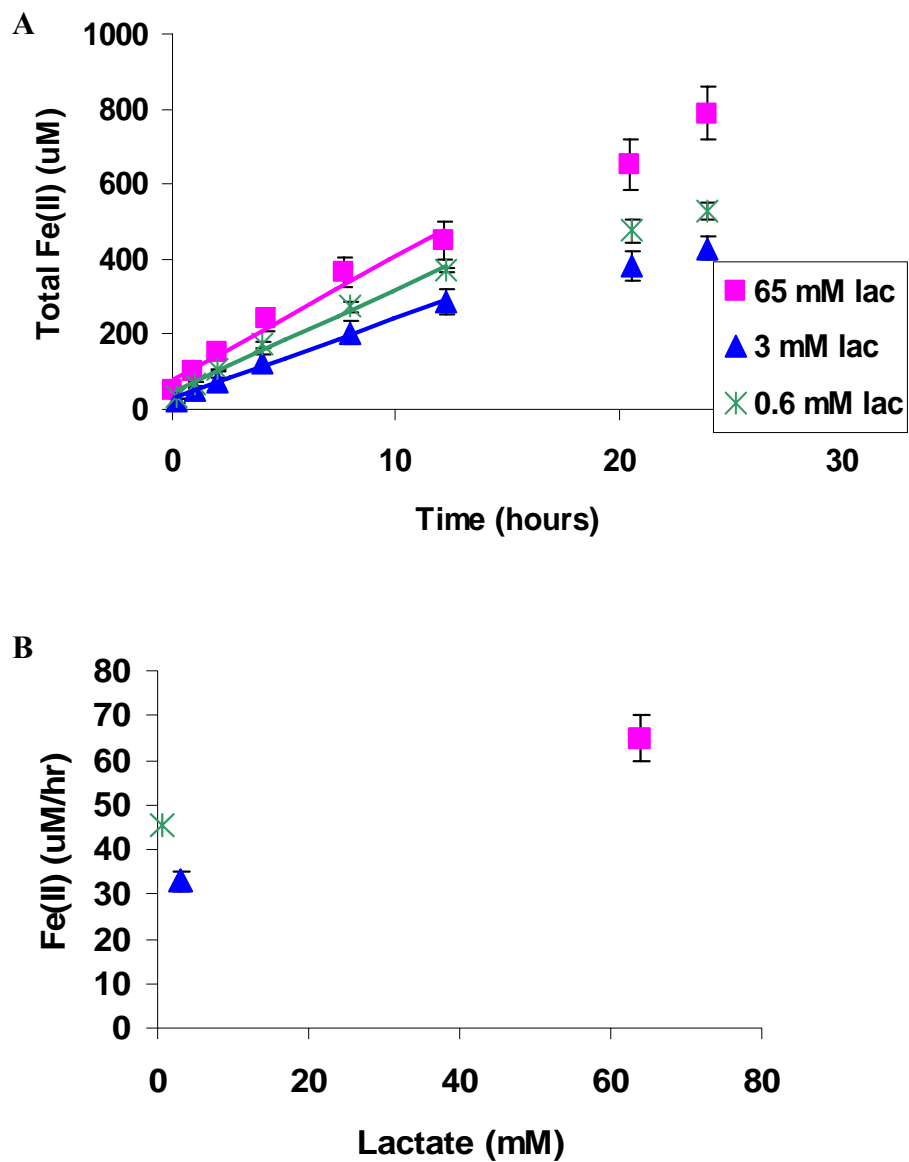Figure A.3 Varied Lactate concentrations in mM. (A) The first twelve hours of each batch experimental condition was used to determine the rate. (B) Rate plotted against batch experimental condition to determine reaction order.
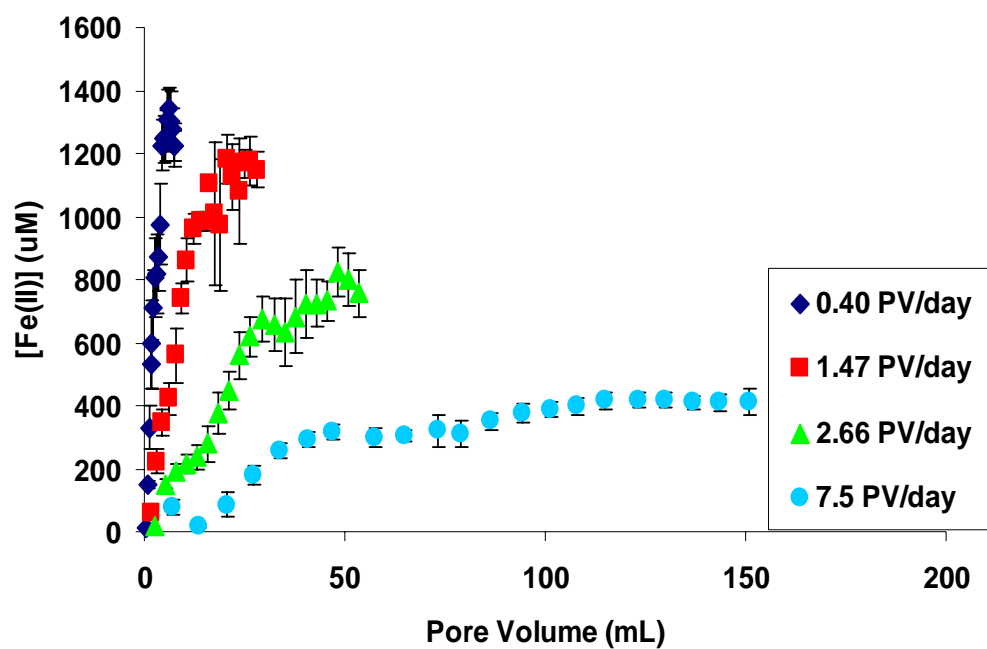
Figure A.4 Raw data form four column experiments run in triplicate or quadruplicate.

LIST OF REFERENCES

American Water Works Association, 1999. Water Quality & Treatment, 13.1−13.19.

Arnold, R.G., Olson, T.M., and Hoffman, M.R., 1986. Kinetic and mechanism of dissimilative Fe(III) reduction by Pseudomonas sp. 200, Biotechnol Bioeng 28:1657−1671.

Brooks, S.C., Carroll, S.L., and Jardine, P.M., 1999. Sustained bacterial reduction of Co(III)EDTA- in the presence of competing geochemical oxidation during dynamic flow. Env. Sci. Tech. 33, 3002–3011.

Burgos, W.D., Royer R.A., Fang, Y., Yeh, G.T., Fisher, A.S., Jeon, B.H., and Dempsey, B.A., 2002. Theoretical and experimental considerations related to reaction-based modeling: A case study using iron(III) oxide bioreduction. Geomicrobio. J. 19(2), 1–35.

Burgos, W.D., Fang, Y.L., Royer, R.A., Yeh, G.T., Stone, J.J., Jeon, B.H., and Dempsey, B.A., 2003. Reaction-based modeling of quinone-mediated bacterial iron (III) reduction. Elsevier Ltd, 2735-2748.

Caccavo, F., Lonergan D.J., Lovley, D.R., Davis, M., Stolz, J.F., and McInerney, M.J., 1994. A hydrogen-and acetate-oxidizing dissimilatory metal-reducing microorganism. Appl. Env. Microbio. 60, 3752–3759.

Chilakapati, A.R., 1995. A simulator for reactive flow and transport of groundwater contaminants. PNL Report 10636, 1995.

Chilakapati, A.R., Ginn T., and Szecsody, J., 1998. An analysis of complex reaction networks in groundwater modeling. Water Resour. Res., 34(7), 1767–1780.

Chilakapati, A.R, Yabusaki S., Szecsody J., and MacEvoy W., 2000. Groundwater flow, multicomponent transport and biogeochemistry: Development and application of a coupled process model. Hydrol., 43, 303–325.

Curtis, GP and Reihard, M. 1994. Reductive dehalogenation of hexachloroethane, carbon tetrachloride, and bromoform by anthrhydroquinone and humic acid. Environ Sci Technol 28:2393-2401.

Fang, Y.L., Yeh, G.T. and Burgos, W.D., 2003. A General Paradigm to Model Reaction Based Biogeochemical Processes in Batch Systems. Water Resours. Res., 2.1-2.25.

Fang, Y.L., and Yeh, G.T., 2002. Numerical modeling of reactive chemical transport under multiphase systems, paper presented at XIV International Conference on Computational Methods in Water Resources, Delft Univ. of Technol., Delft, Netherlands, 23– 28.

Fredrickson, J.K., Zachara, J.M., Kennedy, D.W., Dong, H., Onstott, T.C., Hinman, N.W., and Li, S.M., 1998. Biogenic iron mineralization accompanying the dissimilatory reduction of hydrous ferric oxide by a groundwater bacterium. Geochim Cosmochim Acta 62(19–20), 3239–3257.

Fredrickson, J.K., Zachara, J.M., Kennedy, D.W., Duff, M.C., Gorby, Y.A., Li, S-M.W., and Krupka, K.M., 2000. Reduction of U(VI) ingoethite (alpha-FeOOH) suspensions by a dissimilatory metal-reducing bacterium. Geochim Cosmochim Acta 64(18), 3085–3098.

Friedly, J. and Rubin, J., 1992. Solute transport with multiple equilibrium-controlled or kinetically controlled chemical reactions. Water Resour. Res., 28(6), 1935– 1953.

Irwin, H.S., 1993. Enzyme kinetic behavior and analysis of rapid equilibrium and steady-state enzyme system, 19–96, 102–115.

Kim, S. and Picardal, F.W., 1999. Enhanced anaerobic biotransformation of carbon tetrachloride in the presence of reduced iron oxides. Env. Toxicol. Chem. 18, 2142–2150.

Klausen, J., Trober, S.P., Haderlein, S.B., and Schwarzenbach, R.P., 1995. Reduction of substituted nitrobenzenes by Fe(II) in aqueous mineral suspensions. Env. Sci. Technol. 29, 2396–2404.

Lovley, D.R. and Phillips, E.J.P., 1986. Availability of ferric Fe for microbial reduction in bottom sediments of freshwater tidal Potomac River. Appl. Environ. Microbiol. 52, 751–757.

Lovley, D.R., Woodward, J.C., and Chapelle, F.H., 1994. Simulate anoxic biodegradation of aromatic hydrocarbons using Fe(III) ligands. Nature 370:128–131.

Metaclf & Eddy, 2003. Water engineering treatment and reuse, 551–584, 1138–1149.

Morgan, 2005. Kinetics of Biological Iron(III) Reduction of Natural Sediments in Batch and Column Reactors. Dept. of Civil and Environmental Engineering, The Pennsylvania State University, University Park, PA 16802.

Randall, J.C., 2000. Groundwater hydraulics and pollutant transport, 366–383.

Roden, E.E. and Zachara, J.M., 1996. Microbial reduction of crystalline iron(III) oxides: Influence of oxide surface area and potential for cell growth. Env. Sci. Technol. 30(5), 1618–1628.

Roden, E.E. and Urrutia, M.M., 1999. Ferrous iron removal promotes microbial reduction of crystalline iron(III) oxides. Env. Sci. Technol. 33(11), 1847–1853.

Rubin, J., 1983. Transport of reacting solutes in porous media: relation between mathematical nature of problem formulation and chemical nature of reactions. Water Resours. Res., 19: 493-502.

Steefel, C.I. and MacQuarrie, K.T.B., 1996. Approaches to modeling of reactive transport in porous media. In Reviews in Mineralogy, (eds. P. C. Lichtner, C. I. Steefel, and G. H. Oelkers), vol. 34 pp. 84–129. Mineralogical Society of America.

Steefel, C.I. and van Cappellen P., 1998. Preface: Reactive transport modeling of natural systems. J. Hydrol. 209, 1–7.

Wildung, R.E., Gorby, Y.A., Krupka, K.M., Hess, N.J., Li, S.W., Plymale, A.E., McKinley, J.P., and Fredrickson, J.K., 2000. Effect of Electron Donor and Solution Chemistry on Products of Dissimilatory Reduction of Technetium by Shewanella putrefaciens. Appl. Env. Microbiol. 66(6), 2451–2460.

Yeh, G.T., Iskra, G.A., Szecsody, J.E., Zachara, J.M., and Streile, G.P., 1995. KEMOD: A Mixed Chemical Kinetic and Equilibrium Model of Aqueous and Solid Phase Reactions. PNL-10380, Pacific Northwest Laboratory, Richland, WA.

Yeh, G.T., 1999. Computational Subsurface Hydrology Fluid Flows. Kluwer Academic Publishers. 277 pages.

Yeh, G.T., 2000. Computational subsurface hydrology reaction, transport and fate, 42–60.

Yeh, G.T., Burgos, W.D., and Zachara, J.M., 2001. Modeling and measuring biogeochemical reactions: System consistency, data needs, and rate formulation, Adv. Environ. Res., 5, 219– 237.

Yeh, G.T., Li, Y., Jardine, P.M., Burger, W.D., Fang, Y.L., Li, M.H., and Siegel, M.D., 2004. HYDROGEOCHEM 4.0: A Coupled Model of Fluid Flow, Thermal Transport, and HYDROGEOCHEMICAL Transport through Saturated-Unsaturated Media - Version 4.0. ORNL/TM-2004/103, Oak Ridge National Laboratory, Oak Ridge, TN 37831

Yeh, G.T., Fang, Y.L. and Burgos, W.D., 2005a. BIOGEOCHEM 1.0: A Numerical Model to Simulate BIOGEOCHEMICAL Reactions under Multiple Phase Systems in Batches. Technical Report. Dept. of Civil and Environmental Engineering, University of Central Florida, Orlando, FL 32816

Yeh, G.T., Fang, Y.L. and Burgos, W.D., 2005b. BIOGEOCHEM 2.0: A Numerical Model to Simulate BIOGEOCHEMICAL Reactions under Multiple Phase Systems: A Reaction Module for Transport Systems. Technical Report. Dept. of Civil and Environmental Engineering, University of Central Florida, Orlando, FL 32816

Zachara, J.M., Smith S.C., and Fredrickson, J.K., 2000. The effect of biogenic Fe(II) on the stability of Co(II)EDTA^{2-} to goethite and a subsurface sediment. Geochim. Cosmochim. Acta 64:1345–1362.

Zhang, F. and Yeh, G.T., 2005. Sediment and Reactive Chemical Transport Modeling In River/Stream Networks of Watershed Systems: Part (I) Numerical Strategies. Submitted to the Journal of Hydrologic Engineering, ASCE. April (2005)